Androgen Deprivation as an Immune Modulating Therapy in Combination with Targeted Immunotherapy for Prostate Cancer

By

Anusha Muralidhar

A dissertation submitted in partial fulfilment of

the requirements for the degree of

Doctor of Philosophy
(Cancer Biology)

at the

UNIVERSITY OF WISCONSIN-MADISON

2024

Date of final oral examination: 05/29/2024

The dissertation is approved by the following members of the Final Oral Committee:
Douglas G. McNeel, Professor, Medicine
Zachary Morris, Associate Professor, Human Oncology
Jamey P. Weichert, Professor, Radiology
William Ricke, Professor, Urology
Suresh Marulasiddappa, Professor, Veterinary Medicine

Acknowledgements

I am very grateful to all those who have contributed to the successful completion of this PhD thesis.

I express my heartfelt gratitude to my supervisor, Dr. Douglas McNeel, for his unwavering support, invaluable guidance, and boundless patience, which have been instrumental throughout this journey. His expertise, encouragement, and constructive feedback have profoundly shaped my work.

I am deeply thankful to the members of my lab, past and present, including Laura Johnson, Chris Zahm, Melissa Gamat-Huber, Jena Moseman, Ichwaku Rastogi, Heron Jeon, and Ellen Wargowski, for their collaboration and insightful discussions. Special thanks to Dr. Hemanth Potluri for his training and preliminary experiments that initiated this project, as well as to my undergraduate trainees, Sita Vakkalanka and Alec Chase Lewis, for their keen interest in learning and their valuable contributions to my project.

My appreciation extends to the faculty and staff of the UW Carbone Cancer Center and McArdle Cancer Research for providing a conducive academic environment and essential resources. I am grateful for the invaluable support of the flow cytometry core and the small animal imaging and radiation facility, particularly Justin Jeffery, Ashley Weichmann, and Zack Rosenkrans, for their

unwavering assistance and countless intravenous injections. I extend my thanks to Dr. Reinier Hernandez, Hansel Comas Rojas, and Orou Robert Malick for their assistance in ordering radioisotopes and radiolabeling NM600.

I acknowledge the funding agencies and organizations that have generously supported my research endeavors. Lastly, I extend my deepest appreciation to my committee members for their invaluable contributions to advancing scientific knowledge and understanding.

To my friends and family, your unwavering support, understanding, and encouragement, especially during challenging times, have been my greatest source of strength.

To everyone who has played a role, large or small, in achieving this academic milestone, I am sincerely grateful for your support and encouragement.

Dedication

Words don't suffice to express my appreciation and gratitude for the innumerable people who have played such an important role throughout my graduate school. This thesis is a tribute to those who have supported, encouraged, and inspired me along this journey.

Thank you to Doug for making our lab feel like a family. Madison has become home to me because of you and Linda. I have many warm memories of holiday parties, barbecues, and will always remember getting the GPA in 2021 as my biggest award in graduate school. I have learned so much from you about how to think like a scientist and will take many lessons from your mentorship and support. I could never have made it this far without all the unconditional support I have received from family, friends, and colleagues. To the McNeel lab, I thank each of you for your friendship and advice. Thank you to my cohort, Vu Tran, Gayathri Ramakrishnan, Cristina Paz, Donna Li, Sean Kraus, Mike Ohman, and Jena Moseman, who have made this long journey less isolating especially during our COVID days.

To my friends, Gayathri Ramakrishnan, Mayuri Dutta, Samridhi Garg, Tanaya Purohith, Miranda Salazar, Dimuth Pandhitharathne, Neeraj Deshingkar, Simone Shen, Carmen, Shubham Attri who have stood by me with words of encouragement, laughter, and understanding. Your friendship has made the challenging moments more bearable and the joyous ones even sweeter.

I extend my heartfelt gratitude to my late grandparents, Lalitha Sathyanarayan, Sathyanarayan, and Saraswathi, for their enduring inspiration and unwavering support throughout my childhood. Though they may not be here today, I hope they are proud of the person I have become.

To my parents, Muralidhar and Girija Muralidhar, who have been my guiding lights since the very beginning, I am forever indebted for the opportunities they have provided and for cheering me on at every step of my career journey. To my sister, Dr. Apoorva Muralidhar, and my brother-in-law, Dr. Arjun Prakash, your unwavering encouragement, and belief in me have been invaluable sources of strength. I am also thankful to my uncle, Jayaram Sathyanarayan, my cousin brother, Siddharth Jayaram, and my aunt, Savitha Jayaram, for their continuous support and love from halfway across the world. Their celebration of even the smallest of my achievements has always meant a great deal to me. To my brother-in-law, Darshan Chowdary, and my soon to be in-laws, Dhananjaya Naidu and Suma Kandra, your love and encouragement have been truly supportive throughout my journey.

Lastly, to my fiancée, Chandu Choudary, thank you for listening to all my frustrations and tolerating the long days in lab. You have been **my rock**. I have leaned on you most of all for support during the toughest parts of these five years.

This work is dedicated to you all with deepest gratitude and affection.

Abstract

Androgen deprivation as an immune modulating therapy in combination with targeted immunotherapy for prostate cancer

Anusha Muralidhar

Under the supervision of Professor, Douglas G. McNeel

at the University of Wisconsin-Madison

Metastatic prostate cancer poses a significant clinical challenge due to its lethal nature and the eventual development of resistance to conventional therapies, including androgen deprivation therapy (ADT). While therapies targeting the androgen receptor signaling are effective initially, the emergence of resistance necessitates the exploration of alternative treatment modalities. In recent years, targeted radionuclide therapy (TRT) has emerged as a promising systemic radiation modality for metastatic disease, offering the potential to deliver therapeutic doses to all sites of metastasis with minimal damage to healthy tissues. However, the impact of TRT on the prostate tumor microenvironment and its potential to enhance the efficacy of immunotherapies remains largely unknown.

In our study, we investigated the use of a novel TRT agent, ^{90}Y-NM600, in combination with ADT in murine prostate tumor models. Our findings revealed a sequence preference in the delivery of ADT and TRT, mediated by differences in T cells and myeloid cells within the tumor immune microenvironment. Importantly, we demonstrated that the addition of agents targeting Gr-1+

myeloid-derived suppressor cells significantly improved the antitumor efficacy of this combination therapy.

Furthermore, we explored the combination of ADT with tumor-specific vaccination using a DNA vaccine encoding the ligand-binding domain of the androgen receptor. Our previous research has shown that this vaccine elicits antigen-specific CD8+ T cell responses in both rodent models and humans. By investigating the timing and sequencing of ADT with vaccination, we observed that vaccinating prior to ADT significantly enhanced anti-tumor responses, mediated in part by increased infiltration of CD8+ T cells following ADT. Additionally, targeting myeloid-derived suppressor cell recruitment following ADT with cyclical use of testosterone further augmented anti-tumor responses.

Lastly, we delved into the complex interactions between ADT and T-cell responses, comparing various ADT approaches, including AR degraders and AR antagonists, to determine their synergy with AR-specific immunization. Our study highlights the potential of combining ADT with AR-specific immunization to enhance AR-specific CD8+ T cell infiltration, laying the groundwork for identifying optimal combinations for enhancing anti-tumor responses using checkpoint blockade.

Overall, our findings underscore the importance of exploring novel therapeutic combinations involving ADT and immunotherapy in prostate cancer treatment. Further investigation into these combinations is warranted, given their highly translatable nature and potential to improve clinical outcomes for patients with metastatic prostate cancer.

Table of Contents

List of Figures

Chapter 2:

Chapter 3:

Chapter 4:

Chapter 1

Introduction to prostate cancer and current treatments for treating prostate cancer.

This work has been published in Cancers 2022, Journal of Pharmaceutics 2023, and Nature Reviews Urology 2023.

1.1 Standard treatments for prostate cancer

Prostate cancer is the most common diagnosed malignancy among men and ranks as the second leading cause of cancer-related deaths in the United States [1]. In cases of hormone-sensitive prostate cancer, the standard of care includes androgen deprivation therapy (ADT) as a standalone or in combination with androgen receptor signaling inhibitors (ARSI), and radiation therapy or chemotherapy yielding significant enhancements in overall survival rates [2]. While localized cancer can be cured, metastatic prostate cancer remains a significant challenge worldwide. For recurrent prostate cancer, ADT remains the cornerstone of treatment, often administered lifelong for patients with metastatic disease. However, as castration resistance develops, chemotherapy has traditionally served as the primary treatment approach [3]. Nonetheless, recent years have witnessed the emergence of novel therapeutic options that have enhanced survival rates following chemotherapy. These options encompass ARSI, PARP inhibitors, and Lu-PSMA radioligand therapy [4].

Immunotherapy's role in prostate cancer remains under continuous investigation, with Sipuleucel-T being the sole approved immunotherapeutic agent [5]. Overall, the dynamic landscape of prostate cancer therapy presents both challenges and promise, as numerous new treatment avenues continue to surface.

1.1.1 Androgen Deprivation Therapy

The advancement of prostate cancer occurs in a sequence of stages, starting from the development of prostatic intraepithelial neoplasia (PIN), progressing to high-grade PIN (HG-PIN), and ultimately leading to adenocarcinoma and metastasis. A key factor driving this progression is the dependence of prostate cells on androgens for their growth and function. As a result, therapies aimed at suppressing androgen production or blocking the androgen receptor (AR) are utilized throughout all phases of prostate cancer. While initially exhibiting high responsiveness to this treatment, these cancers almost inevitably develop resistance. This resistance typically involves acquiring gene amplifications of the AR, mutations occurring in the AR, activation of the AR independent of androgen stimulation through the upregulation of steroidogenic enzymes, including de novo intratumoral androgen synthesis from androstenedione and DHEA and the continued occupation of AR on DNA binding sites regardless of ligand availability [6–9].

1.1.1.1 Types of androgen deprivation therapies

Localized prostate cancer treated with prostatectomy or radiation therapy or a combination of both which leads to complete regression in a third of the cases [10]. In cases of metastatic prostate cancer, patients undergo ADT continued indefinitely with or without docetaxel chemotherapy. FDA-approved LHRH agonists like leuprolide and goserelin, as well as the LHRH antagonist degarelix, effectively decrease luteinizing hormone production, leading to reduced gonadal testosterone production [11]. Despite significantly reducing serum testosterone, adrenal androgen production may persist, and prostate tumors can synthesize androgens. Therefore, additional therapies are often utilized to further suppress androgen levels or signaling [12]. Numerous specific androgen receptor degraders (SARDs) and proteolysis-targeting chimera (PROTACs) are

currently under development for treating advanced metastatic castration-resistant prostate cancer (CRPC).

Abiraterone, a potent Cyp17A1 inhibitor, further reduces testosterone levels by blocking androgen production in non-gonadal tissues [13–15]. The first-generation androgen receptor (AR) antagonists, nilutamide and flutamide, lacked selectivity for prostate tissue over other organs, leading to suboptimal efficacy and significant side effects [16]. These drugs only partially suppressed AR activity and were largely supplanted by bicalutamide, which offered improved selectivity and tolerability [17]. In recent years, second-generation AR antagonists, including enzalutamide, apalutamide, and darolutamide have been approved for the treatment of prostate cancer [18]. Enzalutamide, in particular, exhibited superior binding affinity and efficacy compared to earlier drugs like flutamide and bicalutamide [19]. However, despite its efficacy, enzalutamide treatment can lead to the emergence of resistance mechanisms. For instance, it may induce the expression of AR mutant ARF876L and AR-V7, which contribute to resistance to enzalutamide [20,21]. Additionally, there is evidence to suggest that enzalutamide treatment could potentially enhance the metastasis of prostate cancer [22]. These findings underscore the complexity of treating prostate cancer and the need for continued research into developing alternative treatment strategies that can overcome resistance and improve patient outcomes.

ASC-J9, a curcumin analog, represents another PROTAC which works by disrupting the association between the AR and its co-regulator ARA70. ASC-J9 effectively triggers the degradation of the AR protein [23]. This mechanism of action offers a novel approach to targeting the AR pathway, potentially circumventing resistance mechanisms that arise with traditional AR-targeted therapies. Preclinical studies have demonstrated the efficacy of ASC-J9 in degrading both

wild type AR and the F877L mutant AR, which is known to confer resistance to enzalutamide, a commonly used anti-androgen drug in the treatment of prostate cancer [24]. These findings highlight the potential utility of ASC-J9 in overcoming treatment resistance and improving outcomes for patients with advanced prostate cancer. Despite its promising preclinical data, ASC-J9's efficacy and safety profile in clinical settings have yet to be fully evaluated. ARV-110, also belonging to the class of PROTACs has shown remarkable efficacy in inducing degradation of the AR protein in pre-clinical studies in Enzalutamide-Insensitive PDX models [25]. Moreover, in phase I/II clinical trials, ARV-110 has shown promise in a heavily pretreated metastatic castration-resistant prostate cancer (mCRPC) patient population [26] Notably, patients with AR T878 and/or H875 mutations, which are associated with resistance to standard therapies, demonstrated the greatest PSA50 activity and RECIST responses to ARV-110. This subset of patients appears to be particularly sensitive to ARV-110 treatment [27]. However, further investigation is warranted to fully understand the efficacy and safety profile of ARV-110 in larger phase clinical trials.

Another agent, galeterone, which not only inhibits testosterone production by targeting Cyp17A1 but also competitively inhibits the androgen receptor (AR), prevents AR binding to DNA, and enhances degradation of both wild type and mutant AR [28,29]. However, phase 3 trials of galeterone were recently halted because the data monitoring committee determined that it would not improve patient survival compared to enzalutamide [30].

While historically androgen receptor (AR)-targeted agents have primarily focused on the ligand-binding domain of the AR, a new class of AR inhibitors has emerged, directing attention to the N-terminal domain, which plays a significant role in interacting with transcriptional proteins. Preclinical studies involving EPI-001, which specifically targets the AF1 domain of the AR,

thereby blocking AR transactivation, have demonstrated regression of castration-resistant prostate cancer (CRPC) xenografts with minimal toxicity effects [31,32]. Additionally, EPI-506, which similarly targets the N-terminal domain of the .AR, is presently under evaluation in phase 1/2 clinical trials (NCT02606123) [33].

In summary, ADT results in tumor regression, through the induction of tumor cell apoptosis and senescence. There are several ways to decrease circulating androgen levels, using either LHRH agonists or antagonists, Cyp17A1 inhibitors, or compounds to target the AR itself, such as anti-androgens, AR degrading agents, or compounds that use several strategies at once. Invariably, prostate tumors develop mechanisms of resistance to these various methods of ADT.

1.1.1.2 Effects of Androgen deprivation therapy on immune function

Androgens have been associated with direct adverse effects on T-cell function. When splenic CD4+ T cells were cultured in Leydig cell conditioned media, which contains testosterone, or exposed directly to testosterone, there was a dose-dependent rise in the number of CD4+ CD25+Foxp3+ regulatory T cells (Tregs) and increased the production of IL-10. This effect was reversed with concurrent administration of the anti-androgen flutamide that abolished IL-10 production, indicating the androgen dependency of CD4+ CD25+ Foxp3+ Treg function [34].

Interestingly, elevated levels of regulatory T cells (Tregs) in the prostate are correlated with decreased PSA recurrence-free survival. Moreover, this increase in Tregs is significantly linked to higher tumor grade and increased Ki67 labeling in tumors [35]

However, the castration of aged mice led to an enlargement of the thymus, which was linked to increased proliferation and decreased apoptosis of thymocytes in castrated aged mice compared to

intact aged mice [36]. Morse et al showed that shortly after androgen deprivation in mice, there was an increase in the numbers of circulating naïve T cells and these were of the T_H-1phenotype [37]. In addition, studies using short-term androgen deprivation prior to prostatectomy, an increase in oligoclonal T-cell infiltration into prostate tissue was observed [38].

In separate rodent investigations, castration prompted the infiltration of T cells into the prostate. Initially, these cells exhibited a bias towards the Th1 subset, but later shifted towards theTh17 subset, persisting for at least 90 days post-castration [37]. In studies of prostate tumor-bearing mice, castration with immunization similarly elicited a greater number of antigen-specific CD8+ T cells, however with prolonged treatment an increase in Tregs was observed[39]. Together, these studies all demonstrate that androgen deprivation can enhance T cell function. Furthermore, in patients, castration resulted in elevated absolute levels of T cells circulating in the peripheral blood [40]. Taken together, these findings underscore the intricate relationship between androgens and T-cell function, highlighting the potential impact of androgen deprivation on immune modulation in the context of prostate cancer.

1.1.2 Radiation Therapy

Radiation therapy that is used in both localized and advanced stage disease and can be categorized into three main categories: external-beam radiation therapy (EBRT), which uses an x-ray machine (linear accelerator) to produce gamma rays outside the body that target cancer cells, brachytherapy (BT), which uses radioactive seeds administered internally, and TRT which involves administering radionuclides coupled to cancer targeting compounds to irradiate tumor cells.

1.1.2.1 External beam radiation therapy

EBRT is a potentially curative treatment for localized prostate cancer, and typically prioritized for patients who are not candidates for prostatectomy and/or have adverse pathologic features [41–43]. The standard regimen for treating low risk disease is 75-80Gy and for intermediate-risk and high-risk prostate cancer EBRT is often combined with short-term androgen deprivation [44,45].

During the past three decades, technological advances have greatly improved radiation therapy delivery with emphasis on improving target definition with smaller radiation fields [46]. To achieve dose escalation, 3-dimensional conformal radiation therapy (3D-CRT) was developed using computed tomography simulations (CT) and as reported in the RTOG 9406, phase I/II trial, yielded favorable outcomes for localized prostate cancer [47]. With the development of more sophisticated treatment-planning software in the mid-1990s, intensity-modulated radiation therapy (IMRT) emerged as an advanced form of conformal therapy. In addition to IMRT, image-guided radiotherapy (IGRT) is an essential adjunct for dealing with daily changes to the target anatomy [48]. It has been reported that IMRT may be more effective than 3D-CRT for higher dose treatments [49].

Several studies have indicated that prostate cancer responds well to EBRT delivered in fewer fractions with higher doses (hypofractionation) [50–52]. Stereotactic body radiation therapy (SBRT), also called stereotactic ablative radiotherapy (SABR), is a technique that can deliver higher doses in hypofractionated regimens and has shown comparable biochemical control and morbidity to standard fractionation schedules in prospective randomized trials [50,53]. Results

with SBRT in limited numbers of patients with low-risk prostate cancer suggest that this approach is feasible, with comparable efficacy and safety to other forms of radiation therapy [54–56].

In contrast to conventional photon (X-ray) therapies, proton beam therapy (PBT) can also confer several advantages in terms of tumor targeting and dose exposure. Multi-institutional randomized trials (NCT01617161, NCT03561220) are comparing IMRT versus PBT for impacts on treatment-related toxicity and quality of life, however no prospective trials have evaluated the efficacy of PBT relative to EBRT [57].

1.1.2.2 Brachytherapy

In the early 19th century, Pasteau and DeGrais explored treatments for prostate cancer by implanting radium sources through a catheter in the urethra or rectum. This initial approach led to developments in techniques and instruments for brachytherapy using radioactive sources by multiple others. In particular, the interest in brachytherapy was revived by Bagshaw and colleagues in the late 1950s with a series of patients being cured by high energy cobalt treatment [58]. In the early 1980s, Whitmore experimented with a variety of different radioisotopes implanted as permanent brachytherapy sources in patients, and found this approach was well tolerated [59] . Holm and colleagues applied transrectal ultrasound to the guidance of Iodine-125 seed placement [60]. Iodine-125, palladium-103, and cesium-131 are now the three isotopes routinely used for low-dose-rate (LDR) prostate brachytherapy [61]. Neither isotope appears to be more effective than another based on the available data [62]. In some cases LDR brachytherapy is used in combination with EBRT in men with intermediate- or high-risk prostate cancer [63]. Escalating

the dose of radiation through high-dose-rate (HDR) brachytherapy with iridium-192 has also been used as a monotherapy and/or in combination with EBRT, and this has been a promising approach for treating locally advanced prostate cancers [64–66].

There have been no randomized prospective trials to compare the efficacy of EBRT and BT treatments. However, a meta-analysis of randomized clinical trials provided evidence to support the use of BT boost after EBRT to improve biochemical progression-free survival (bPFS) in intermediate and high-risk patients [67].

1.1.2.3 Targeted radionuclide therapy

Despite potentially curative therapy for localized prostate cancer, nearly 1/3 of patients will ultimately progress to metastatic disease [68–70]. Due to the inability to feasibly target all metastatic lesions, EBRT has typically been used only for palliative purposes in this setting [71,72]. However, in recent years, targeted radionuclide therapy (TRT) has emerged as a promising treatment strategy for metastatic prostate cancer. Strontium-89 (Sr-89) and Samarium-153 (Sm-153) were the first TRT agents approved for palliative use due to their ability to target metastatic bone disease, although they did not improve overall survival [73,74]. Radium-223, which is a calcium mimetic, similarly targets bone metastatic disease, and was the first alpha emitting radionuclide approved by FDA as a treatment for mCRPC based on evidence of extended survival [75,76].

While these TRT agents have been useful for patients with disease localized exclusively to the bone, they are not effective for those with other disease sites. Hence, other investigations have

focused on compounds that specifically target cancer cells rather than the bone. One of the most studied targets for these approaches has been prostate-specific membrane antigen (PSMA) which is highly expressed in prostate cancer cells [77]. As the first PSMA-targeting antibody, capromab pendetide was initially used as an imaging tool for prostate cancer. Labeling of this agent with therapeutic isotypes demonstrated limited clinical efficacy, probably because it binds to an intracellular epitope of PSMA, requiring the internal domain of PSMA to be exposed externally [78]. However, J591, a monoclonal antibody that binds the extracellular domain of PSMA, has been conjugated to multiple radionuclides and evaluated in trials for patients with mCRPC. Using an activated monoclonal antibody-fluorophore conjugate of J591, Nakajima and colleagues successfully imaged prostate cancer *in vivo* in murine prostate tumor models [79]. Bander et al conducted several trials assessing dose limiting toxicities and efficacy of radiolabeled J591 and demonstrated that the agent can accurately target metastatic prostate cancer sites in bone and soft tissue, and may be useful for targeting diagnostic or therapeutic imaging agents [80,81]. In particular, a phase II clinical trial evaluating a single administration of 177-Lu-J591 found this to be well tolerated and capable of targeting metastatic sites. Of 47 patients with mCRPC treated, 59.6% experienced a decrease in PSA, and 1/12 with measurable disease achieved a partial response. Those with low PSMA expression by imaging were less likely to respond [82]. As a mixed alpha and beta emitter, bismuth-213 (213Bi) has also demonstrated pre-clinical activity when tagged to the PSMA-targeting antibody J591 [83–86]. However, 213-Bi-J591 has not yet been evaluated in patients with prostate cancer.

More recently, a small molecule ligand that binds PSMA, PSMA-617, has been radiolabeled with different radionuclides and investigated for both diagnostic imaging and therapeutics (theranostic

agent). 68Ga-PSMA-617 was the first approach to utilize PSMA-617 for the diagnosis of prostate cancer. As reported by Liu and others, PET/CT imaging of 68Ga-PSMA-617 was useful as an imaging biomarker to assess metastatic disease not detectable by conventional imaging, to stratify the risk of metastatic prostate cancer [57,87,88]. Preclinical studies of PSMA-617 with the 177-Lu beta emitting radioligand yielded encouraging results for safety and efficacy as reported by Ruigroket et al [89]. 177Lu-PSMA-617 (Lu-PSMA) was evaluated in a prospective single-arm phase 2 study in which 57% of patients experienced PSA declines greater than 50%. Patients also experienced pain improvements, and median PFS and OS of 7.6 months and 13.5 months, respectively, were identified [90]. This was confirmed in a randomized phase 3 trial in which patients with mCRPC, who had received prior taxane chemotherapy and at least one AR pathway inhibitor agent, were randomized to receive 177Lu-PSMA-617 or a non-chemotherapy standard of care (SOC). This trial demonstrated that Lu-PSMA therapy was effective in generating a longer radiological progression-free survival (8.7 months) in patients with PSMA+ mCRPC who previously received standard of care therapies, as well as overall survival (15.3 months), compared to 3.4 and 11.3 months, respectively, for the SOC group. These findings led to FDA approval in 2022 for the use of LuPSMA as a treatment for mCRPC following previous treatment with chemotherapy and a second generation AR pathway targeting agent [91,92].

PSMA-617 has also been evaluated conjugated to other radioisotopes, notably with the higher energy alpha emitter ^{225} Ac. A series of small studies have evaluated ^{225}Ac PSMA-617 in patients with mCRPC, including patients resistant to 177-Lu PSMA-617 [93–96]. A retrospective meta-analysis of 6 trials comprising 201 patients treated, showed that PSA declines >50% occurred in 66.1% of patients, with low rates of hematological toxicity. The most common adverse effect, as

with Lu-PSMA, was xerostomia, which occurred in 77.1% of all patients. Further prospective clinical trials with this agent are anticipated [97].

1.1.2.3.1. ^{90}Y-NM600 as a theranostic agent

^{90}Y-NM600 represents a novel theranostic agent that can be utilized as a diagnostic tracer and therapeutic radiopharmaceutical therapy. It comprises NM600, a small molecule, conjugated with the radioisotope yttrium-90 (^{90}Y). Yttrium-90, being a high-energy beta emitter with a half-life of 64.1 hours. Upon administration, ^{90}Y-NM600 selectively accrues in tumor tissue, delivering therapeutic radiation doses directly to cancer cells while preserving adjacent healthy tissue. Preclinical studies have shown that ^{90}Y-NM600 is effective in treating T cell lymphoma models [98]. Further work has demonstrated that ^{90}Y-NM600 in combination with CTLA-4 blockade can result in strong anti-tumor efficacy in melanoma, breast, and neuroblastoma models by eliciting a cytotoxic and memory CD8+ T cell response [99]. However, this compound has been studied in the context of prostate cancer with anti-PD-1 and has shown combination 90Y-NM600 and PD-1 blockade is ineffective in these models due to the persistence of Tregs and the activating effects of PD-1 blockade on this population and careful evaluation of the effects of other radioisotopes or TRT agents on the tumor microenvironment could be crucial for successful combination with checkpoint blockade in prostate cancer [100].

1.1.2.4 Effect of Radiation therapy on tumor immune microenvironment

Radiation therapy (RT) has effects on both tumor cells and immune cells within the tumor microenvironment, potentially making immunotherapies more effective against poorly immunogenic tumors. The optimal dose and fractionation of radiotherapy are likely important and may differ for each tumor type and immune microenvironment. Radiation at optimal doses can cause release of proinflammatory cytokines such as IL-1β and TNFα, increase FAS expression on tumor cells rendering them susceptible to Fas-ligand expressing lymphocytes [101], and increase MHC-I expression on tumor cells making them more readily detected by CD8+ T cells [102]. In addition, RT-induced dsDNA fragments can be sensed by cGAS within dendritic cells (DCs), activating STING signaling, and leading to a type I IFN response and increased cross-presentation by DCs. Radiation therapy can also increase CD86 and CD70 expression on intratumoral DCs, as well as promote DC maturation, increased expression of MHC II, and migration to the tumor draining lymph nodes to present antigens to CD8 T cells [103,104]. Moreover, as the dose of radiation increases, greater accumulation of DNA damage occurs [105]. DNA damage leads to cell death, which is accompanied by release of damage-associated molecular patterns and a cascade of inflammatory response activation known as immunogenic cell death [106]. RT induced immunogenic cell death can lead to the release of tumor-associated antigens that, cross-presented by activated DC, may elicit an adaptive immune response and lead to further increased T-cell infiltration into tumors [107]. In addition to the extensive literature demonstrating that RT has immunostimulatory effects, it has been shown that a significant portion of the anti-tumor effects of radiation are mediated by immune populations. Immunocompromised mice require much higher

doses of radiation to result in tumor eradication than do immunocompetent mice [108]. Additionally, when CD8+ T cells are depleted from tumor-bearing mice, the anti-tumor effect of radiation is greatly reduced [104]. Although RT initially results in temporary depletion of CD8+ T cells, this population is eventually activated and infiltrates the tumor, as reported in both preclinical models and human cancers [109–111]. It has also been shown that RT skews tumor-infiltrating CD8+ T cell populations towards resident memory phenotypes, in part because these memory cells are more radioresistant [112,113]. There is also some evidence that RT can facilitate NK expansion, activation, and accumulation in draining lymph nodes, resulting in improved anti-tumor efficacy *in vivo* [114,115]. While conceptually radiation can be used to stimulate the development of an anti-tumor cytotoxic response, many tumors also have an increased number of immunosuppressive cell populations (tumor-associated macrophages (TAMs), MDSC, and Tregs) that are more radioresistant than the other immune subtypes. These populations can cause NK cell and T cell anergy and block DC maturation [116,117]. The dose of RT can therefore significantly affect the phenotype of immune cells and alter the signaling within the tumor microenvironment, making them pro- or antitumorigenic. For instance, RT can affect the functional polarization of macrophages that can activate either anti-tumor M1-like macrophages or immunosuppressive M2 macrophages, encouraging angiogenesis and remodeling of the stromal matrix to help tumor establishment [118]. However, high doses of RT have been correlated with increased TGF- β release that has potent immunosuppressive properties, including polarization of CD4 T cells into Tregs, suggesting that targeted chemokine receptor antagonists might be effectively combined with RT [119,120] Additionally, radiation can increase T-cell checkpoint molecule/ligand expression. Specifically, high-dose radiation results in upregulation of PD-L1 on tumor cells [121].

This explains the rationale behind treatment combinations with radiation and checkpoint blockade. Because prostate cancer is associated with multiple immunosuppressive pathways, combining immunotherapy that targets these immunosuppressive pathways with radiotherapy may be a promising approach for increasing antitumor responses and preventing immune escape.

1.1.3 Immunotherapy

The concept of immunotherapy for prostate cancer dates back to the 1970s when Ablin and colleagues reported anecdotal cases of metastatic prostate cancers that regressed after being treated locally with cryotherapy [122]. The identification of autologous antibodies that recognized the prostate tissue suggested that this abscopal-type treatment response was immune mediated [123]. This led to significant interest in developing immune-based strategies for prostate cancer treatment. Early efforts focused on vaccines aimed at generating T cell and antibody responses to the prostate. This concept was ideal for prostate cancer since the prostate is a non-essential organ, and therefore an immune response directed against prostate cancer need not be necessarily limited to malignant cells. Since then, there have been several approaches to developing anti-tumor vaccines, most commonly delivering inactivated or modified tumor cells (antigen non-specific), or delivering components of tumors to stimulate immune responses to specific antigenic targets (antigen-specific vaccines). Five phase 3 clinical trials have been conducted in patients with mCRPC using different vaccine approaches. Four of these approaches did not demonstrate improved overall survival [124–128]. To date, only sipuleucel-T met its primary endpoint of extending survival in patients with advanced metastatic prostate cancer and was approved by FDA

in 2010 [128]. Sipuleucel-T is comprised of autologous antigen-presenting cells loaded *ex vivo* with a fusion protein of a tissue-specific antigen (prostatic acid phosphatase, PAP) and GM-CSF. The approval of sipuleucel-T has demonstrated that vaccine therapies can be useful in the treatment of prostate cancer, however the absence of significant objective radiographic responses or substantial changes in serum prostate specific antigen (PSA) with sipuleucel-T, or other vaccines when used as monotherapies, has led to the exploration of vaccines as a part of combination therapies.

More recently, efforts have been directed toward recruiting effector T cells to the sites of tumor with the development of bispecific T-cell engagers (BiTE). These agents consist of a tumor-specific domain and a T-cell activating domain. Several such agents targeting PSMA are in clinical stages of development. In particular, pasotuxizumab (AMG 212) and acapatamab (AMG 160) have demonstrated objective responses in patients with mCRPC [129,130]. A phase 1 clinical trial with JNJ-081, a similar bispecific antibody for targeting PSMA and CD3, demonstrated transient reductions in PSA in patients with mCRPC [88]. A second generation BiTE approach, HPN424, has also recently completed evaluation in a phase 1/II clinical trial [88]. More BiTE approaches targeting other prostate-specific surface molecules are being explored.

Although all the vaccine approaches evaluated in phase 3 trials were effective in activating antigen-specific T cells, most did not improve clinical outcomes when used alone in treating advanced prostate cancer. Similarly, despite immune checkpoint blockade therapy being effective for many different cancer types, these treatments have been relatively ineffective as monotherapies for advanced prostate cancer. Together, these findings suggest that mechanisms of immune

suppression are active in prostate cancer. Prostate cancer is known to have an immunologically "cold" tumor microenvironment characterized by a low mutational burden and limited infiltration of effector CD8 T cells. In addition, the secretion of immune-suppressive cytokines like TGF-β and CXCR2 by prostate tumor cells leads to the recruitment of immunosuppressive populations, such as regulatory T cells (Treg) and myeloid-derived suppressor cells (MDSC) that have been also been associated with poor clinical outcomes [131,132]. The expression of nitrous oxide synthase and indoleamine2,3-dioxygenase by these populations can further suppress the activity of CD8+T cells [132,133]. Consequently, these immunotherapeutic approaches may be most active when used in combination with agents that target the mechanisms that underlie tumor-associated resistance and immune evasion.

1.1.3.1. DNA vaccines for prostate cancer

The shift towards DNA vaccines in cancer treatment stems from their unique advantages over traditional vaccine approaches. DNA vaccines offer simplicity in design, ease of manufacturing, and a favorable safety profile, making them an attractive option for combating tumors. The first target of DNA vaccines to be explored for prostate cancer treatment was PSA. Pisa and colleagues reported a phase I dose-escalation study using a plasmid encoding full length PSA that was given intramuscularly and intradermally to patients with advanced CRPC in monthly cycles for five months. The highest dose (900μg of DNA) elicited PSA-specific cellular and humoral antibody responses [134]. To further improve the immunogenicity of this PSA vaccine, this group tested a DNA vaccine encoding the rhesus PSA gene administered intradermally and with electroporation

[135] . Immune responses to PSA were detected in several patients, and 4/15 patients demonstrated a > 50% increase in PSA doubling time. This approach has not been pursued further.

The most studied antigen in DNA vaccine trials for prostate cancer has been PAP, the same target as for the sipuleucel-T vaccine. A phase I dose-escalation study was conducted using a plasmid encoding PAP, pTVG-HP, in 22 patients with PSA-recurrent, non-metastatic prostate cancer and was found to be safe and elicit CD8 T cell immune responses at each dose level tested [136]. In a separate phase I trial, two different schedules of pTVG-HP were assessed in 17 patients with non-metastatic, CRPC. This study identified that multiple DNA immunizations were required to elicit and maintain PAP-specific immune responses. In both studies, increases in PSA doubling time were observed [137]. Based on these findings, a randomized phase II study was conducted to determine whether vaccination could delay the development of metastatic disease in patients with non-metastatic, castration-sensitive prostate cancer. Ninety-nine patients with a pre-treatment PSA doubling time of less than 12 months were randomized to receive pTVG-HP and GM-CSF adjuvant or GM-CSF alone. No difference in overall two-year metastasis-free survival (MFS) was observed between the two cohorts. However, the subset of patients with most rapidly progressing disease did have longer MFS, and decreases in sodium fluoride uptake in micro-metastatic bone disease detected by ^{18}F-NaF PET/CT was observed in vaccine-treated patients [138]

Together, these findings suggested that while there was evidence of biological activity, this pTVG-HP vaccine should not be further pursued as a single agent, and that DNA vaccines might best be evaluated in combination with other vaccines or other immune-activating agents. As a result of these findings, a subsequent trial evaluated the pTVG-HP vaccine given following sipuleucel-T,

as a prime-boost approach targeting the same PAP target antigen [139]. Although small, this trial demonstrated that DNA booster immunizations could augment the antibody response to PAP that were elicited with sipuleucel-T, but differences in T-cell responses or longer TTP were not observed. Preclinical murine studies, however, demonstrated that DNA vaccination led to an increase in PD-1 expression on activated CD8+T cells and that combining vaccination with PD-1/PD-L1 blockade led to superior anti-tumor outcomes, suggesting that DNA vaccination might best be used with concurrent PD-1 blockade [140] . This was initially demonstrated in a pilot trial in patients with mCRPC. Patients were vaccinated with pTVG-HP either concurrently with pembrolizumab over 12 weeks or receiving pembrolizumab after a 12-week course of vaccination. In that trial, objective radiographic changes were observed in 4/5 patients with measurable disease treated with the agents in combination, with 1/5 experiencing an unconfirmed PR. Similarly, any PSA decline from baseline was identified in 8/13 patients receiving the agents in combination compared with 1/12 receiving the agents sequentially (p=0.01) [141]. Of these PSA declines, declines >50% occurred in 2/13 patients receiving the agents in combination, but not sequentially. As a result, this trial was expanded to include 66 patients total with mCRPC, evaluating the effect of treatment on TTP. While few objective responses were observed, the overall radiographic PFS rate at 6 months was 47%, overall median time on treatment was 5.6 months (95% CI: 5.4 to 10.8 months), and 32% of patients remained on trial beyond 6 months without progression. The median overall survival was 22.9 months (95% CI: 16.2 to 25.6 months) [142]. Given these findings, this approach using pTVG-HP in combination with PD-1 blockade is being pursued in trials in patients with early recurrent prostate cancer with nivolumab and in combination with a DNA vaccine encoding another antigen (pTVG-AR) and pembrolizumab in patients with mCRPC [143].

PSMA has also been evaluated as a target antigen for DNA vaccines. A DNA vaccine encoding an HLA-A2 binding epitope of the PSMA gene fused to a fragment of the tetanus toxin was tested in a phase I/II dose escalation trial [144] .Patients received vaccine with or without electroporation, and this demonstrated a significant increase in PSA doubling time compared to an unvaccinated patient control cohort. While the investigators deemed this worthy of evaluation in a randomized trial, to our knowledge there has been no further clinical development of this approach. In another approach, investigators evaluated a DNA vaccine encoding fragments of PSMA and preferentially-expressed-antigen-in-melanoma (PRAME). In this trial, patients with several cancer types were immunized by intralymph node injection with DNA followed by immunization with peptides derived from PSMA and PRAME [145]. While safe and demonstrating evidence of immunological activity, this approach has not been further pursued in patients with prostate cancer, likely given that only 1/10 (10%) experienced a PSA decline >50%, and no partial or complete radiographic responses were detected. A more recent trial, however, evaluated INO-5150, a DNA vaccine consisting of plasmids encoding both PSMA and PSA, and delivered by electroporation with or without a plasmid DNA encoding IL-12 (INO-9012). This trial, conducted in 62 patients with biochemically recurrent prostate cancer, demonstrated no safety concerns, and patients overall experienced an increase in PSA doubling time that was associated with the development of immune response to the target antigens [146]. This approach is currently being evaluated in combination with PD-1 blockade (nivolumab) and flt3 ligand (CDX-301) in a multi-arm trial in patients with mCRPC.

The androgen receptor (AR), the primary pharmacological target of prostate cancer, has also been investigated as a vaccine antigen. Preclinical studies had demonstrated the safety and anti-tumor

efficacy of a DNA vaccine encoding the ligand-binding domain (LBD) of the AR (pTVG-AR) [147]. In particular, anti-tumor efficacy was demonstrated when pTVG-AR was used with androgen deprivation, the primary treatment for prostate cancer that can lead to overexpression of the AR. A phase I trial evaluated pTVG-AR in one of two treatment schedules, and with or without GM-CSF given as a vaccine adjuvant, in patients with newly metastatic prostate cancer who had recently begun androgen deprivation [148]. This vaccination was demonstrated to be safe, and one schedule was demonstrated to elicit more AR-specific IFNγ-secreting T cells; GM-CSF was not found to augment immune responses. Immune response to the AR LBD target was associated with a longer PSA progression-free survival compared to patients who did not develop immune responses. The pTVG-AR vaccine is being further explored in combination with pTVG-HP and pembrolizumab in patients with mCRPC, and in patients with high-risk newly diagnosed prostate cancer in sequence with androgen deprivation and with or without PD-1 blockade using nivolumab [143].

Prostate cancer has traditionally been associated with low mutational burden, suggesting a lower number of potential tumor-specific mutation-associated neoantigens (MANA)[149]. This, and the availability of prostate cancer-specific targets as described above, has impeded the development of personalized vaccines for prostate cancer targeting MANA that have been explored as vaccine antigens for other cancer types[150]. However, a pilot clinical trial is evaluating a personalized vaccine approach using a DNA vaccine encoding MANA, following treatment with the PROSTVAC vaccine, and delivered with ipilimumab and nivolumab, in patients with metastatic castration-sensitive prostate cancer [151].

Plasmid DNA vaccines have also been used as parts of heterologous immunization approaches [152]. In an approach known as VBIR, studies in preclinical models suggested that potent T cell responses could be elicited by means of a chimpanzee adenovirus vector encoding a target used for priming, followed by plasmid DNA encoding the same antigen. This could be further augmented using antibodies targeting PD-1 and CTLA-4 delivered subcutaneously. This approach was attempted in a large phase I trial of patients with different stages of prostate cancer, and targeting three antigens (PSA, PSMA and prostate stem cell antigen (PSCA)). This trial demonstrated few objective tumor responses, and grade 3 or 4 adverse events were observed in 38% of patients [153]. As a consequence, this approach is not being further pursued.

1.1.3.2 Immune checkpoint blockade therapy in prostate cancer

Since 2010, the success of immune checkpoint blockade therapies for multiple cancer types has led to their exploration in the treatment of prostate cancer as well. Single-agent trials using agents blocking either CTLA-4 or PD-1 have advanced through clinical testing and have also been evaluated in randomized phase 3 clinical trials. Unfortunately, the results of these trials have been relatively disappointing in prostate cancer. In particular, two phase 3 trials using CTLA-4 blockade (ipilimumab), either alone or combined with bone metastasis-targeted radiation therapy, did not demonstrate prolonged overall survival [154,155]. Clinical trials using PD-1/L1 blocking agents have similarly demonstrated little evidence of single-agent activity in earlier phase clinical trials for patients with metastatic prostate cancer [156,157]. Combined PD-1 and CTLA-4 blockade demonstrated slightly more clinical activity against advanced prostate cancer, but with

significantly more toxicity, hence is not being further pursued [158]. A phase 3 trial using enzalutamide with or without atezolizumab found no difference in overall survival [159]. Similarly, a recently completed phase 3 trial using docetaxel with or without pembrolizumab (KEYNOTE-921) for patients with advanced prostate cancer showed no improvement in overall survival. Earlier phase clinical trials have suggested that checkpoint blockade therapies may have efficacy in combination with other agents, including vaccines, and hence combination trials are being further pursued [142,160] with the hypothesis that combining vaccines with checkpoint blockade therapies will enhance the overall anti-cancer immune responses.

1.2 Rationale for combining ADT with TRT

While androgen deprivation therapy (ADT) and RT are standard treatments for localized prostate cancer, there has been relatively limited exploration of ADT combined specifically with TRT [161]. Apart from their independent cytotoxic effects, there is evidence to suggest that ADT synergistically works with RT by preventing DNA repair [162,163]. However, the order in which ADT and TRT are best administered has not been rigorously studied [164]. Recent data indicates that RT and ADT can distinctly influence the tumor immune microenvironment [165]. ADT enhances vulnerability to CD8+ T cell-mediated destruction, triggers thymus regeneration, amplifies naive T cell production, augments immune cell infiltration from myeloid and lymphocyte populations, and elevates antibody responses against prostate-specific antigens [39,166–169]. However, ADT also triggers a significant secretion of IL-8 in human prostate tumors, which can lead to the accumulation of intratumoral myeloid-derived suppressor cells (MDSCs), which may impede T-cell activity [170]. Conversely, RT elicits inflammatory responses, including the

upregulation of MHC-I expression on tumor cells, enhancement of antigen cross-presentation by antigen-presenting cells, activation of the Fas/Fas ligand (Fas-L) signaling pathway, targeting of immune-suppressive populations like regulatory T cells (Tregs), and the induction of immunogenic cell death [171,172]. In combination, ADT and RT can synergistically enhance tumor immunity, modulating both local and systemic anti-tumor immune responses [173]. Therefore, investigating effective strategies for their combination, including considerations such as the timing and sequence of ADT with RT, as well as the integration of newer systemic TRT agents, is crucial.

1.3 Rationale for combining ADT with immunotherapy

ADT leads to increased infiltration of T cells into both the prostate and prostate tumors [174]. In patients, tumor-infiltrating lymphocytes consist of both effector CD8+ T cells and CD4+ T cells, including regulatory T cells [175]. The diverse immunomodulatory effects of ADT underscore its potential utility in combination with vaccine-based therapies. Clinical trials have explored the sequential administration of Sip-T (PA2024, the PAP/GM-CSF fusion protein vaccine antigen) and androgen deprivation therapy in patients with biochemically recurrent prostate cancer at high risk of metastasis [5]. Additionally, randomized trials have evaluated the efficacy of the viral PROSTVAC vaccine compared to the AR antagonist nilutamide in patients with biochemically recurrent castration-resistant prostate cancer. While initial monotherapy trials did not reveal significant differences in time to treatment failure, combination therapy following PSA progression showed promising results [176]. Studies examining GVAX with the T-reg depleting agent cyclophosphamide followed by degarelix demonstrated significantly increased time to PSA

progression and time to next treatment compared to degarelix alone. However, it's noteworthy that treatment with ADT also results in the infiltration of CD8+ T cells into the tumor, albeit alongside an increase in T-regs and likely immunosuppressive myeloid cells [177].

The exploration of ADT in combination with DNA vaccines presents another avenue for therapeutic advancement. Preclinical studies in murine models using the pTVG-AR DNA vaccine have demonstrated significant antitumor activity when combined with androgen deprivation therapy, possibly attributable to increased expression of the androgen receptor within prostate tumors following androgen deprivation [147]. Clinical trials evaluating this approach have shown that patients developing immunity to AR exhibit prolonged time to castration resistance, suggesting the potential benefits of DNA vaccines in combination with ADT. Moreover, the emergence of immune checkpoint blockade has revolutionized cancer immunotherapy, with notable targets including CTLA-4 and PD-1. While monotherapy trials in patients with metastatic castration-resistant prostate cancer (mCRPC) have shown limited efficacy, combination therapies targeting multiple checkpoints simultaneously have shown promise, albeit with increased toxicity. Furthermore, the addition of vaccination strategies may enhance the response to checkpoint blockade by activating or expanding tumor-associated T-cell populations [141]. Preclinical studies have demonstrated the potential of combining vaccination and immune checkpoint blockade in various models, highlighting synergistic effects and improved survival outcomes.

In conclusion, the intricate interplay between androgen deprivation therapy and the immune system offers promising opportunities for the development of novel therapeutic strategies in

prostate cancer. Combination approaches integrating ADT with vaccine-based therapies and immune checkpoint blockade represent a paradigm shift in the treatment landscape, offering the potential for enhanced antitumor immunity and improved clinical outcomes for patients with prostate cancer. Further research is warranted to elucidate optimal treatment regimens and refine therapeutic strategies to maximize efficacy while minimizing adverse effects.

1.4 Doctoral Thesis Objectives

The aims of the thesis are:

1. **To determine whether, and by what mechanism ADT in combination with Targeted Radionuclide therapy (TRT using 90Y-NM600) improves anti-tumor responses..**

a. Determine whether ADT in combination with TRT specifically using ^{90}Y-NM600 leads to better anti-tumor responses.
b. Determine whether the timing of ADT with respect to TRT using ^{90}Y-NM600 affects the tumor immune microenvironment.
c. Determine the mechanism underlying the dependence on the sequence of therapies in combination that leads to better anti-tumor responses.

2. **Determine the effects timing and sequencing of ADT in combination with AR-targeted DNA vaccination that leads to better anti-tumor responses in murine prostate tumor models.**

a. Determine whether the timing and sequencing of ADT and AR-specific vaccination affects the anti-tumor responses.
b. Determine whether AR-specific vaccination leads to antigen specific CD8+T cells.
c. Determine if intermittent schedules of ADT lead to reduction in MDSCs and therefore improve anti-tumor responses.

3. Determine whether and by what mechanisms ADT in combination with AR-targeted therapies and immune checkpoint blockade lead to enhanced anti-tumor responses in murine prostate models.

a. Determine the effect of different AR-targeted agents on the upregulation of AR expression in tumor cells in vitro.
b. Determine the effect of AR targeted agents on tumor cells that affect CD8+T cell recognition in vitro.
c. Determine the efficacy of AR degraders or AR antagonists in combination with AR-specific vaccination in vivo.
d. Determine the optimal AR targeted agent to combine with immune checkpoint blockade to enhance anti-tumor responses.

1.5 References

1. Siegel RL, Miller KD, Wagle NS, Jemal A. Cancer statistics, 2023. CA Cancer J Clin. 2023; 73: 17–48.

2. Zattoni F, Rajwa P, Gandaglia G. Optimal combination therapy for metastatic hormone-sensitive prostate cancer: new evidence, challenges, and unanswered questions. Curr Opin Urol. 2023; 33: 445–51.

3. Zhao J, Guercio BJ, Sahasrabudhe D. Current Trends in Chemotherapy in the Treatment of Metastatic Prostate Cancer. Cancers. 2023; 15: 3969.

4. Aurilio G, Cimadamore A, Santoni M, et al. New Frontiers in Prostate Cancer Treatment: Are We Ready for Drug Combinations with Novel Agents? Cells. 2020; 9: 1522.

5. Gardner TA, Elzey BD, Hahn NM. Sipuleucel-T (Provenge) autologous vaccine approved for treatment of men with asymptomatic or minimally symptomatic castrate-resistant metastatic prostate cancer. Hum Vaccin Immunother. 2012; 8: 534–9.

6. Visakorpi T, Hyytinen E, Koivisto P, et al. In vivo amplification of the androgen receptor gene and progression of human prostate cancer. Nat Genet. 1995; 9: 401–6.

7. Eisermann K, Wang D, Jing Y, Pascal LE, Wang Z. Androgen receptor gene mutation, rearrangement, polymorphism. Transl Androl Urol. 2013; 2: 137–47.

8. Cai C, He HH, Chen S, et al. Androgen Receptor Gene Expression in Prostate Cancer Is Directly Suppressed by the Androgen Receptor Through Recruitment of Lysine-Specific Demethylase 1. Cancer Cell. 2011; 20: 457–71.

9. Decker KF, Zheng D, He Y, Bowman T, Edwards JR, Jia L. Persistent androgen receptor-mediated transcription in castration-resistant prostate cancer under androgen-deprived conditions. Nucleic Acids Research. 2012; 40: 10765–79.

10. Brawley S, Mohan R, Nein CD. Localized Prostate Cancer: Treatment Options. afp. 2018; 97: 798–805.

11. Clinton TN, Woldu SL, Raj GV. Degarelix versus luteinizing hormone-releasing hormone agonists for the treatment of prostate cancer. Expert Opin Pharmacother. 2017; 18: 825–32.

12. Rice MA, Malhotra SV, Stoyanova T. Second-Generation Antiandrogens: From Discovery to Standard of Care in Castration Resistant Prostate Cancer. Front Oncol [Internet]. 2019 [cited 29 April 2024]; 9. Available at: https://www.frontiersin.org/journals/oncology/articles/10.3389/fonc.2019.00801/full

13. Gravis G, Boher J-M, Joly F, et al. Androgen Deprivation Therapy (ADT) Plus Docetaxel Versus ADT Alone in Metastatic Non castrate Prostate Cancer: Impact of Metastatic Burden and Long-term Survival Analysis of the Randomized Phase 3 GETUG-AFU15 Trial. European Urology. 2016; 70: 256–62.

14. Sathianathen NJ, Oestreich MC, Brown SJ, et al. Abiraterone acetate in combination with androgen deprivation therapy compared to androgen deprivation therapy only for metastatic hormone-sensitive prostate cancer. Cochrane Database of Systematic Reviews [Internet]. 2020 [cited 29 April 2024]; Available at: https://www.cochranelibrary.com/cdsr/doi/10.1002/14651858.CD013245.pub2/full

15. Shah S, Ryan C. Abiraterone acetate for castration resistant prostate cancer. Expert Opinion on Investigational Drugs. 2010; 19: 563–70.

16. Brown TR. Nonsteroidal Selective Androgen Receptors Modulators (SARMs): Designer Androgens with Flexible Structures Provide Clinical Promise. Endocrinology. 2004; 145: 5417–9.

17. Gao W, Kim J, Dalton JT. Pharmacokinetics and pharmacodynamics of nonsteroidal androgen receptor ligands. Pharm Res. 2006; 23: 1641–58.

18. Chen Y, Zhou Q, Hankey W, Fang X, Yuan F. Second generation androgen receptor antagonists and challenges in prostate cancer treatment. Cell Death Dis. 2022; 13: 1–11.

19. Tran C, Ouk S, Clegg NJ, et al. Development of a Second-Generation Antiandrogen for Treatment of Advanced Prostate Cancer. Science. 2009; 324: 787–90.

20. Antonarakis Emmanuel S., Lu Changxue, Wang Hao, et al. AR-V7 and Resistance to Enzalutamide and Abiraterone in Prostate Cancer. New England Journal of Medicine. 2014; 371: 1028–38.

21. Korpal M, Korn JM, Gao X, et al. An F876L Mutation in Androgen Receptor Confers Genetic and Phenotypic Resistance to MDV3100 (Enzalutamide). Cancer Discovery. 2013; 3: 1030–43.

22. Chen J, Li L, Yang Z, Luo J, Yeh S, Chang C. Androgen-deprivation therapy with enzalutamide enhances prostate cancer metastasis *via* decreasing the EPHB6 suppressor expression. Cancer Letters. 2017; 408: 155–63.

23. Yamashita S, Lai K-P, Chuang K-L, et al. ASC-J9 Suppresses Castration-Resistant Prostate Cancer Growth through Degradation of Full-length and Splice Variant Androgen Receptors. Neoplasia. 2012; 14: 74-IN12.

24. Wang R, Lin W, Lin C, Li L, Sun Y, Chang C. ASC-J9® suppresses castration resistant prostate cancer progression *via* degrading the enzalutamide-induced androgen receptor mutant AR-F876L. Cancer Letters. 2016; 379: 154–60.

25. Neklesa T, Snyder LB, Willard RR, et al. Abstract 5236: ARV-110: An androgen receptor PROTAC degrader for prostate cancer. Cancer Research. 2018; 78: 5236.

26. Gao X, Burris III HA, Vuky J, et al. Phase 1/2 study of ARV-110, an androgen receptor (AR) PROTAC degrader, in metastatic castration-resistant prostate cancer (mCRPC). JCO. 2022; 40: 17–17.

27. Durgeau A, Virk Y, Corgnac S, Mami-Chouaib F. Recent Advances in Targeting CD8 T-Cell Immunity for More Effective Cancer Immunotherapy. Front Immunol [Internet]. 2018 [cited 6 June 2021]; 9. Available at: https://www.ncbi.nlm.nih.gov/pmc/articles/PMC5786548/

28. Njar VCO, Brodie AMH. Discovery and Development of Galeterone (TOK-001 or VN/124-1) for the Treatment of All Stages of Prostate Cancer. J Med Chem. 2015; 58: 2077–87.

29. Yu Z, Cai C, Gao S, Simon NI, Shen HC, Balk SP. Galeterone Prevents Androgen Receptor Binding to Chromatin and Enhances Degradation of Mutant Androgen Receptor. Clinical Cancer Research. 2014; 20: 4075–85.

30. Taplin M-E, Antonarakis ES, Ferrante KJ, et al. Androgen Receptor Modulation Optimized for Response—Splice Variant: A Phase 3, Randomized Trial of Galeterone Versus Enzalutamide in Androgen Receptor Splice Variant-7–expressing Metastatic Castration-resistant Prostate Cancer. European Urology. 2019; 76: 843–51.

31. De Mol E, Fenwick RB, Phang CTW, et al. EPI-001, a compound active against castration-resistant prostate cancer, targets transactivation unit 5 of the androgen receptor. ACS Chem Biol. 2016; 11: 2499–505.

32. Myung J-K, Banuelos CA, Fernandez JG, et al. An androgen receptor N-terminal domain antagonist for treating prostate cancer. J Clin Invest. 2013; 123: 2948–60.

33. Ban F, Leblanc E, Cavga AD, et al. Development of an Androgen Receptor Inhibitor Targeting the N-Terminal Domain of Androgen Receptor for Treatment of Castration Resistant Prostate Cancer. Cancers (Basel). 2021; 13: 3488.

34. Walecki M, Eisel F, Klug J, et al. Androgen receptor modulates Foxp3 expression in CD4+CD25+Foxp3+ regulatory T-cells. MBoC. 2015; 26: 2845–57.

35. Flammiger A, Weisbach L, Huland H, et al. High tissue density of FOXP3+ T cells is associated with clinical outcome in prostate cancer. Eur J Cancer. 2013; 49: 1273–9.

36. Sutherland JS, Goldberg GL, Hammett MV, et al. Activation of Thymic Regeneration in Mice and Humans following Androgen Blockade. The Journal of Immunology. 2005; 175: 2741–53.

37. Morse MD, McNeel DG. T cells localized to the androgen-deprived prostate are TH1 and TH17 biased. The Prostate. 2012; 72: 1239–47.

38. Mercader M, Bodner BK, Moser MT, et al. T cell infiltration of the prostate induced by androgen withdrawal in patients with prostate cancer. Proceedings of the National Academy of Sciences. 2001; 98: 14565–70.

39. Tang S, Moore ML, Grayson JM, Dubey P. Increased CD8+ T-cell function following castration and immunization is countered by parallel expansion of regulatory T cells. Cancer Res. 2012; 72: 1975–85.

40. Olsen NJ, Kovacs WJ. Evidence that Androgens Modulate Human Thymic T Cell Output. Journal of Investigative Medicine. 2011; 59: 32–5.

41. Thompson IM, Tangen CM, Paradelo J, et al. Adjuvant Radiotherapy for Pathologically Advanced Prostate CancerA Randomized Clinical Trial. JAMA. 2006; 296: 2329–35.

42. Hamdy FC, Donovan JL, Lane JA, et al. 10-Year Outcomes after Monitoring, Surgery, or Radiotherapy for Localized Prostate Cancer. N Engl J Med. 2016; 375: 1415–24.

43. Bolla M, van Poppel H, Collette L, et al. Postoperative radiotherapy after radical prostatectomy: a randomised controlled trial (EORTC trial 22911). The Lancet. 2005; 366: 572–8.

44. Pollack A, Hanlon AL, Horwitz EM, et al. Dosimetry and preliminary acute toxicity in the first 100 men treated for prostate cancer on a randomized hypofractionation dose escalation trial. International Journal of Radiation Oncology*Biology*Physics. 2006; 64: 518–26.

45. Kupelian PA, Willoughby TR, Reddy CA, Klein EA, Mahadevan A. Hypofractionated Intensity-Modulated Radiotherapy (70 Gy at 2.5 Gy Per Fraction) for Localized Prostate Cancer: Cleveland Clinic Experience. International Journal of Radiation Oncology*Biology*Physics. 2007; 68: 1424–30.

46. Baskar R, Lee KA, Yeo R, Yeoh K-W. Cancer and Radiation Therapy: Current Advances and Future Directions. Int J Med Sci. 2012; 9: 193–9.

47. Michalski J, Winter K, Roach M, et al. Clinical Outcome of Patients Treated with 3D Conformal Radiation Therapy 3D-CRT for Prostate Cancer on RTOG 9406. Int J Radiat Oncol Biol Phys. 2012; 83: e363–70.

48. Dang A, Kupelian PA, Cao M, Agazaryan N, Kishan AU. Image-guided radiotherapy for prostate cancer. Transl Androl Urol. 2018; 7: 308–20.

49. Bakiu E, Telhaj E, Kozma E, Ruçi F, Malkaj P. Comparison of 3D CRT and IMRT Tratment Plans. Acta Inform Med. 2013; 21: 211–2.

50. Dearnaley D, Syndikus I, Mossop H, et al. Conventional versus hypofractionated high-dose intensity-modulated radiotherapy for prostate cancer: 5-year outcomes of the randomised, non-inferiority, phase 3 CHHiP trial. Lancet Oncol. 2016; 17: 1047–60.

51. Brower JV, Forman JD, Kupelian PA, et al. Quality of life outcomes from a dose-per-fraction escalation trial of hypofractionation in prostate cancer. Radiother Oncol. 2016; 118: 99–104.

52. Yeoh EE, Botten RJ, Butters J, Di Matteo AC, Holloway RH, Fowler J. Hypofractionated Versus Conventionally Fractionated Radiotherapy for Prostate Carcinoma: Final Results of Phase III Randomized Trial. International Journal of Radiation Oncology*Biology*Physics. 2011; 81: 1271–8.

53. Kalbasi A, Li J, Berman A, et al. Dose-Escalated Irradiation and Overall Survival in Men With Nonmetastatic Prostate Cancer. JAMA Oncol. 2015; 1: 897–906.

54. Anwar M, Weinberg V, Chang AJ, Hsu I-C, Roach M, Gottschalk A. Hypofractionated SBRT versus conventionally fractionated EBRT for prostate cancer: comparison of PSA slope and nadir. Radiation Oncology. 2014; 9: 42.

55. Boike TP, Lotan Y, Cho LC, et al. Phase I dose-escalation study of stereotactic body radiation therapy for low- and intermediate-risk prostate cancer. J Clin Oncol. 2011; 29: 2020–6.

56. Gómez-Aparicio MA, Valero J, Caballero B, et al. Extreme Hypofractionation with SBRT in Localized Prostate Cancer. Curr Oncol. 2021; 28: 2933–49.

57. Liu Y, Patel SA, Jani AB, et al. Overall Survival After Treatment of Localized Prostate Cancer With Proton Beam Therapy, External-Beam Photon Therapy, or Brachytherapy. Clin Genitourin Cancer. 2021; 19: 255-266.e7.

58. Bagshaw MA. Definitive Radiotherapy in Carcinoma of the Prostate. JAMA. 1969; 210: 326–7.

59. Whitmore WF, Hilaris B, Grabstald H. Retropubic implantation to iodine 125 in the treatment of prostatic cancer. J Urol. 1972; 108: 918–20.

60. Holm HH, Juul N, Pedersen JF, Hansen H, Strøyer I. Transperineal 125Iodine Seed Implantation in Prostatic Cancer Guided by Transrectal Ultrasonography. The Journal of Urology. 1983; 130: 283–6.

61. Stish BJ, Davis BJ, Mynderse LA, Deufel CL, Choo R. Brachytherapy in the Management of Prostate Cancer. Surg Oncol Clin N Am. 2017; 26: 491–513.

62. Wallner K, Merrick G, True L, Sutlief S, Cavanagh W, Butler W. 125I versus 103Pd for low-risk prostate cancer: preliminary PSA outcomes from a prospective randomized multicenter trial. International Journal of Radiation Oncology*Biology*Physics. 2003; 57: 1297–303.

63. Kent AR, Matheson B, Millar JL. Improved survival for patients with prostate cancer receiving high-dose-rate brachytherapy boost to EBRT compared with EBRT alone. Brachytherapy. 2019; 18: 313–21.

64. Grills IS, Martinez AA, Hollander M, et al. High dose rate brachytherapy as prostate cancer monotherapy reduces toxicity compared to low dose rate palladium seeds. J Urol. 2004; 171: 1098–104.

65. Hoskin PJ, Rojas AM, Bownes PJ, Lowe GJ, Ostler PJ, Bryant L. Randomised trial of external beam radiotherapy alone or combined with high-dose-rate brachytherapy boost for localised prostate cancer. Radiother Oncol. 2012; 103: 217–22.

66. Zaorsky NG, Doyle LA, Yamoah K, et al. High dose rate brachytherapy boost for prostate cancer: A systematic review. Cancer Treatment Reviews. 2014; 40: 414–25.

67. Kee DLC, Gal J, Falk AT, et al. Brachytherapy versus external beam radiotherapy boost for prostate cancer: Systematic review with meta-analysis of randomized trials. Cancer Treatment Reviews. 2018; 70: 265–71.

68. Weiner AB, Matulewicz RS, Eggener SE, Schaeffer EM. Increasing incidence of metastatic prostate cancer in the United States (2004-2013). Prostate Cancer Prostatic Dis. 2016; 19: 395–7.

69. Harris WP, Mostaghel EA, Nelson PS, Montgomery B. Androgen deprivation therapy: progress in understanding mechanisms of resistance and optimizing androgen depletion. Nat Clin Pract Urol. 2009; 6: 76–85.

70. Agarwal PK, Sadetsky N, Konety BR, Resnick MI, Carroll PR, Cancer of the Prostate Strategic Urological Research Endeavor (CaPSURE). Treatment failure after primary and salvage therapy for prostate cancer: likelihood, patterns of care, and outcomes. Cancer. 2008; 112: 307–14.

71. Ost P, Reynders D, Decaestecker K, et al. Surveillance or Metastasis-Directed Therapy for Oligometastatic Prostate Cancer Recurrence: A Prospective, Randomized, Multicenter Phase II Trial. JCO. 2018; 36: 446–53.

72. Rogowski P, Trapp C, von Bestenbostel R, et al. Outcomes of metastasis-directed therapy of bone oligometastatic prostate cancer. Radiat Oncol. 2021; 16: 125.

73. Reddy EK, Robinson RG, Mansfield CM. Strontium 89 for Palliation of Bone Metastases. J Natl Med Assoc. 1986; 78: 27–32.

74. Sartor O, Reid RH, Hoskin PJ, et al. Samarium-153-Lexidronam complex for treatment of painful bone metastases in hormone-refractory prostate cancer. Urology. 2004; 63: 940–5.

75. Hoskin P, Sartor O, O'Sullivan JM, et al. Efficacy and safety of radium-223 dichloride in patients with castration-resistant prostate cancer and symptomatic bone metastases, with or without previous docetaxel use: a prespecified subgroup analysis from the randomised, double-blind, phase 3 ALSYMPCA trial. The Lancet Oncology. 2014; 15: 1397–406.

76. Sartor O, Coleman R, Nilsson S, et al. Effect of radium-223 dichloride on symptomatic skeletal events in patients with castration-resistant prostate cancer and bone metastases: results from a phase 3, double-blind, randomised trial. The Lancet Oncology. 2014; 15: 738–46.

77. Schülke N, Varlamova OA, Donovan GP, et al. The homodimer of prostate-specific membrane antigen is a functional target for cancer therapy. Proceedings of the National Academy of Sciences. 2003; 100: 12590–5.

78. Nagda SN, Mohideen N, Lo SS, et al. Long-term follow-up of 111In-capromab pendetide (ProstaScint) scan as pretreatment assessment in patients who undergo salvage radiotherapy for rising prostate-specific antigen after radical prostatectomy for prostate cancer. International Journal of Radiation Oncology, Biology, Physics. 2007; 67: 834–40.

79. Nakajima T, Mitsunaga M, Bander NH, Heston WD, Choyke PL, Kobayashi H. Targeted, Activatable, IN VIVO Fluorescence Imaging of Prostate-specific Membrane Antigen (PSMA)-positive Tumors Using the Quenched Humanized J591 Antibody-ICG Conjugate. Bioconjug Chem. 2011; 22: 1700–5.

80. Bander NH, Trabulsi EJ, Kostakoglu L, et al. Targeting Metastatic Prostate Cancer With Radiolabeled Monoclonal Antibody J591 to the Extracellular Domain of Prostate Specific Membrane Antigen. The Journal of Urology. 2003; 170: 1717–21.

81. Bander NH, Milowsky MI, Nanus DM, Kostakoglu L, Vallabhajosula S, Goldsmith SJ. Phase I Trial of ^{177} Lutetium-Labeled J591, a Monoclonal Antibody to Prostate-Specific

Membrane Antigen, in Patients With Androgen-Independent Prostate Cancer. JCO. 2005; 23: 4591–601.

82. Tagawa ST, Milowsky MI, Morris M, et al. Phase II study of Lutetium-177-labeled anti-prostate-specific membrane antigen monoclonal antibody J591 for metastatic castration-resistant prostate cancer. Clin Cancer Res. 2013; 19: 5182–91.

83. In vitro and preclinical targeted alpha therapy of human prostate cancer with Bi-213 labeled J591 antibody against the prostate specific membrane antigen | Prostate Cancer and Prostatic Diseases [Internet]. [cited 19 November 2022]. Available at: https://www.nature.com/articles/4500543

84. McDevitt MR, Barendswaard E, Ma D, et al. An α-Particle Emitting Antibody ([213Bi]J591) for Radioimmunotherapy of Prostate Cancer1. Cancer Research. 2000; 60: 6095–100.

85. Sathekge M, Knoesen O, Meckel M, Modiselle M, Vorster M, Marx S. 213Bi-PSMA-617 targeted alpha-radionuclide therapy in metastatic castration-resistant prostate cancer. Eur J Nucl Med Mol Imaging. 2017; 44: 1099–100.

86. Kratochwil C, Schmidt K, Afshar-Oromieh A, et al. Targeted alpha therapy of mCRPC: Dosimetry estimate of 213Bismuth-PSMA-617. Eur J Nucl Med Mol Imaging. 2018; 45: 31–7.

87. Afshar-Oromieh A, Hetzheim H, Kratochwil C, et al. The Theranostic PSMA Ligand PSMA-617 in the Diagnosis of Prostate Cancer by PET/CT: Biodistribution in Humans, Radiation Dosimetry, and First Evaluation of Tumor Lesions. Journal of Nuclear Medicine. 2015; 56: 1697–705.

88. Lim EA, Schweizer MT, Chi KN, et al. Safety and preliminary clinical activity of JNJ-63898081 (JNJ-081), a PSMA and CD3 bispecific antibody, for the treatment of metastatic castrate-resistant prostate cancer (mCRPC). JCO. 2022; 40: 279–279.

89. Ruigrok EAM, van Vliet N, Dalm SU, et al. Extensive preclinical evaluation of lutetium-177-labeled PSMA-specific tracers for prostate cancer radionuclide therapy. Eur J Nucl Med Mol Imaging. 2021; 48: 1339–50.

90. Hofman MS, Violet J, Hicks RJ, et al. [177Lu]-PSMA-617 radionuclide treatment in patients with metastatic castration-resistant prostate cancer (LuPSMA trial): a single-centre, single-arm, phase 2 study. The Lancet Oncology. 2018; 19: 825–33.

91. Dosimetry of 177Lu-PSMA-617 in Metastatic Castration-Resistant Prostate Cancer: Correlations Between Pretherapeutic Imaging and Whole-Body Tumor Dosimetry with

Treatment Outcomes | Journal of Nuclear Medicine [Internet]. [cited 30 September 2022]. Available at: https://jnm.snmjournals.org/content/60/4/517.short

92. Sartor O, de Bono J, Chi KN, et al. Lutetium-177–PSMA-617 for Metastatic Castration-Resistant Prostate Cancer. N Engl J Med. 2021; 385: 1091–103.

93. Kratochwil C, Bruchertseifer F, Giesel FL, et al. ^{225} Ac-PSMA-617 for PSMA-Targeted α-Radiation Therapy of Metastatic Castration-Resistant Prostate Cancer. J Nucl Med. 2016; 57: 1941–4.

94. Sathekge M, Bruchertseifer F, Lawal I, et al. Treatment of brain metastases of castration-resistant prostate cancer with 225Ac-PSMA-617. European Journal of Nuclear Medicine and Molecular Imaging. 2019; 46.

95. Kratochwil C, Bruchertseifer F, Rathke H, et al. Targeted Alpha Therapy of mCRPC with 225Actinium-PSMA-617: Dosimetry estimate and empirical dose finding. Journal of Nuclear Medicine [Internet]. 2017 [cited 19 November 2022]; Available at: https://jnm.snmjournals.org/content/early/2017/04/12/jnumed.117.191395

96. Feuerecker B, Tauber R, Knorr K, et al. Activity and Adverse Events of Actinium-225-PSMA-617 in Advanced Metastatic Castration-resistant Prostate Cancer After Failure of Lutetium-177-PSMA. European Urology. 2021; 79: 343–50.

97. Ma J, Li L, Liao T, Gong W, Zhang C. Efficacy and Safety of 225Ac-PSMA-617-Targeted Alpha Therapy in Metastatic Castration-Resistant Prostate Cancer: A Systematic Review and Meta-Analysis. Frontiers in Oncology [Internet]. 2022 [cited 14 December 2022]; 12. Available at: https://www.frontiersin.org/articles/10.3389/fonc.2022.796657

98. Hernandez R, Walker KL, Grudzinski JJ, et al. 90 Y-NM600 targeted radionuclide therapy induces immunologic memory in syngeneic models of T-cell Non-Hodgkin's Lymphoma. Commun Biol. 2019; 2: 1–12.

99. Patel RB, Hernandez R, Carlson P, et al. Low-dose targeted radionuclide therapy renders immunologically cold tumors responsive to immune checkpoint blockade. Sci Transl Med. 2021; 13: eabb3631.

100. Potluri HK, Ferreira CA, Grudzinski J, et al. Antitumor efficacy of 90Y-NM600 targeted radionuclide therapy and PD-1 blockade is limited by regulatory T cells in murine prostate tumors. J Immunother Cancer. 2022; 10: e005060.

101. Chakraborty M, Abrams SI, Camphausen K, et al. Irradiation of Tumor Cells Up-Regulates Fas and Enhances CTL Lytic Activity and CTL Adoptive Immunotherapy. J Immunol. 2003; 170: 6338–47.

102. Klein B, Loven D, Lurie H, et al. The effect of irradiation on expression of HLA class I antigens in human brain tumors in culture. Journal of Neurosurgery. 1994; 80: 1074–7.

103. Gupta A, Probst HC, Vuong V, et al. Radiotherapy Promotes Tumor-Specific Effector CD8 $^{+}$ T Cells via Dendritic Cell Activation. JI. 2012; 189: 558–66.

104. Lee Y, Auh SL, Wang Y, et al. Therapeutic effects of ablative radiation on local tumor require CD8+ T cells: changing strategies for cancer treatment. Blood. 2009; 114: 589–95.

105. Lomax ME, Folkes LK, O'Neill P. Biological Consequences of Radiation-induced DNA Damage: Relevance to Radiotherapy. Clinical Oncology. 2013; 25: 578–85.

106. Golden EB, Frances D, Pellicciotta I, Demaria S, Helen Barcellos-Hoff M, Formenti SC. Radiation fosters dose-dependent and chemotherapy-induced immunogenic cell death. OncoImmunology. 2014; 3: e28518.

107. Nikitina EYu, Gabrilovich DI. Combination of γ-irradiation and dendritic cell administration induces a potent antitumor response in tumor-bearing mice: Approach to treatment of advanced stage cancer. International Journal of Cancer. 2001; 94: 825–33.

108. Slone HB, Peters LJ, Milas L. Effect of Host Immune Capability on Radiocurability and Subsequent Transplantability of a Murine Fibrosarcoma2. JNCI: Journal of the National Cancer Institute. 1979; 63: 1229–35.

109. Ganss R, Ryschich E, Klar E, Arnold B, Hammerling GJ. Combination of T-Cell Therapy and Trigger of Inflammation Induces Remodeling of the Vasculature and Tumor Eradication. Cancer Research. 2002; 62: 1462–70.

110. Zhang T, Yu H, Ni C, et al. Hypofractionated stereotactic radiation therapy activates the peripheral immune response in operable stage I non-small-cell lung cancer. Sci Rep. 2017; 7: 4866.

111. Nakamura N, Kusunoki Y, Akiyama M. Radiosensitivity of CD4 or CD8 Positive Human T-Lymphocytes by an in Vitro Colony Formation Assay. Radiation Research. 1990; 123: 224–7.

112. Arina A, Beckett M, Fernandez C, et al. Tumor-reprogrammed resident T cells resist radiation to control tumors. Nat Commun. 2019; 10: 3959.

113. Dovedi SJ, Cheadle EJ, Popple AL, et al. Fractionated Radiation Therapy Stimulates Antitumor Immunity Mediated by Both Resident and Infiltrating Polyclonal T-cell Populations when Combined with PD-1 Blockade. Clin Cancer Res. 2017; 23: 5514–26.

114. Finkel P, Frey B, Mayer F, et al. The dual role of NK cells in antitumor reactions triggered by ionizing radiation in combination with hyperthermia. Oncoimmunology. 2016; 5: e1101206.

115. Lee H-R, Son C-H, Koh E-K, et al. Expansion of cytotoxic natural killer cells using irradiated autologous peripheral blood mononuclear cells and anti-CD16 antibody. Sci Rep. 2017; 7: 11075.

116. Xu J, Escamilla J, Mok S, et al. CSF1R Signaling Blockade Stanches Tumor-Infiltrating Myeloid Cells and Improves the Efficacy of Radiotherapy in Prostate Cancer. Cancer Research. 2013; 73: 2782–94.

117. Muroyama Y, Nirschl TR, Kochel CM, et al. Stereotactic Radiotherapy Increases Functionally Suppressive Regulatory T Cells in the Tumor Microenvironment. Cancer Immunology Research. 2017; 5: 992–1004.

118. Shi X, Shiao SL. The Role of Macrophage Phenotype in Regulating the Response to Radiation Therapy. Transl Res. 2018; 191: 64–80.

119. Jones E, Pu H, Kyprianou N. Targeting TGF-beta in prostate cancer: therapeutic possibilities during tumor progression. Expert Opin Ther Targets. 2009; 13: 227–34.

120. Jiao S, Subudhi SK, Aparicio A, et al. Differences in Tumor Microenvironment Dictate T Helper Lineage Polarization and Response to Immune Checkpoint Therapy. Cell. 2019; 179: 1177-1190.e13.

121. Deng L, Liang H, Burnette B, et al. Irradiation and anti–PD-L1 treatment synergistically promote antitumor immunity in mice [Internet]. American Society for Clinical Investigation; 2014 [cited 1 October 2022]. Available at: https://www.jci.org/articles/view/67313/pdf

122. Soanes WA, Ablin RJ, Gonder MJ. Remission of metastatic lesions following cryosurgery in prostatic cancer: immunologic considerations. J Urol. 1970; 104: 154–9.

123. Ablin RJ, Soanes WA, Gonder MJ. Elution of in vivo bound antiprostatic epithelial antibodies following multiple cryotherapy of carcinoma of prostate. Urology. 1973; 2: 276–9.

124. Cell Genesys. A Phase III Randomized, Open-Label Study of Docetaxel in Combination With CG1940 and CG8711 Versus Docetaxel and Prednisone in Taxane-Naïve Patients With Metastatic Hormone-Refractory Prostate Cancer With Pain [Internet]. clinicaltrials.gov; 2008 Sep [cited 21 November 2022]. Report No.: NCT00133224. Available at: https://clinicaltrials.gov/ct2/show/NCT00133224

125. Vuky J, Corman JM, Porter C, Olgac S, Auerbach E, Dahl K. Phase II trial of neoadjuvant docetaxel and CG1940/CG8711 followed by radical prostatectomy in patients with high-risk clinically localized prostate cancer. Oncologist. 2013; 18: 687–8.

126. Gulley JL, Borre M, Vogelzang NJ, et al. Phase III Trial of PROSTVAC in Asymptomatic or Minimally Symptomatic Metastatic Castration-Resistant Prostate Cancer. J Clin Oncol. 2019; 37: 1051–61.

127. Noguchi M, Fujimoto K, Arai G, et al. A randomized phase III trial of personalized peptide vaccination for castration-resistant prostate cancer progressing after docetaxel. Oncol Rep. 2021; 45: 159–68.

128. Kantoff PW, Higano CS, Shore ND, et al. Sipuleucel-T immunotherapy for castration-resistant prostate cancer. N Engl J Med. 2010; 363: 411–22.

129. Deegen P, Thomas O, Nolan-Stevaux O, et al. The PSMA-targeting Half-life Extended BiTE Therapy AMG 160 has Potent Antitumor Activity in Preclinical Models of Metastatic Castration-resistant Prostate Cancer. Clinical Cancer Research. 2021; 27: 2928–37.

130. Hummel H-D, Kufer P, Grüllich C, et al. Pasotuxizumab, a BiTE® immune therapy for castration-resistant prostate cancer: Phase I, dose-escalation study findings. Immunotherapy. 2021; 13: 125–41.

131. Brusa D, Simone M, Gontero P, et al. Circulating immunosuppressive cells of prostate cancer patients before and after radical prostatectomy: Profile comparison. International Journal of Urology. 2013; 20: 971–8.

132. Tuomela K, Ambrose AR, Davis DM. Escaping Death: How Cancer Cells and Infected Cells Resist Cell-Mediated Cytotoxicity. Frontiers in Immunology [Internet]. 2022 [cited 22 November 2022]; 13. Available at: https://www.frontiersin.org/articles/10.3389/fimmu.2022.867098

133. Koinis F, Xagara A, Chantzara E, Leontopoulou V, Aidarinis C, Kotsakis A. Myeloid-Derived Suppressor Cells in Prostate Cancer: Present Knowledge and Future Perspectives. Cells. 2021; 11: 20.

134. Miller AM, Ozenci V, Kiessling R, Pisa P. Immune monitoring in a phase 1 trial of a PSA DNA vaccine in patients with hormone-refractory prostate cancer. J Immunother. 2005; 28: 389–95.

135. Eriksson F, Tötterman T, Maltais A-K, Pisa P, Yachnin J. DNA vaccine coding for the rhesus prostate specific antigen delivered by intradermal electroporation in patients with relapsed prostate cancer. Vaccine. 2013; 31: 3843–8.

136. McNeel DG, Dunphy EJ, Davies JG, et al. Safety and Immunological Efficacy of a DNA Vaccine Encoding Prostatic Acid Phosphatase in Patients With Stage D0 Prostate Cancer. J Clin Oncol. 2009; 27: 4047–54.

137. McNeel DG, Becker JT, Eickhoff JC, et al. Real-Time Immune Monitoring to Guide Plasmid DNA Vaccination Schedule Targeting Prostatic Acid Phosphatase in Patients with Castration-Resistant Prostate Cancer. Clinical Cancer Research. 2014; 20: 3692–704.

138. McNeel DG, Eickhoff JC, Johnson LE, et al. Phase II Trial of a DNA Vaccine Encoding Prostatic Acid Phosphatase (pTVG-HP [MVI-816]) in Patients With Progressive, Nonmetastatic, Castration-Sensitive Prostate Cancer. J Clin Oncol. 2019; 37: 3507–17.

139. Wargowski E, Johnson LE, Eickhoff JC, et al. Prime-boost vaccination targeting prostatic acid phosphatase (PAP) in patients with metastatic castration-resistant prostate cancer (mCRPC) using Sipuleucel-T and a DNA vaccine. J Immunother Cancer. 2018; 6: 21.

140. Zahm CD, Moseman JE, Delmastro LE, G. Mcneel D. PD-1 and LAG-3 blockade improve anti-tumor vaccine efficacy. Oncoimmunology. 10: 1912892.

141. McNeel DG, Eickhoff JC, Wargowski E, et al. Concurrent, but not sequential, PD-1 blockade with a DNA vaccine elicits anti-tumor responses in patients with metastatic, castration-resistant prostate cancer. Oncotarget. 2018; 9: 25586–96.

142. McNeel DG, Eickhoff JC, Wargowski E, et al. Phase 2 trial of T-cell activation using MVI-816 and pembrolizumab in patients with metastatic, castration-resistant prostate cancer (mCRPC). J Immunother Cancer. 2022; 10: e004198.

143. McNeel DG, Emamekhoo H, Eickhoff JC, et al. Phase 2 trial of a DNA vaccine (pTVG-HP) and nivolumab in patients with castration-sensitive non-metastatic (M0) prostate cancer. J Immunother Cancer. 2023; 11: e008067.

144. Chudley L, McCann K, Mander A, et al. DNA fusion-gene vaccination in patients with prostate cancer induces high-frequency CD8(+) T-cell responses and increases PSA doubling time. Cancer Immunol Immunother. 2012; 61: 2161–70.

145. Weber JS, Vogelzang NJ, Ernstoff MS, et al. A Phase 1 Study of a Vaccine Targeting Preferentially Expressed Antigen in Melanoma and Prostate-specific Membrane Antigen in Patients With Advanced Solid Tumors. J Immunother. 2011; 34: 556–67.

146. Shore ND, Morrow MP, McMullan T, et al. CD8+ T Cells Impact Rising PSA in Biochemically Relapsed Cancer Patients Using Immunotherapy Targeting Tumor-Associated Antigens. Mol Ther. 2020; 28: 1238–50.

147. Olson BM, Gamat M, Seliski J, et al. Prostate Cancer Cells Express More Androgen Receptor (AR) Following Androgen Deprivation, Improving Recognition by AR-Specific T Cells. Cancer Immunol Res. 2017; 5: 1074–85.

148. Kyriakopoulos CE, Eickhoff JC, Ferrari AC, et al. Multicenter Phase 1 Trial of a DNA Vaccine Encoding the Androgen Receptor Ligand Binding Domain (pTVG-AR, MVI-118) in Patients with Metastatic Prostate Cancer. Clin Cancer Res. 2020; 26: 5162–71.

149. Alexandrov LB, Nik-Zainal S, Wedge DC, et al. Signatures of mutational processes in human cancer. Nature. 2013; 500: 415–21.

150. Ott PA, Hu Z, Keskin DB, et al. An immunogenic personal neoantigen vaccine for patients with melanoma. Nature. 2017; 547: 217–21.

151. Study Details | Neoantigen DNA Vaccine in Combination With Nivolumab/Ipilimumab and PROSTVAC in Metastatic Hormone-Sensitive Prostate Cancer | ClinicalTrials.gov [Internet]. [cited 22 May 2024]. Available at: https://clinicaltrials.gov/study/NCT03532217

152. Cho H, Binder J, Weeratna R, et al. Preclinical development of a vaccine-based immunotherapy regimen (VBIR) that induces potent and durable T cell responses to tumor-associated self-antigens. Cancer Immunol Immunother. 2023; 72: 287–300.

153. First-in-human, phase I study of PF-06753512, a vaccine-based immunotherapy regimen (PrCa VBIR), in biochemical relapse (BCR) and metastatic castration-resistant prostate cancer (mCRPC). | Journal of Clinical Oncology [Internet]. [cited 22 May 2024]. Available at: https://ascopubs.org/doi/10.1200/JCO.2021.39.15_suppl.2612

154. Kwon ED, Drake CG, Scher HI, et al. Ipilimumab versus placebo after radiotherapy in patients with metastatic castration-resistant prostate cancer that had progressed after docetaxel chemotherapy (CA184-043): a multicentre, randomised, double-blind, phase 3 trial. Lancet Oncol. 2014; 15: 700–12.

155. Beer TM, Kwon ED, Drake CG, et al. Randomized, Double-Blind, Phase III Trial of Ipilimumab Versus Placebo in Asymptomatic or Minimally Symptomatic Patients With Metastatic Chemotherapy-Naive Castration-Resistant Prostate Cancer. J Clin Oncol. 2017; 35: 40–7.

156. Petrylak DP, Loriot Y, Shaffer DR, et al. Safety and Clinical Activity of Atezolizumab in Patients with Metastatic Castration-Resistant Prostate Cancer: A Phase I Study. Clin Cancer Res. 2021; 27: 3360–9.

157. Antonarakis ES, Piulats JM, Gross-Goupil M, et al. Pembrolizumab for Treatment-Refractory Metastatic Castration-Resistant Prostate Cancer: Multicohort, Open-Label Phase II KEYNOTE-199 Study. J Clin Oncol. 2020; 38: 395–405.

158. Sharma P, Pachynski RK, Narayan V, et al. Nivolumab Plus Ipilimumab for Metastatic Castration-Resistant Prostate Cancer: Preliminary Analysis of Patients in the CheckMate 650 Trial. Cancer Cell. 2020; 38: 489-499.e3.

159. Powles T, Yuen KC, Gillessen S, et al. Atezolizumab with enzalutamide versus enzalutamide alone in metastatic castration-resistant prostate cancer: a randomized phase 3 trial. Nat Med. 2022; 28: 144–53.

160. van den Eertwegh AJM, Versluis J, van den Berg HP, et al. Combined immunotherapy with granulocyte-macrophage colony-stimulating factor-transduced allogeneic prostate cancer cells and ipilimumab in patients with metastatic castration-resistant prostate cancer: a phase 1 dose-escalation trial. Lancet Oncol. 2012; 13: 509–17.

161. Coulter JB, Song DY, DeWeese TL, Yegnasubramanian S. Mechanisms, Challenges, and Opportunities in Combined Radiation and Hormonal Therapies. Seminars in Radiation Oncology. 2022; 32: 76–81.

162. Polkinghorn WR, Parker JS, Lee MX, et al. Androgen receptor signaling regulates DNA repair in prostate cancers. Cancer Discov. 2013; 3: 1245–53.

163. Sekhar KR, Wang J, Freeman ML, Kirschner AN. Radiosensitization by enzalutamide for human prostate cancer is mediated through the DNA damage repair pathway. PLOS ONE. 2019; 14: e0214670.

164. Dal Pra A, Cury FL, Souhami L. Combining radiation therapy and androgen deprivation for localized prostate cancer—a critical review. Curr Oncol. 2010; 17: 28–38.

165. Wang C, Zhang Y, Gao W-Q. The evolving role of immune cells in prostate cancer. Cancer Letters. 2022; 525: 9–21.

166. Long X, Hou H, Wang X, et al. Immune signature driven by ADT-induced immune microenvironment remodeling in prostate cancer is correlated with recurrence-free survival and immune infiltration. Cell Death Dis. 2020; 11: 779.

167. Qin C, Wang J, Du Y, Xu T. Immunosuppressive environment in response to androgen deprivation treatment in prostate cancer. Front Endocrinol (Lausanne). 2022; 13: 1055826.

168. Roden AC, Moser MT, Tri SD, et al. Augmentation of T cell levels and responses induced by androgen deprivation. J Immunol. 2004; 173: 6098–108.

169. Gamat M, McNeel DG. Androgen deprivation and immunotherapy for the treatment of prostate cancer. Endocr Relat Cancer. 2017; 24: T297–310.

170. Lopez-Bujanda ZA, Haffner MC, Chaimowitz MG, et al. Castration-mediated IL-8 Promotes Myeloid Infiltration and Prostate Cancer Progression [Internet]. Immunology; 2019 May [cited 12 February 2021]. Available at: http://biorxiv.org/lookup/doi/10.1101/651083

171. Lee Y, Auh SL, Wang Y, et al. Therapeutic effects of ablative radiation on local tumor require CD8+ T cells: changing strategies for cancer treatment. Blood. 2009; 114: 589–95.

172. Demaria S, Bhardwaj N, McBride WH, Formenti SC. Combining radiotherapy and immunotherapy: a revived partnership. Int J Radiat Oncol Biol Phys. 2005; 63: 655–66.

173. Kalina J, Neilson D, Comber A, et al. Immune Modulation by Androgen Deprivation and Radiation Therapy: Implications for Prostate Cancer Immunotherapy. Cancers. 2017; 9: 13.

174. Gamat-Huber M, McNeel DG. Androgen deprivation as a tumour-immunomodulating treatment. Nat Rev Urol. 2020; 17: 371–2.

175. Sfanos KS, Bruno TC, Maris CH, et al. Phenotypic Analysis of Prostate-Infiltrating Lymphocytes Reveals TH17 and Treg Skewing. Clinical Cancer Research. 2008; 14: 3254–61.

176. Madan RA, Arlen PM, Mohebtash M, Hodge JW, Gulley JL. Prostvac-VF: a vector-based vaccine targeting PSA in prostate cancer. Expert Opin Investig Drugs. 2009; 18: 1001–11.

177. Obradovic A, Dallos MC, Zahurak ML, et al. T-Cell Infiltration and Adaptive Treg Resistance in Response to Androgen Deprivation With or Without Vaccination in Localized Prostate Cancer. Clin Cancer Res. 2020; 26: 3182–92.

Chapter 2

Myeloid Derived Suppressor Cells Attenuate the Antitumor Efficacy of Radiopharmaceutical Therapy Using 90Y-NM600 in Combination with Androgen Deprivation Therapy in Murine Prostate Tumors

This work is published in the Journal for ImmunoTherapy of Cancer.

Muralidhar A, Hernandez R, Morris ZS*, et al*
Myeloid-derived suppressor cells attenuate the antitumor efficacy of radiopharmaceutical therapy using ^{90}Y-NM600 in combination with androgen deprivation therapy in murine prostate tumors
Journal for ImmunoTherapy of Cancer 2024;**12:**e008760. doi: 10.1136/jitc-2023-008760

2.1Abstract

Rationale: Androgen deprivation therapy (ADT) is pivotal in treating recurrent prostate cancer and is often combined with external beam radiation therapy (EBRT) for localized disease. However, for metastatic castration-resistant prostate cancer (mCRPC), EBRT is typically only used in the palliative setting, because of the inability to radiate all sites of disease. Systemic radiation treatments that preferentially irradiate cancer cells, known as radiopharmaceutical therapy or targeted radionuclide therapy (TRT), have demonstrable benefit for treating metastatic prostate cancer. Here, we explored the use of a novel TRT, ^{90}Y-NM600, specifically in combination with ADT, in murine prostate tumor models.

Methods: 6-week-old male FVB mice were implanted subcutaneously with Myc-CaP tumor cells and given a single intravenous injection of ^{90}Y-NM600, in combination with ADT (degarelix). The combination and sequence of administration was evaluated for effect on tumor growth and infiltrating immune populations were analyzed by flow cytometry. Sera were assessed to determine treatment effects on cytokine profiles.

Results: ADT delivered prior to TRT (ADT→TRT) resulted in a significantly greater anti-tumor response and overall survival than if delivered after TRT (TRT→ADT). Studies conducted in immunodeficient NRG mice failed to show a difference in treatment sequence, suggesting an immunological mechanism. MDSCs significantly accumulated in tumors following TRT→ADT treatment and retained immune suppressive function. However, CD4+ and CD8+T cells with an activated and memory phenotype were more prevalent in the ADT→TRT group. Depletion of Gr1+ MDSCs led to greater anti-tumor response following either treatment sequence. Chemotaxis assays suggested that tumor cells secreted chemokines that recruited MDSCs, notably CXCL1 and

CXCL2. Use of a selective CXCR2 antagonist, reparixin, further improved anti-tumor responses and overall survival when used in tumor-bearing mice treated with TRT→ADT.

Conclusion: The combination of ADT and TRT improved anti-tumor responses in murine models of prostate cancer, however this was dependent on the order of administration. This was found to be associated with one treatment sequence leading to an increase in infiltrating MDSCs. Combining treatment with a CXCR2 antagonist improved the anti-tumor effect of this combination, suggesting a possible approach for treating advanced human prostate cancer.

2.2 Introduction

Radiation therapy (RT) has been one of the mainstay treatments for prostate cancer. External beam radiation therapy (EBRT) can be curative for localized prostate cancer but has traditionally been limited to palliation for widely metastatic disease due to the inability to radiate all sites of metastasis [1]. Systemic administration of radionuclides that are preferentially taken up in bone has been used to treat painful bone metastases. These radionuclides include beta-emitting ^{89}Sr and ^{153}Sm, and FDA-approved alpha-emitting $^{223}RaCl_2$ (Xofigo) for the treatment of metastatic castration resistant prostate cancer (mCRPC) with bone metastases [2–4]. This approach, utilizing targeted radionuclides to treat all metastatic diseases simultaneously, with relative sparing of healthy tissue, is called radiopharmaceutical therapy or targeted radionuclide therapy (TRT).

While these TRT agents have been useful for patients with disease metastasized exclusively to the bone, they are not effective for those with other disease sites. Hence, other investigations have focused on compounds that specifically target cancer cells rather than the bone. One of the most studied targets for prostate tumor-directed radiation delivery is prostate-specific membrane antigen (PSMA) which is highly expressed on prostate cancer cells. Early attempts used ^{177}Lu or ^{90}Y conjugated to an antibody specific for PSMA (J591), which was well tolerated and promising in early clinical trials [5,6]. Further efforts focused on the development of small molecules such as [^{18}F]DCFPyL and PSMA-11, which have both been utilized in PET/CT diagnostic imaging [7,8]. Another PSMA analog, PSMA-617, has also been labeled with radionuclides suitable for therapy (e.g., ^{177}Lu, ^{225}Ac) of recurrent prostate cancer [9]. ^{177}Lu-PSMA-617 was the first cancer-targeted TRT agent that received FDA approval for the treatment of mCRPC on the basis of it

demonstrating a survival benefit compared to standard of care androgen receptor-targeted therapy, albeit by only 4 months [10].

While androgen deprivation therapy (ADT) and RT are standard treatments for localized prostate cancer, there has been relatively limited exploration of ADT combined specifically with TRT [11]. Apart from their independent cytotoxic effects, there is evidence to suggest that ADT synergistically works with RT by preventing DNA repair [12,13]. However, the order in which ADT and TRT are best administered has not been rigorously studied [14]. Recent data indicates that RT and ADT can distinctly influence the tumor immune microenvironment [15]. ADT enhances vulnerability to CD8+ T cell-mediated destruction, triggers thymus regeneration, amplifies naive T cell production, augments immune cell infiltration from myeloid and lymphocyte populations, and elevates antibody responses against prostate-specific antigens [16–20]. However, ADT also triggers a significant secretion of IL-8 in human prostate tumors, which can lead to the accumulation of intratumoral myeloid-derived suppressor cells (MDSCs), which may impede T-cell activity [21]. Conversely, RT elicits inflammatory responses, including the upregulation of MHC-I expression on tumor cells, enhancement of antigen cross-presentation by antigen-presenting cells, activation of the Fas/Fas ligand (Fas-L) signaling pathway, targeting of immune-suppressive populations like regulatory T cells (Tregs), and the induction of immunogenic cell death [22,23]. In combination, ADT and RT can synergistically enhance tumor immunity, modulating both local and systemic anti-tumor immune responses [24]. Therefore, investigating effective strategies for their combination, including considerations such as the timing and sequence of ADT with RT, as well as the integration of newer systemic TRT agents, is crucial.

Our group has employed alkylphosphocholines (APCs) as TRT agents given that they have the ability to specifically accumulate within tumor cells by integrating into lipid rafts [25]. First

generation ^{131}I-NM404 is currently under investigation as a potential monotherapy treatment for metastatic multiple myeloma and other cancer types [26–28]. We have recently focused on the assessment of a second-generation APC chelate, called NM600, which can be tagged with different radiometals. By employing the radiometal ^{86}Y, one can visualize tumors and perform dosimetry measurements by PET/CT imaging [29]. Alternatively, through labeling with the isotopic pair, ^{90}Y, one can administer therapeutic radiation [30,31]. This innovative approach, utilizing Y-NM600 for both imaging and therapy, has demonstrated success in numerous preclinical models [29,30,32]. However, its applicability to prostate cancer used in conjunction with ADT has not been previously investigated.

In this report, we explored the combination of TRT using ^{90}Y-NM600 with ADT in murine prostate models and specifically examined the effects of this combination on the tumor immune microenvironment. Our findings revealed that the effectiveness of this combination was influenced by the order of administration. ADT followed by TRT (ADT→TRT) showed superior enhancement of anti-tumor responses compared to the reverse sequence of TRT followed by ADT (TRT→ADT). We demonstrated that this disparity was due, in part, to the presence of infiltrating MDSCs, which impaired the function of CD8+ T cells. Furthermore, we showed that the efficacy of anti-tumor responses could be improved by inhibiting the migration of MDSCs *in vivo* using a CXCR2 antagonist. These findings underscore the significance of understanding the mechanisms through which ADT and TRT influence the tumor microenvironment, enabling the optimal timing and choice of combination therapies for prostate cancer.

2.3 Results

2.3.1 Combination of ADT and TRT with ADT prior to TRT (ADT→ TRT) significantly improved anti-tumor responses in murine prostate tumor models.

We studied the effects of ^{90}Y-NM600 in combination with ADT in two separate murine prostate tumor models, Myc-CaP and TRAMP-C1. As depicted in Figure 1A, MyC-CaP tumor cells were implanted subcutaneously in male FVB mice, and when tumors reached a volume of 0.2-0.3cm^3 they were treated with degarelix. TRT (250μCi ~ 9.25MBq of ^{90}Y- NM600, delivering ~16Gy) was given one week before or after degarelix. When ADT was delivered prior to TRT (ADT→TRT) there was a significant tumor growth delay (Figure 1B and Figure 2A) and improved overall survival (Figure 1C). Because ADT and TRT can have different effects depending on the day they are administered relative to tumor volume, in a second study, ADT was again used before or after TRT, but this time fixing the day on which TRT was administered (Figure 1D). As before, the ADT→TRT combination significantly delayed tumor growth (Figure 1E and Figure 2B) and improved overall survival (Figure 1F) compared to the monotherapies or TRT→ADT combination. ADT→TRT also significantly improved anti-tumor responses and overall survival in a prostate tumor model in which TRAMP-C1 tumor cells were implanted in C57BL/6 mice (Figures 1G, 1H, 1I and Figure 2C). However, there was no evidence of improved treatment response or overall survival when Myc-CaP cells were implanted in NRG mice lacking functional T cells (Figures 1J, 1K and 1L and Figure 2D). Overall, these findings demonstrated that ADT and TRT had a stronger anti-tumor effect in combination and was dependent on the order of administration, with ADT→TRT leading to superior anti-tumor responses, and this was likely immune cell dependent.

2.3.2 CD4+ T and CD8+ T cells persisted in the tumor microenvironment in the ADT→TRT sequence whereas significant increases in MDSCs were observed in the TRT→ADT sequence.

We next sought to understand the effect of sequencing of these treatments on the tumor immune microenvironment. A similar study was performed as in Figure 1D, but tumors were collected at several time points following treatment for evaluation of immune cell compositions via flow cytometry, as shown in Figure 3A. Representative flow plots for T cells and MDSCs are shown in Figure 3B (and gating strategy shown in Appendix). We found that CD4+T and CD8+T cells persisted in the tumor microenvironment until day 32 in the ADT→TRT treated mice (Figures 3C and 3D) compared to the TRT→ADT treated mice (Figures 3E and 3F, and Supplemental Figure 4). Increases in MDSCs were not observed in ADT→TRT mice until day 39, and there were no significant changes in regulatory CD4+ T cells following treatment (Figures 3G and 3H). Notably, MDSCs were significantly increased in the TRT→ADT group immediately after TRT treatment and this increase was further accentuated with the subsequent administration of ADT (Figure 3I), whereas there were no significant changes in regulatory CD4+ T cells (Figure 3J). Taken together, these data suggested that the balance of CD4+ T cells, CD8+ T cells and MDSC affected by these treatments might have contributed to the preferred treatment sequence.

2.3.3 ADT→TRT led to persistence of activated and memory CD8+ T cells while these were significantly reduced in the TRT→ADT group.

A similar study was performed to further characterize CD8+ T cells (Figure 4A) with the gating strategy shown in Appendix. Tumor-infiltrating CD8+ T cells from mice treated in the ADT→TRT sequence were found to have increased proliferation (Ki67+) and activation (CD69) (Figures 4B and 4C) compared to the TRT→ADT treatment sequence (Figures 4D and 4E). Notably, memory CD8+ T cells in the ADT→TRT sequence persisted, including effector and resident memory populations (Figures 4F, 4G, 4J and 4K). Conversely, the TRT→ADT sequence led to a significant reduction in memory CD8+ T cells, notably effector and resident memory populations (Figures 4H, 4I, 4L and 4M). In summary, these findings indicate that the ADT→TRT treatment sequence facilitated the sustained presence of activated and memory CD8+ T cells, whereas these populations were substantially diminished in mice initially treated with TRT.

2.3.4 T cell depletion reduces the anti-tumor efficacy of the combination of ADT and TRT.

We next sought to understand if T cells were required in mediating differences in anti-tumor responses by depleting these populations immediately after ADT or TRT (Figure 5A). In the ADT→TRT group, depleting CD4+T or CD8+T cells resulted in a slightly accelerated tumor growth, although the difference was not statistically significant. However, in the TRT→ADT group, CD8+ T cell depletion led to significantly more rapid tumor growth (Figure 5B and Figure 6). Regardless of the combination sequence, depletion of T cells worsened survival (Figure 5C).

2.3.5 MDSC depletion significantly improved anti-tumor responses and increased infiltration of CD4+ and CD8+ T cells into prostate tumors.

We next wished to determine whether tumor infiltrating MDSCs that were present following TRT were functionally immunosuppressive. MDSC were obtained from mice treated with TRT with or without ADT and evaluated for their effects on CD8+ T cell proliferation (Figure 7A). We found that MDSCs obtained from tumors of mice treated with TRT alone had a slight suppressive effect on CD8+ T cell proliferation, however MDSCs from mice subjected to the TRT→ADT treatment markedly suppressed CD8+ T cell proliferation (Figure 7B). MDSC from mice treated with either TRT alone or TRT→ADT similarly suppressed IFNγ secretion from CD8+ T cells stimulated with anti-CD3/anti-CD28 beads (Figure 7C). These data demonstrate that MDSCs infiltrating tumors in mice treated with TRT were still functionally active. We next used clodronate liposomes or anti-Gr1 antibody to deplete these myeloid populations in mice treated with TRT→ADT (Figure 7D). Either of these treatments resulted in significantly greater tumor control compared to control mice (Figure 7E and Figure 8). These treatments led to a significant decrease in tumor-infiltrating MDSCs (Figure 7F), as well as slight increases in tumor-infiltrating CD4+ (Figure 7G) and CD8+ (Figure 7H) T cells.

2.3.6 Cytokines and chemokines secreted by tumor cells promote MDSC infiltration into tumors.

We next explored the potential mechanism of tumor infiltration by MDSCs by investigating the effects of the combination treatments on the cytokines and chemokines present in the sera

following these different treatments (Figure 9A). As shown in Figure 9B-F, CXCL1, CXCL2 and CCL5, all chemokines associated with myeloid cell migration, were significantly increased in sera of mice treated with the TRT→ADT sequence relative to the ADT→TRT sequence. To determine which cell types may be involved in MDSC recruitment, a chemotaxis assay was performed using tumor cells, T cells, or the combination, in testosterone-replete or testosterone-deficient medium (Figure 9G). As shown in Figure 9H, tumor cells primarily contributed to MDSC migration. The presence of T cells slightly reduced the migration of MDSC. Similar differences were observed using testosterone replete or testosterone-deficient media containing ^{90}Y (Figure 11A and Figure 12). CXCL1 and CXCL2 were increased significantly in Myc-CaP conditioned media (Figures 9I and 9J) while CCL2, CCL3, CCL5 were increased in conditioned media containing Myc-CaP and T cells (Figures 9K-M). No significant changes were observed in other chemokines and cytokines (Figures 10 and 11B).

2.3.7 CXCR2 blockade improves antitumor efficacy in the TRT→ADT combination.

Because tumor cells appeared primarily responsible for MDSC recruitment, and MDSC recruitment was inhibited in the presence of T cells, this suggested that CXCL1 and CXCL2 produced by tumor cells may be the dominant chemokines involved in MDSC recruitment. Consequently, we next tested if CXCL1 directly contributed to MDSC migration *in vitro*, and whether this might be affected by blockade of the CXCL1/CXCL2 receptor, CXCR2 (Figure 13A). As demonstrated in Figure 13B, we observed that MDSCs exhibited a migratory response toward supernatants containing CXCL1, and this response was significantly reduced when CXCR2 was blocked using reparixin. We next wanted to determine whether blocking CXCR2 could improve

the anti-tumor response of the TRT→ADT treatment sequence (Figure 13C). As demonstrated in Figure 13D (and Figure 14), mice treated with reparixin showed improved anti-tumor responses. Tumors from these mice exhibited a significant reduction in MDSCs (Figure 13E), a slight increase in CD4+ T cells (Figure 13F), and a significant increase in CD8+ T cells (Figure 13G). Similar improved anti-tumor responses were found in mice treated with ADT→TRT and reparixin (Figure 15).

2.4 Discussion

Following the approval of ^{177}Lu-PSMA-617, there has been a growing interest in the utilization of TRT for the treatment of prostate cancer, either as a standalone therapy or in combination with other treatments. However, there is currently a lack of preclinical data that can provide insights into how TRT affects immune cell populations within tumors and how it can be optimally integrated with other immunomodulatory treatments. This report is the first combining TRT using ^{90}Y-NM600 with ADT in immune competent murine prostate tumor models, with an emphasis on investigating the effects of immune modulation and the critical aspects of timing and sequence in this combination therapy approach. Our primary findings can be summarized as follows: 1) Administering ADT→TRT yielded significant advantages compared to the reverse sequence, as demonstrated by both a delayed time to tumor growth and improved overall survival; 2) ADT→TRT was associated with the sustained presence of activated and memory CD8+ T cells within the tumor microenvironment; 3) TRT→ADT group exhibited increased infiltration of MDSCs that were functionally active in suppressing CD8+ T cell function; and 4) inhibiting CXCR2, the receptor for CXCL1 and CXCL2, effectively inhibited the migration of MDSCs and improved the anti-tumor response with TRT→ADT. The observed outcomes highlight the crucial role of the administration sequence of ADT and TRT on modulating the tumor immune microenvironment, thereby influencing therapeutic responses. Moreover, the identification of molecular targets, exemplified by CXCR2 blockade, offers mechanistic insights to guide novel approaches aimed at enhancing treatment outcomes.

The combination of ADT and RT is a standard treatment regimen for localized prostate cancer, supported by evidence from trials such as reported by Bolla, which demonstrated improved

survival for patients with high risk prostate cancer treated with radiation therapy and androgen deprivation compared to radiation therapy alone [37]. Despite the established efficacy of this combined approach, a lingering controversy surrounds the optimal timing and sequence for administering ADT and RT. Individual trials have suggested a similar advantage in progression-free survival using ADT prior to and concurrent (neoadjuvant ADT) with external beam radiation therapy (EBRT), rather than concurrent and following EBRT (adjuvant ADT), such as the Radiation Therapy Oncology Group (RTOG) 94134 trial [38]. A more recent similar trial, however, showed no difference in outcome between these similar approaches [39]. A pooled meta-analysis of 12 randomized trials, however, found that concurrent/adjuvant ADT was associated with improved metastasis-free survival and overall survival compared to patients receiving neoadjuvant/concurrent ADT, at least for patients receiving prostate-only EBRT, compared to patients who received larger field radiation therapy [40]. The time frames of treatment over days in our study to treatment over the course of months in these clinical trials is certainly different and may account for differences in sequence preference. Notwithstanding, the potential impacts of ADT and EBRT on the tumor immune microenvironment has been underappreciated as a potential mechanism for differences observed in clinical trials, particularly since differences were observed if regional lymph nodes were included in the radiation fields.

The investigation into the combined effects of ADT and RT has primarily focused on potential synergies arising from direct cytotoxic effects and the induction of increased DNA damage [41]. However, what remains significantly underexplored is the interplay of these therapies with immune cells within the tumor microenvironment. There is a general consensus that tumor-infiltrating lymphocytes (TILs) have a role in detecting and eradicating tumor cells, and their

presence is linked to improved patient outcomes [42]. More specifically, CD8+T cells correlated with enhanced 5 year-overall survival in patients undergoing radical prostatectomy (98% vs. 91%, $p = 0.01$) and prostate cancer-specific survival (99% vs. 95%, $p = 0.04$) compared to individuals exhibiting low CD8+ TIL density [43]. Our studies substantiate this observation, demonstrating that enhanced overall survival is associated with increased CD8+ T cells in the ADT→TRT sequence. Interestingly, while the use of TRT clearly led to a decrease in tumor-infiltrating T cells in either treatment sequence, as expected since T cells are relatively sensitive to radiation, there were still more tumor-infiltrating T cells when ADT was used prior to TRT. Others have demonstrated that ADT alone can lead to an increase in tumor-infiltrating CD4+ and CD8+ T cells [16,44]. We expect this is due to release of chemokines recruiting T cells following ADT. Conceivably, the use of TRT, in addition to depleting tissue-resident T cells, may have also disrupted the release of these chemokines, leading to this observed difference due to treatment sequence. This will be an area for future studies.

Clinical data indicate that the accumulation of MDSCs in the bloodstream of patients with advanced prostate cancer, and an intra-tumoral myeloid signature, are linked to unfavorable outcomes [45]. Various strategies have been investigated to target MDSCs, encompassing efforts to deplete MDSCs, hinder their function by inhibiting immunosuppressive mediators, and induce their maturation to stimulate differentiation [46]. Efforts to therapeutically target myeloid cells broadly have thus far failed clinically, potentially due to myeloid cell heterogeneity and complexity. Targeting the recruitment of MDSCs has been explored through the inhibition of various chemokines and chemokine receptors, such as the use of CSF-1R antibody, but these approaches have demonstrated limited success in clinical trials [47,48]. Currently, IL-8, which

interacts with the CXCR2 receptor typically secreted by prostate cancer cells, is undergoing testing in a phase Ib/II clinical trial (NCT03689699). It is important to note that IL-8 is naturally absent in mice, suggesting that mice rely on alternative chemokines, notably CXCL1 and CXCL2, to facilitate MDSC recruitment [21,49]. Recent studies have shown that CXCL1 can influence the differentiation and function of MDSCs by promoting the expansion of MDSCs in the tumor microenvironment, contributing to immune suppression and facilitating tumor progression [50]. In addition, CXCL1 can also enhance the suppressive activity of MDSCs, further exacerbating their immunosuppressive effects. Therefore, targeting CXCR2 and its effects on MDSCs may represent a promising therapeutic approach for cancer and other inflammatory diseases [51]. Clinical trials evaluating the efficacy of reparixin, either alone or in combination with other treatments, have been initiated in patients with metastatic breast cancer [52]. In addition to its effects on MDSCs, reparixin also has anti-inflammatory properties and can modulate the function of other immune cells, such as neutrophils and macrophages [53,54]. Thus, selectively blocking chemokine activity emerges as an attractive therapeutic strategy to increase tumor cell sensitivity to immune-modulating treatments. The CXCR2 inhibitor navarixin, which has been utilized in clinical trials for chronic obstructive pulmonary diseases with established safety and toxicity profiles [55], is now also under evaluation in a clinical trial (NCT03473925) for its efficacy in treating advanced prostate cancer.

In conclusion, our study advances the understanding of the interplay between ADT, TRT, and the immune microenvironment in prostate cancer. The sequence-dependent effects on immune populations and treatment resistance emphasize the need for meticulous optimization of treatment timing and sequencing. Tailoring treatment strategies to harness these immunological dynamics

represents a promising avenue for further improving therapeutic outcomes in advanced prostate cancer. We anticipate that the exploration of TRT combined with ADT, as well as other immune modulating agents, will remain an active focus in both preclinical and clinical investigations for prostate cancer, notably given the relatively recent approval of ^{177}Lu-PSMA-617 and the evaluation of other TRT agents for advanced prostate cancer. In future studies we plan to specifically evaluate ^{177}Lu-PSMA-617 in murine models of prostate cancer that express PSMA, to determine if there is a similar sequence-dependent effect on immune populations when that agent is used in combination with ADT. In addition, the use of immune checkpoint inhibitors is actively being pursued in combination with TRT (e.g. NCT03805594, NCT03658447). Based on our results presented here, future studies should also evaluate the additional use of ADT in combination with immune checkpoint inhibition and TRT.

2.5 Figures

Figure 1: Combination of ADT and TRT with ADT prior to TRT (ADT→TRT) significantly improved anti-tumor responses in murine prostate tumor models. FVB mice were implanted with Myc-CaP tumor cells and treated with degarelix (ADT), with TRT delivered before or after ADT, and followed for tumor growth (n=10 per group). Shown is a schema (panel A), tumor growth curves (panel B), and Kaplan-Meier curves depicting survival (time to a tumor size of $2cm^3$ or death, panel C). A similar study fixed the day of TRT with ADT delivered before or after (n=10 per group). Shown is the schema (panel D), tumor growth curves (panel E), and Kaplan-Meier survival curves (time to tumor size of $2cm^3$ or death, panel F). Similarly, male C57BL/6 were implanted with TRAMP-C1 tumor cells (n=5 per group) and treated with ADT delivered before or after TRT. Shown is the schema (panel G), tumor growth curves (panel H), and Kaplan-Meier survival curves (time to tumor size of $2cm^3$ or death, panel I). In addition, Myc-CaP tumor cells were implanted in male NRG T-cell deficient mice, treated with ADT and/or TRT as before (n=10 per group), and followed for tumor growth (schema in panel J). Shown are the tumor growth curves (panel K) and Kaplan-Meier survival curves (panel L). For tumor growth curves, asterisks demonstrate significant (*$p < 0.05$, **$p<0.01$ **$p<0.001$) differences as assessed by linear mixed effects model with Geisser-Greenhouse correction and Tukey's multiple comparisons test with individual variances; Kaplan-Meier curves were compared using the log-rank test with asterisks indicating *$p<0.05$, **$p<0.01$, and ***$p<0.001$. Results are from one experiment and are representative of two independent experiments for each study (Supplemental Figure 2).

.

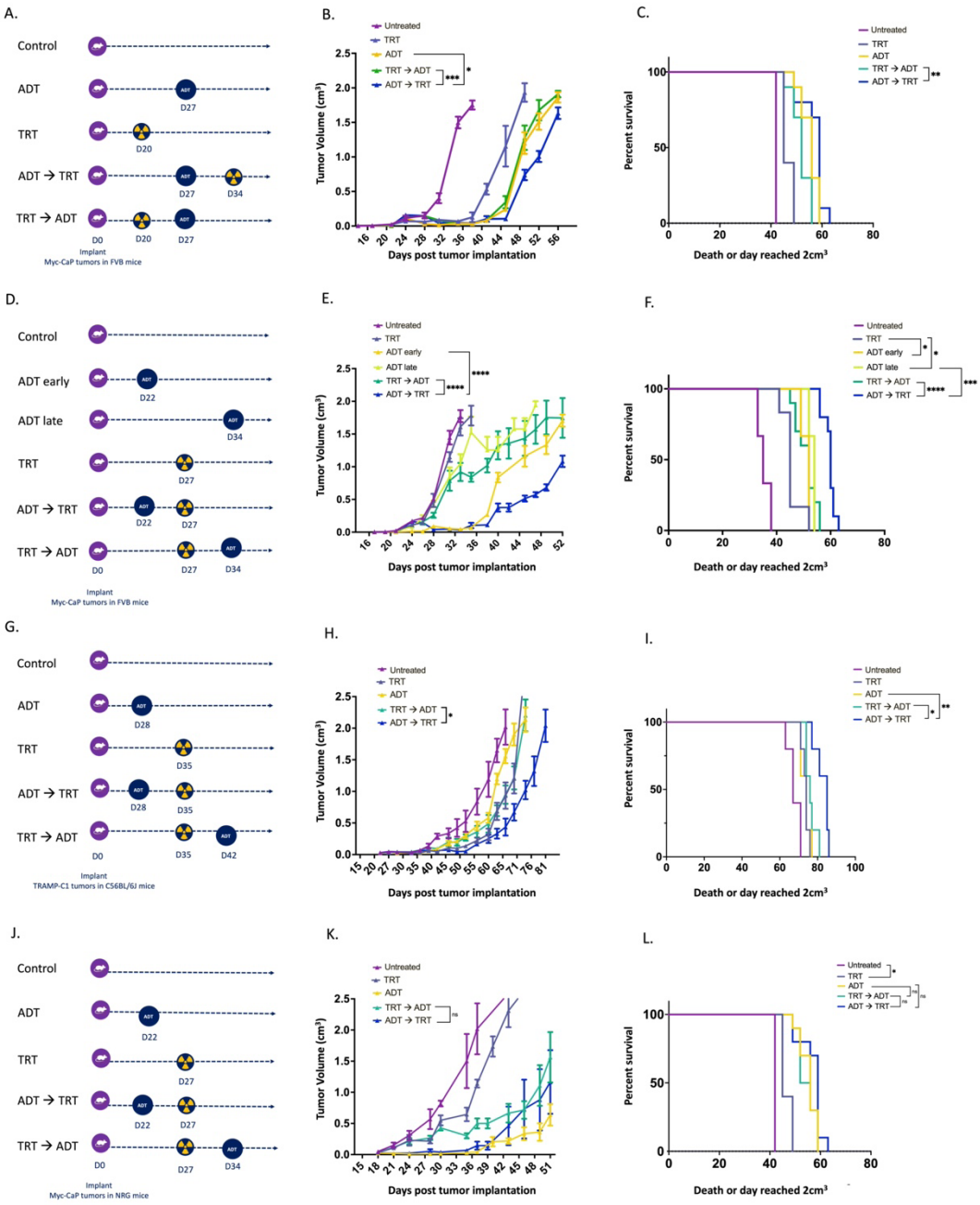

Figure 1: Combination of ADT and TRT with ADT prior to TRT (ADT→TRT) significantly improved anti-tumor responses in murine prostate tumor models.

Figure 2: Combination of vaccination and ADT and TRT, with ADT prior to TRT (ADT→TRT), significantly improved anti-tumor responses. (A) Individual tumor growth curves from experiment shown in Figure 1B (n=5 in the untreated and TRT groups, n=10 in the ADT, TRT→ ADT, ADT→ TRT groups). (B) Individual tumor growth curves from experiment shown in Figure 1E (n=3 in the untreated and ADT early group, n=6 in the TRT, ADT late groups) and n=10 in the ADT→ TRT and TRT → ADT groups). (C) Individual tumor growth curves from experiment shown in Figure 1H (n=5 per group). (D) Individual tumor growth curves from experiment shown in Figure 1K (n=3 in the untreated, TRT and ADT groups and n=10 in the combination groups).

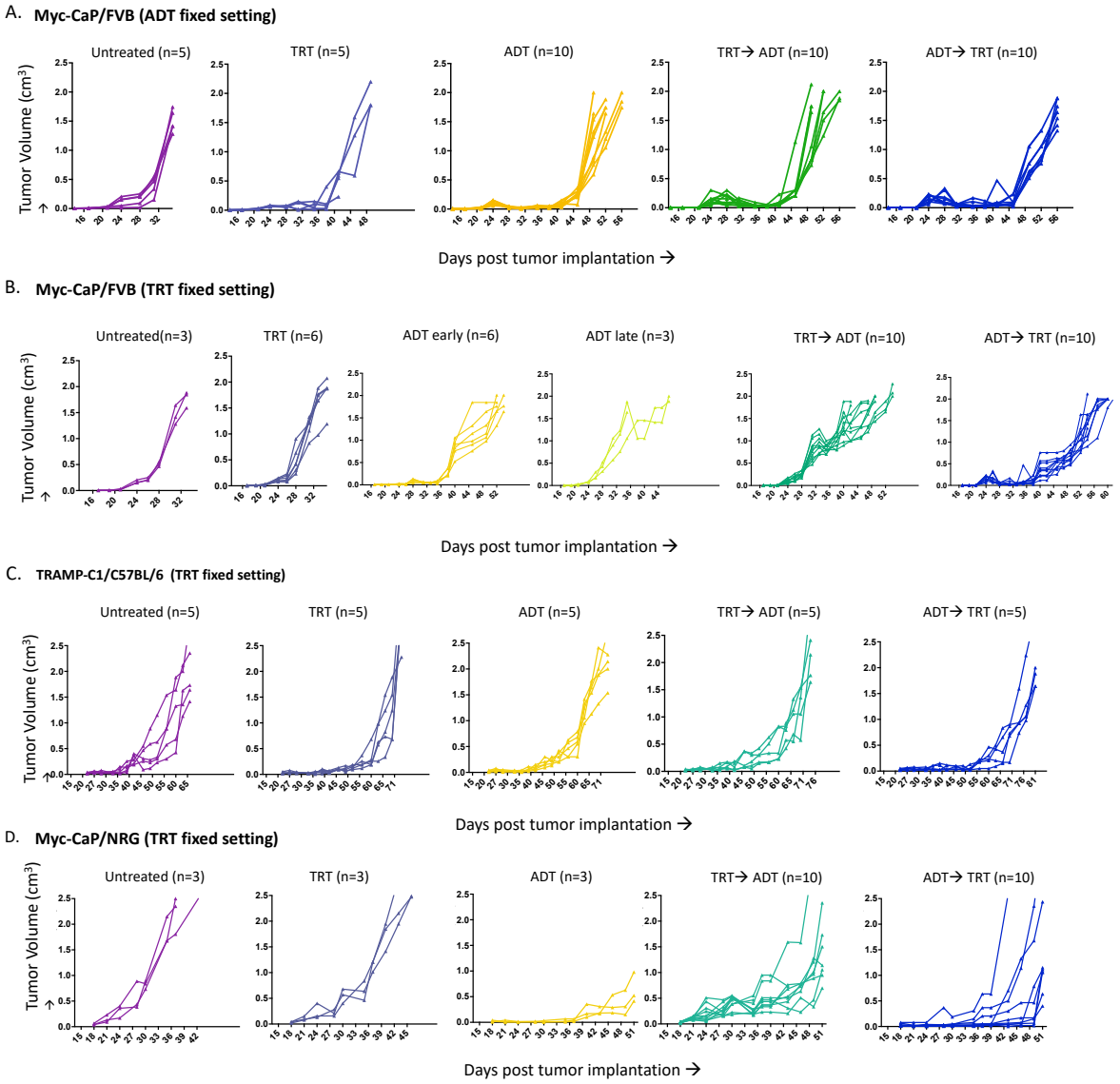

Figure 2: Combination of vaccination and ADT and TRT, with ADT prior to TRT (ADT→ TRT), significantly improved anti-tumor responses.

Figure 3: CD4+ T and CD8+ T cells persist in the tumor microenvironment in the ADT→TRT sequence combination whereas significant increases in MDSCs were observed in the TRT→ADT sequence. Myc-CaP tumor cells were implanted in male FVB mice and treated with ADT and/or TRT, with tumors sampled at different days for flow cytometry analysis (n=6 per group per time point). Shown are a schema (panel A) and representative dot plots (panel B) of CD4+CD3+ and CD8+CD3+ T cells and CD11b+Gr1+ MDSCs in ADT→TRT (left panels) and TRT→ADT groups (right panels) collected on day 32. CD4+ T cells (panels C and E), CD8+ T cells (panels D and F), and CD11b+Gr-1+ MDSC (panels G and I) are shown as a percentage of CD45+ cells. CD4+FoxP3+ Treg (panels H and J) are shown as a percentage of CD4+ cells. Panels C-J were compared using one-way ANOVA with Tukey's multiple comparisons test asterisks indicating *$p<0.05$, **$p<0.01$, and ***$p<0.001$. Results are from one experiment and are representative of two independent experiments (Supplemental Figure 4).

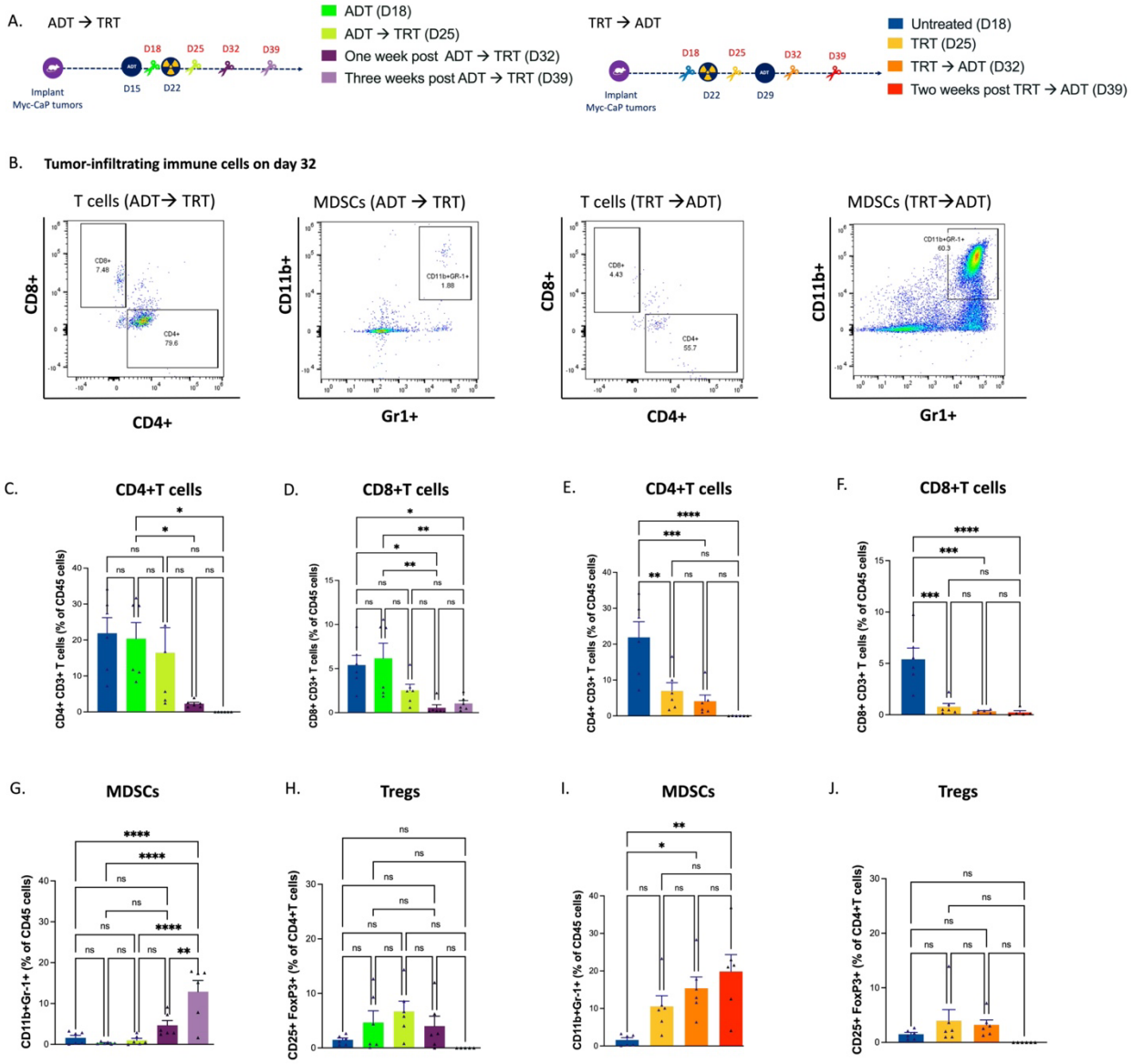

Figure 3: CD4+ T and CD8+ T cells persist in the tumor microenvironment in the ADT→TRT sequence combination whereas significant increases in MDSCs were observed in the TRT→ ADT sequence.

Figure 4: ADT→TRT led to persistence of activated and memory CD8+ T cells while these were significantly reduced in the TRT→ADT group. Myc-CaP tumor cells were implanted in male FVB mice, treated with ADT and/or TRT as before, and tumors were sampled at different days (n=5 per group per time point) for flow cytometry analysis of CD8+CD3+ cells (schema in panel A). Untreated CD8+ T cells were collected from animals on day 18. Left panels indicate data from ADT→TRT treated animals, and right panels indicate data from TRT→ADT treated animals. Data indicate number of each population per gram of tumor for Ki67+CD8+CD3+ T cells (panels B and D), CD69 MFI on CD8+T cells (panels C and E), CD44+ memory CD8+ T cells (panels F and H), CD44+CD27+CD62L+ central memory CD8+ T cells (panels G and I), CD44+CD27-CD62L- effector memory CD8+ T cells (panels J and L), and CD69+CD103+ resident memory CD8+ T cells (panels K and M). Comparisons were made using one-way ANOVA with Tukey's multiple comparisons test asterisks indicating *$p<0.05$, **$p<0.01$, and ***$p<0.001$. Results are from one experiment and are representative of two independent experiments.

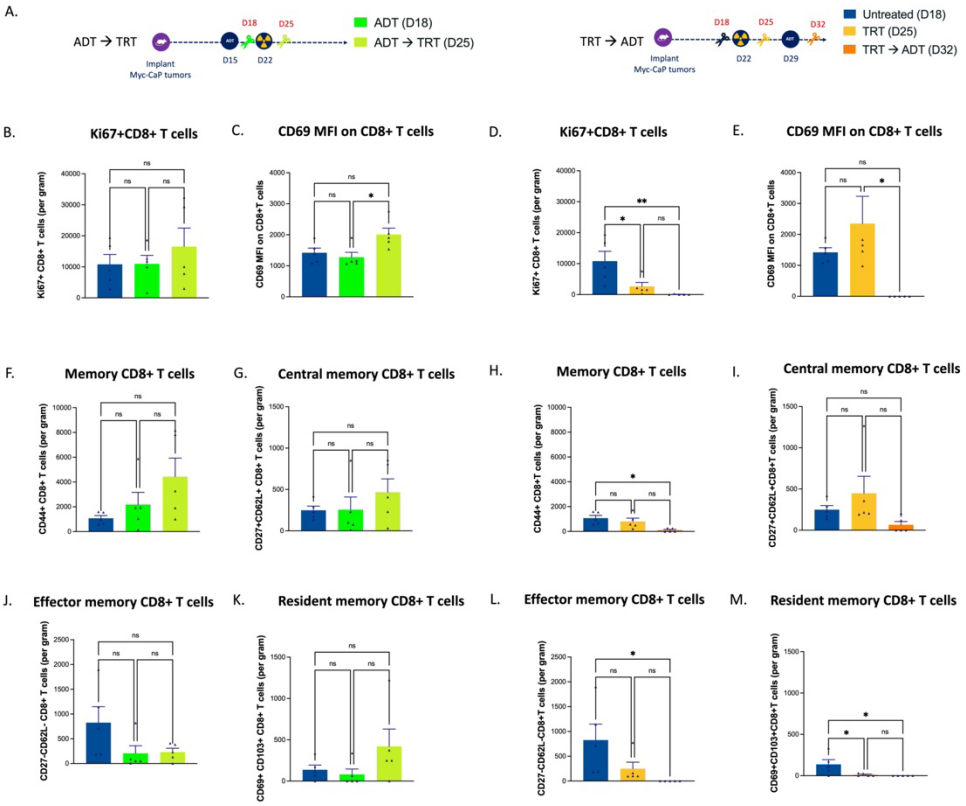

Figure 4: ADT→TRT led to persistence of activated and memory CD8+ T cells while these were significantly reduced in the TRT→ADT group.

Figure 5: The anti-tumor efficacy of the combination of ADT and TRT worsened in the absence of T cells. Myc-CaP tumor cells were implanted in male FVB mice, treated with ADT and/or TRT as before, and mice received IgG, anti-CD4 or anti-CD8 depleting antibodies between these treatments (schema in panel A). Shown are the tumor growth curves (panel B) and Kaplan-Meier survival curves (panel C). For tumor growth curves, comparisons were made by linear mixed effects model with Geisser-Greenhouse correction and Tukey's multiple comparisons test with individual variance; Kaplan-Meier curves were compared using the log-rank test. Asterisks demonstrate significant differences (*$p<0.05$, **$p<0.01$, and ***$p<0.001$). Results shown are each from one experiment (n=7 per group).

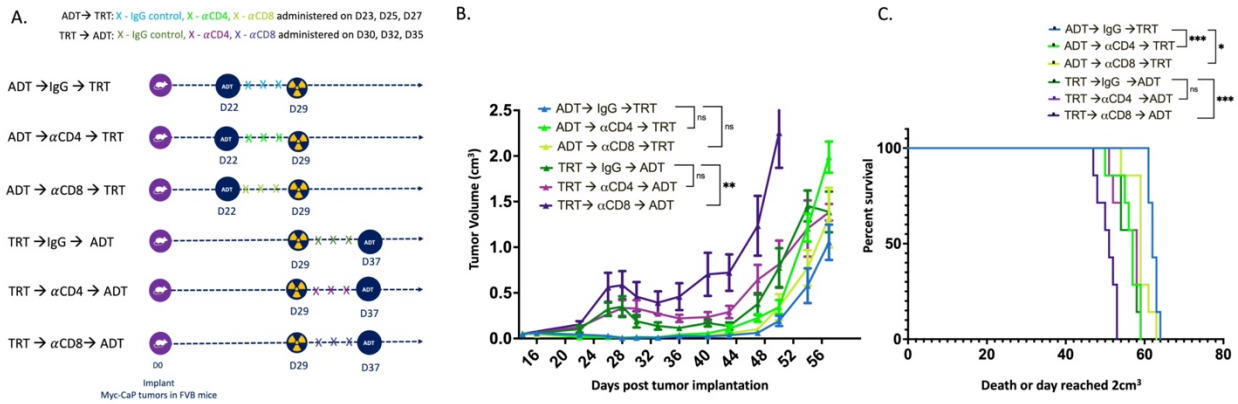

Figure 5: The anti-tumor efficacy of the combination of ADT and TRT worsened in the absence of T cells.

Figure 6: **Anti-tumor efficacy of the combination of ADT and TRT worsens in the absence of T cells.** Individual tumor growth curves from experiment shown in Figure 4B. Results are from one experiment and are representative of two independent experiments (n=7 per group).

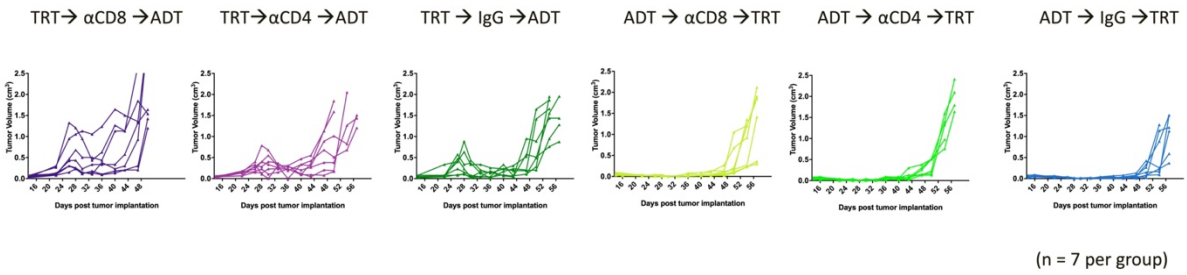

Figure 6: Anti-tumor efficacy of the combination of ADT and TRT worsens in the absence of T cells.

Figure 7: Depletion of MDSCs significantly improved anti-tumor responses and increased infiltration of CD4+ and CD8+ T cells into prostate tumors. CD11b+Gr-1+ MDSC were collected from Myc-CaP tumor-bearing mice that had been treated with TRT alone or TRT→ADT. MDSC were co-cultured with naïve, CFSE-labeled CD8+T cells and stimulated with anti-CD3/anti-CD28 beads (schema in panel A). After 72 hours, flow cytometry was conducted to evaluate CD8+ T cell proliferation by loss of CFSE (panel B), and culture supernatants were evaluated for IFNγ concentration (panel C). Myc-CaP tumor cells were implanted in male FVB mice, treated with TRT→ADT as before, and mice received control liposomes, clodronate liposomes, (n=7 per group) or anti-Gr-1 antibody (n=3) as indicated (schema in panel D). Shown are the tumor growth curves (panel E). Tumors were collected on day 54 (n=3 per group) and evaluated by flow cytometry for CD11b+Gr-1+ MDSC (panel F), CD4+ T cells (panel G), and CD8+ T cells (panel H). For tumor growth curves, asterisks demonstrate significant ($p < 0.05$) differences as assessed by linear mixed effects model with Geisser-Greenhouse correction. For panels F-H, comparisons were made using one-way ANOVA with Tukey's multiple comparisons test; asterisks indicate *$p<0.05$, **$p<0.01$, and ***$p<0.001$. Results are from one experiment, and representative of results from an independent experiment (Supplemental Figure 7B).

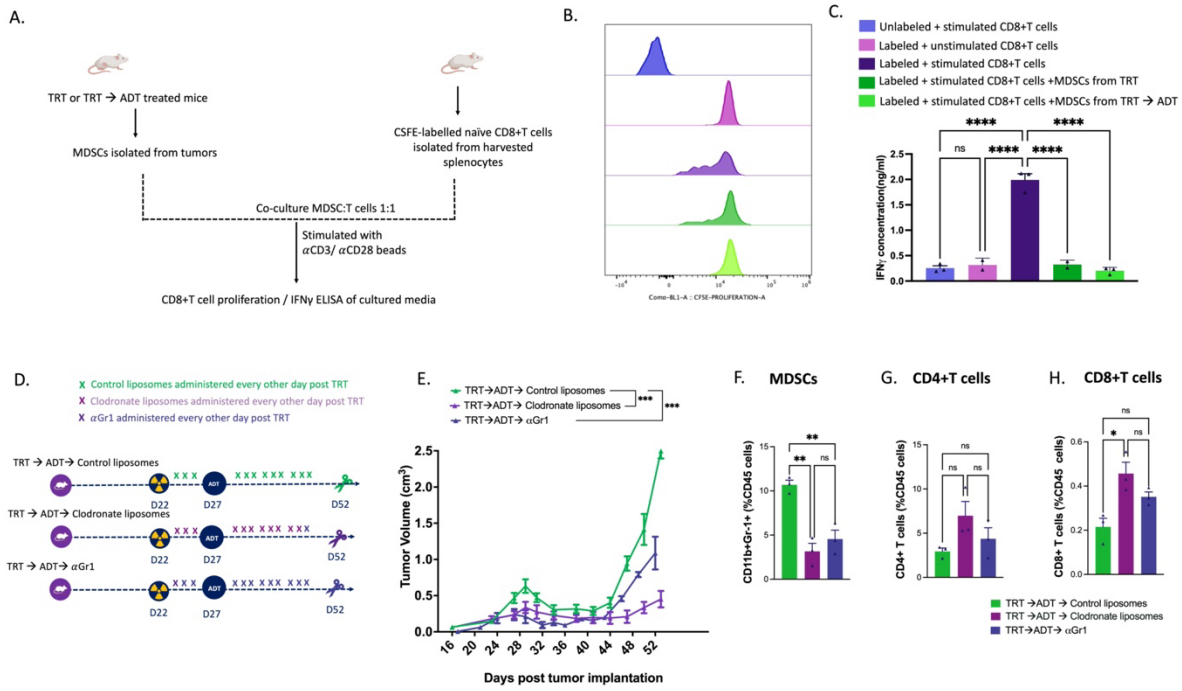

Figure 7: Depletion of MDSCs significantly improved anti-tumor responses and increased infiltration of CD4+ and CD8+ T cells into prostate tumors.

Figure 8: Depletion of MDSCs significantly improves anti-tumor responses.

Individual tumor growth curves from experiment shown in Figure 5E. Results are from one experiment and are representative of two independent experiments with the repeat experiment shown in panel B (n=3-7 per group).

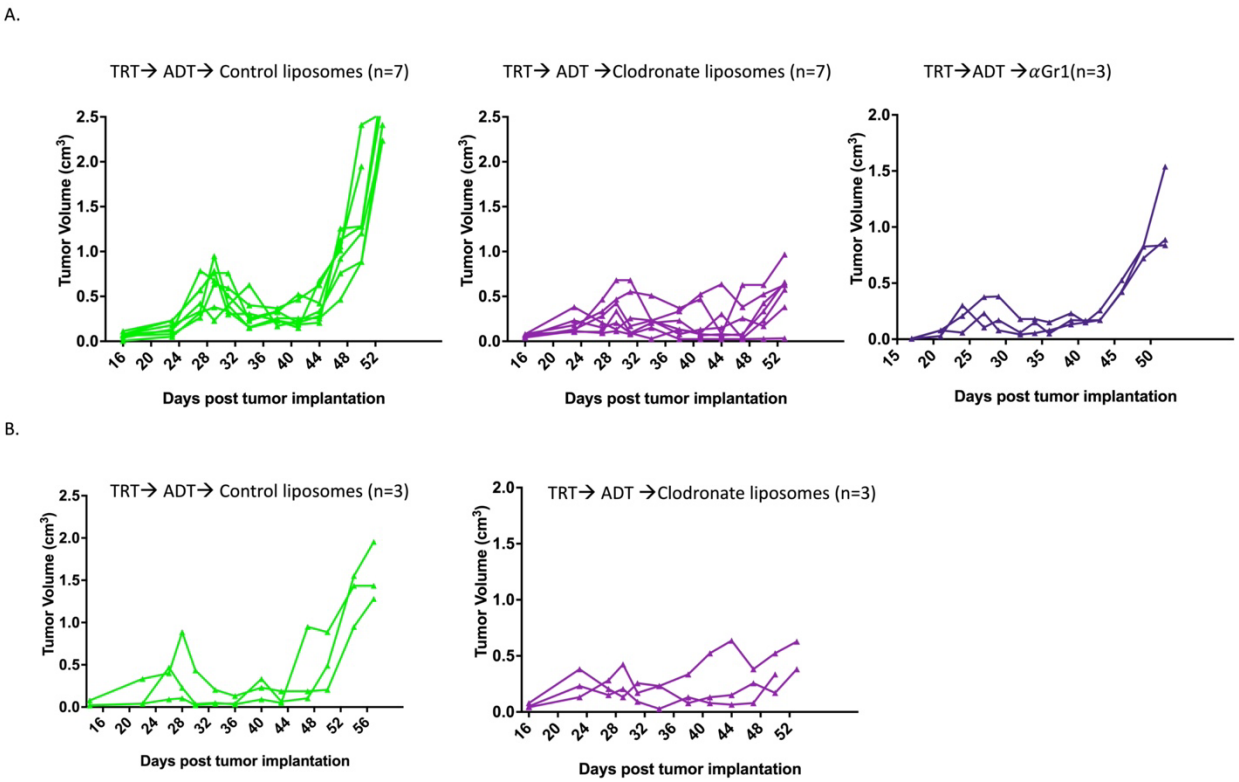

Figure 8:Depletion of MDSCs significantly improves anti-tumor responses.

Figure 9: Cytokines and chemokines secreted by tumor cells promote MDSC infiltration into tumors. Myc-CaP tumor cells were implanted in male FVB mice, treated with ADT and/or TRT as before, and sera were collected at different days (n=2 per group per time point) for cytokine and chemokine quantification (schema in panel A). Shown are concentrations of cytokines in pg/mL for CXCL1 (panel B), CXCL2 (panel C), CCL2 (panel D), CCL3 (panel E), and CCL5 (panel F). Culture supernatant from cultured Myc-CaP cells, naïve CD4+ and CD8+ T cells, the combination, or media alone (containing testosterone-replete or -deficient serum) were placed in the bottom of transwell chambers, with MDSC collected from treated mice placed in the upper chambers (schema in panel G). The % of MDSC that migrated to the bottom chamber was determined by flow cytometry (panel H), and the conditioned media were evaluated for CXCL1 (panel I), CXCL2 (panel J), CCL2 (panel K), CCL3 (panel L), and CCL5 (panel M). Panels B-F and H-M were compared using one-way ANOVA with Tukey's multiple comparisons test with asterisks indicating *$p<0.05$, **$p<0.01$, and ***$p<0.001$. Results are from one experiment with n=3 per condition and are representative of two independent experiments.

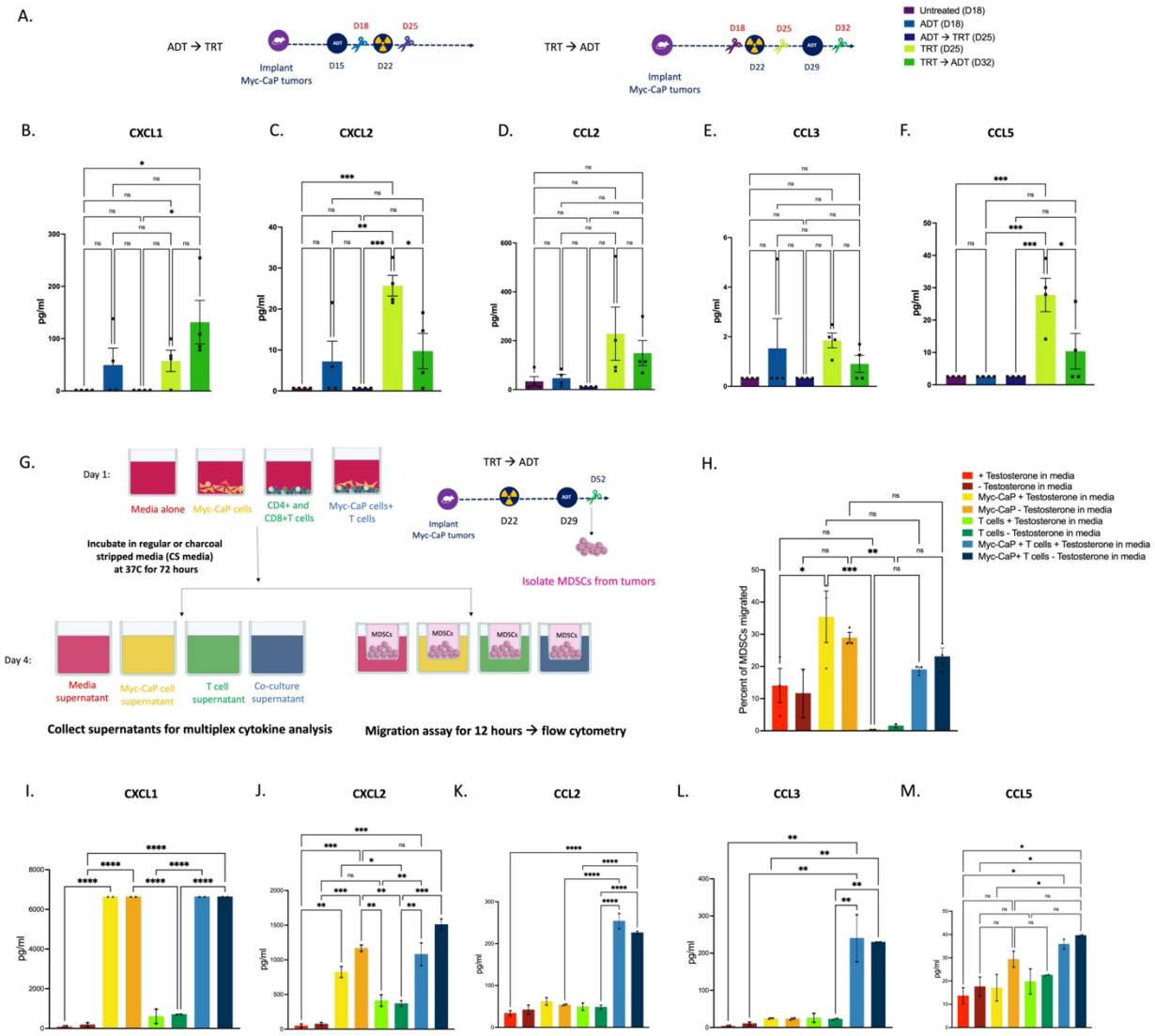

Figure 9:Cytokines and chemokines secreted by tumor cells promote MDSC infiltration into tumors.

Figure 10: Concentrations of cytokines and chemokines from sera collected from mice post treatments. Chemokines and cytokines detected using the multiplex luminex assay using sera from 2 mice per group collected at different time points post treatment. The results were compared using one-way ANOVA with Tukey's multiple comparisons test. Asterisks indicate *$p<0.05$, **$p<0.01$, and ***$p<0.001$. Results are from one experiment.

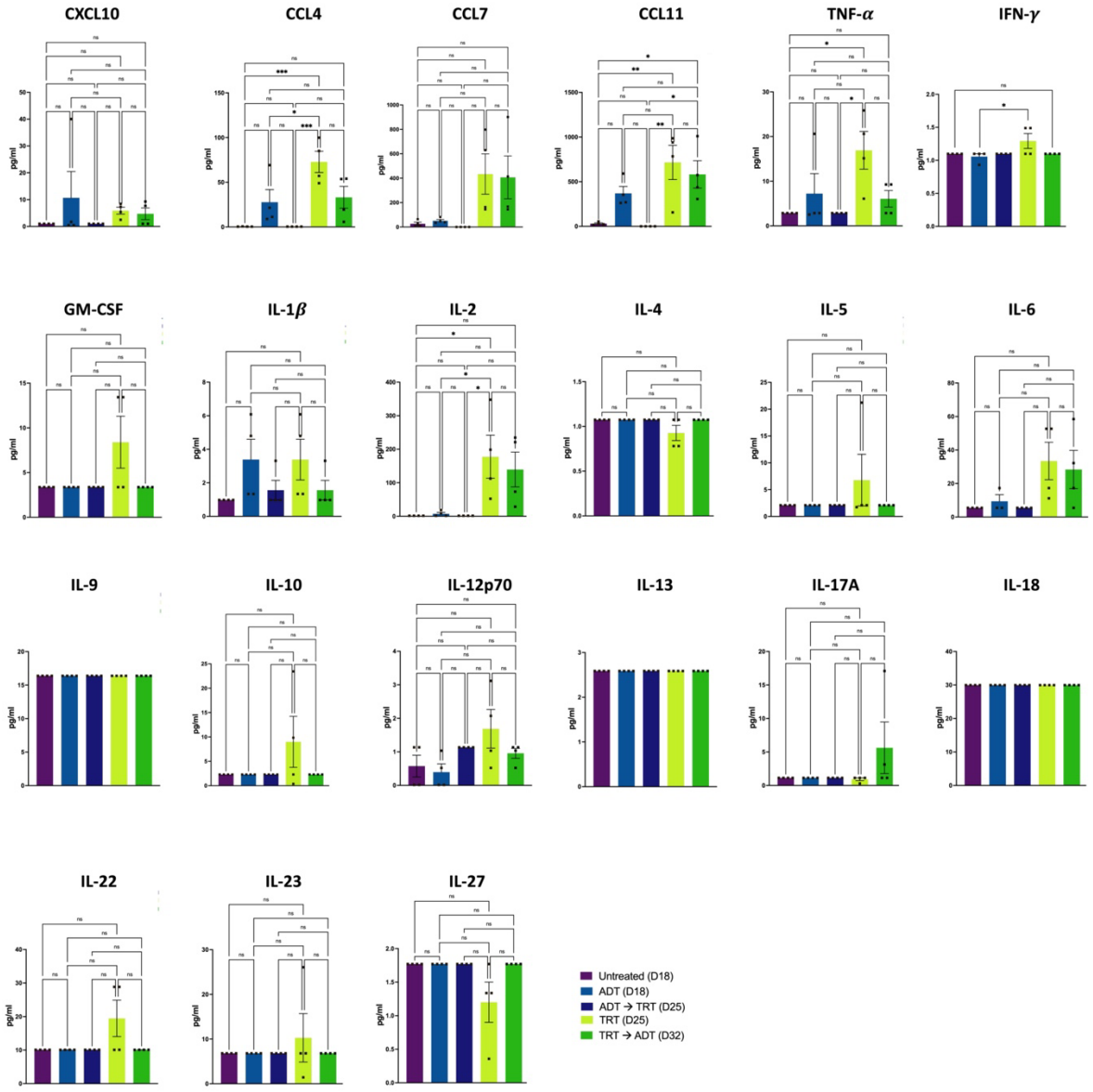

Figure 10:Concentrations of cytokines and chemokines from sera collected from mice post treatments.

Figure 11: Chemotaxis assay and chemokine/cytokine concentrations of conditioned media with ^{90}Y and ^{90}Y-charcoal stripped (^{90}Y-CS) media. Culture supernatant from cultured Myc-CaP cells, naïve CD4+ and CD8+ T cells, the combination, or media alone (containing 69.9uCi of ^{90}Y per 3ml media and testosterone-replete or -deficient serum with n=3 per condition) were placed in the bottom of transwell chambers, with MDSC collected from treated mice placed in the upper chambers. MDSC migration was determined as in Figure 6 (panel A). Chemokines and cytokines were detected in culture supernatants using the multiplex luminex assay (panel B) (n=2 per condition). Comparisons were with one-way ANOVA with Tukey's multiple comparisons test, with asterisks indicating *$p<0.05$, **$p<0.01$, and ***$p<0.001$. Results are from one experiment.

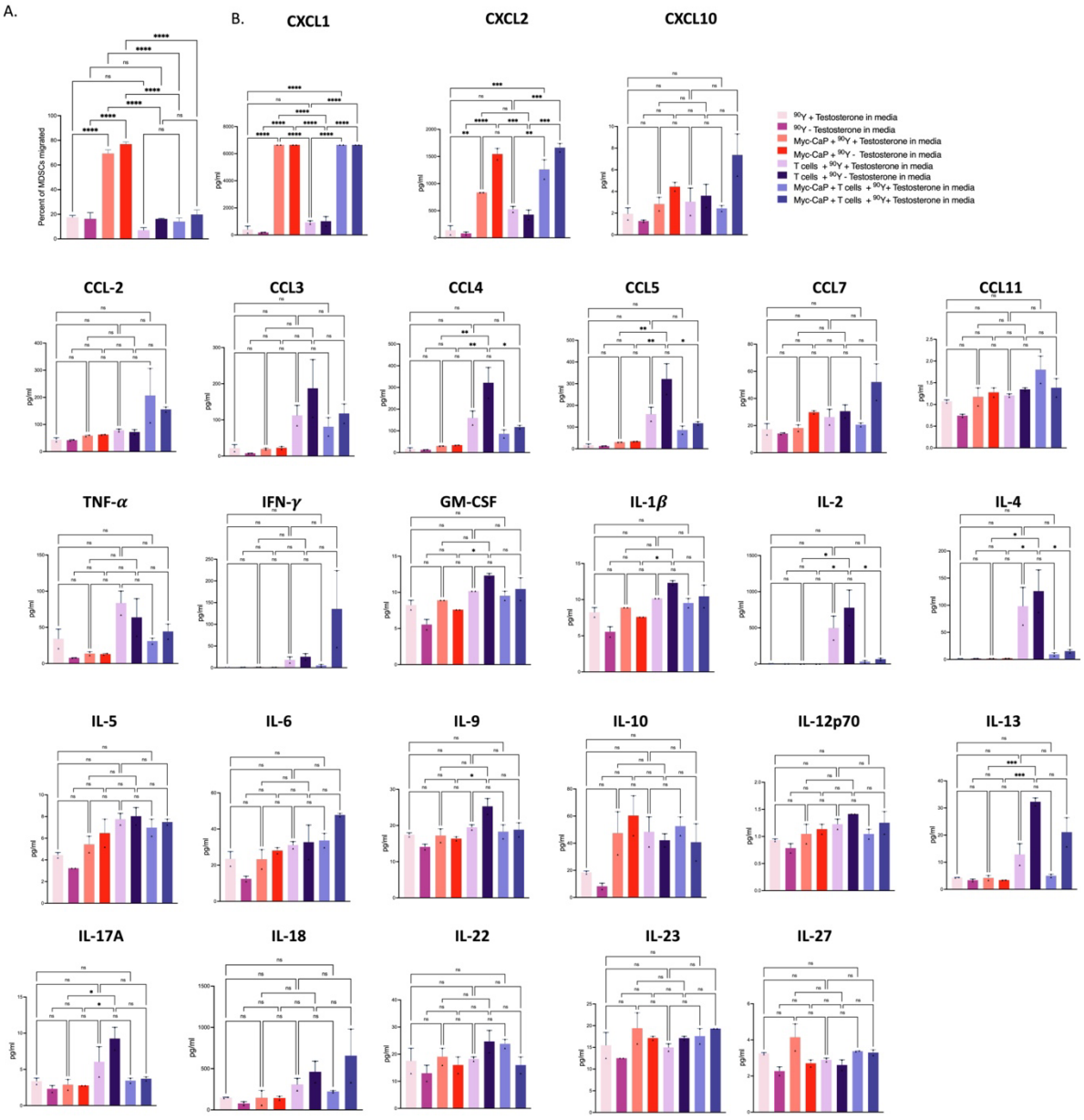

Figure 11:Chemotaxis assay and chemokine/cytokine concentrations of conditioned media with 90Y and 90Y-charcoal stripped (90Y-CS) media.

Figure 12: Concentrations of cytokines and chemokines from conditioned media with testosterone-replete or -deficient media. Chemokines detected using the multiplex luminex assay using conditioned media shown in Figure 6G (n=2 per condition). The results were compared using one-way ANOVA with Tukey's multiple comparisons test asterisks indicating *$p<0.05$, **$p<0.01$, ***$p<0.001$. Results are from one experiment with n=2 per condition.

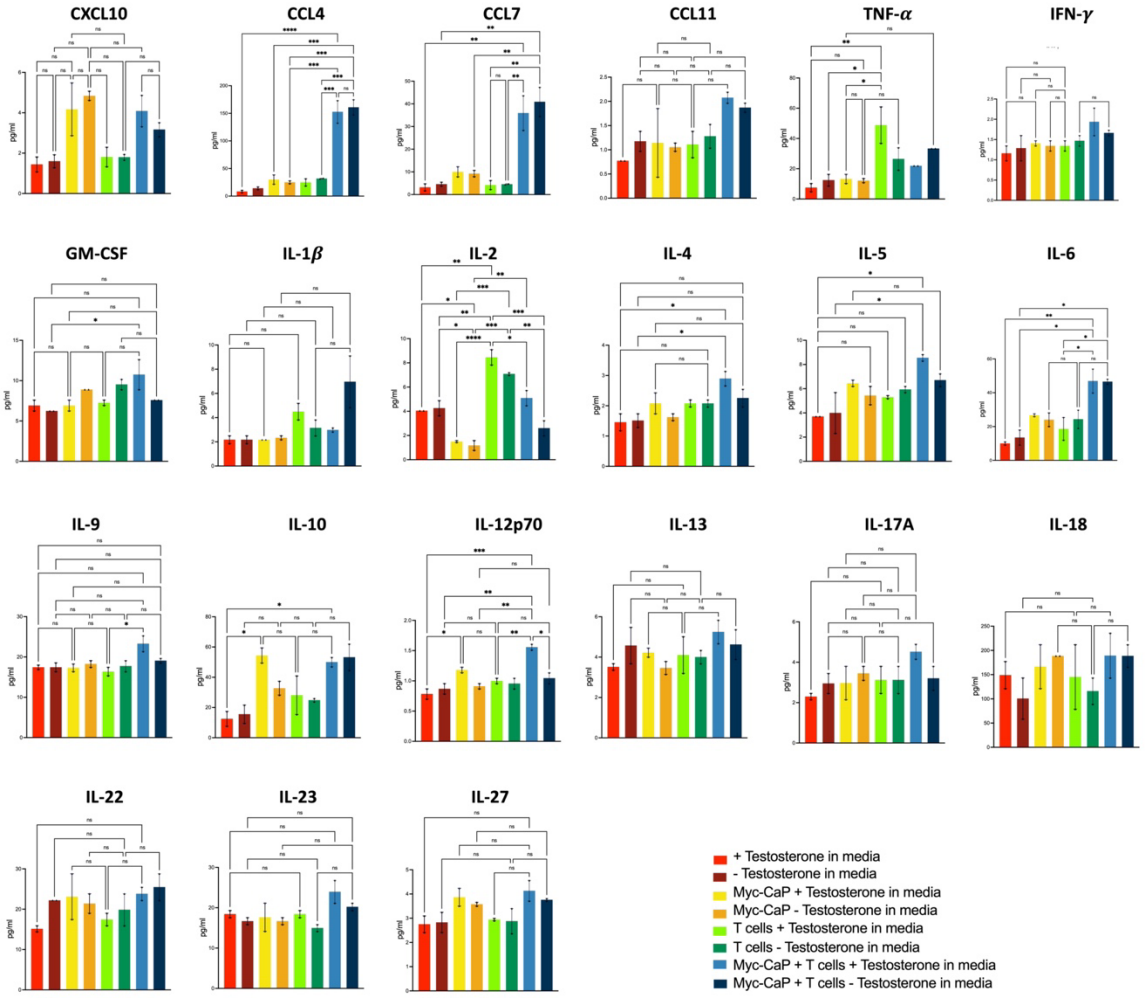

Figure 12: Concentrations of cytokines and chemokines from conditioned media with testosterone-replete or -deficient media.

Figure 13: CXCR2 blockade improves anti-tumor efficacy in the TRT→ADT combination. Culture supernatant from cultured Myc-CaP cells, with or without naïve CD4+ and CD8+ T cells, and with or without CXCL1 or reparixin, were placed in the bottom of transwell chambers, with MDSC collected from treated mice placed in the upper chambers with n =3 per condition (schema in panel A). MDSC migration was determined after 12 hours (panel B). Myc-CaP tumor cells were implanted in male FVB mice (n=7 mice per group), treated with TRT→ADT as before, and then treated with reparixin or vehicle as indicated (schema in panel C). Shown are the tumor growth curves (panel D). Tumors were collected on day 46 (n=3 from each group) and evaluated by flow cytometry for CD11b+Gr-1+ MDSC (panel E), CD4+ T cells (panel F), and CD8+ T cells (panel G). For tumor growth curves, differences were assessed by linear mixed effects model with Geisser-Greenhouse correction. Conditions in panel B were compared using one-way ANOVA with Tukey's multiple comparisons test and panels E-G were compared using unpaired-t tests. Asterisks indicate *$p<0.05$, **$p<0.01$, and ***$p<0.001$. Results shown are each from one experiment.

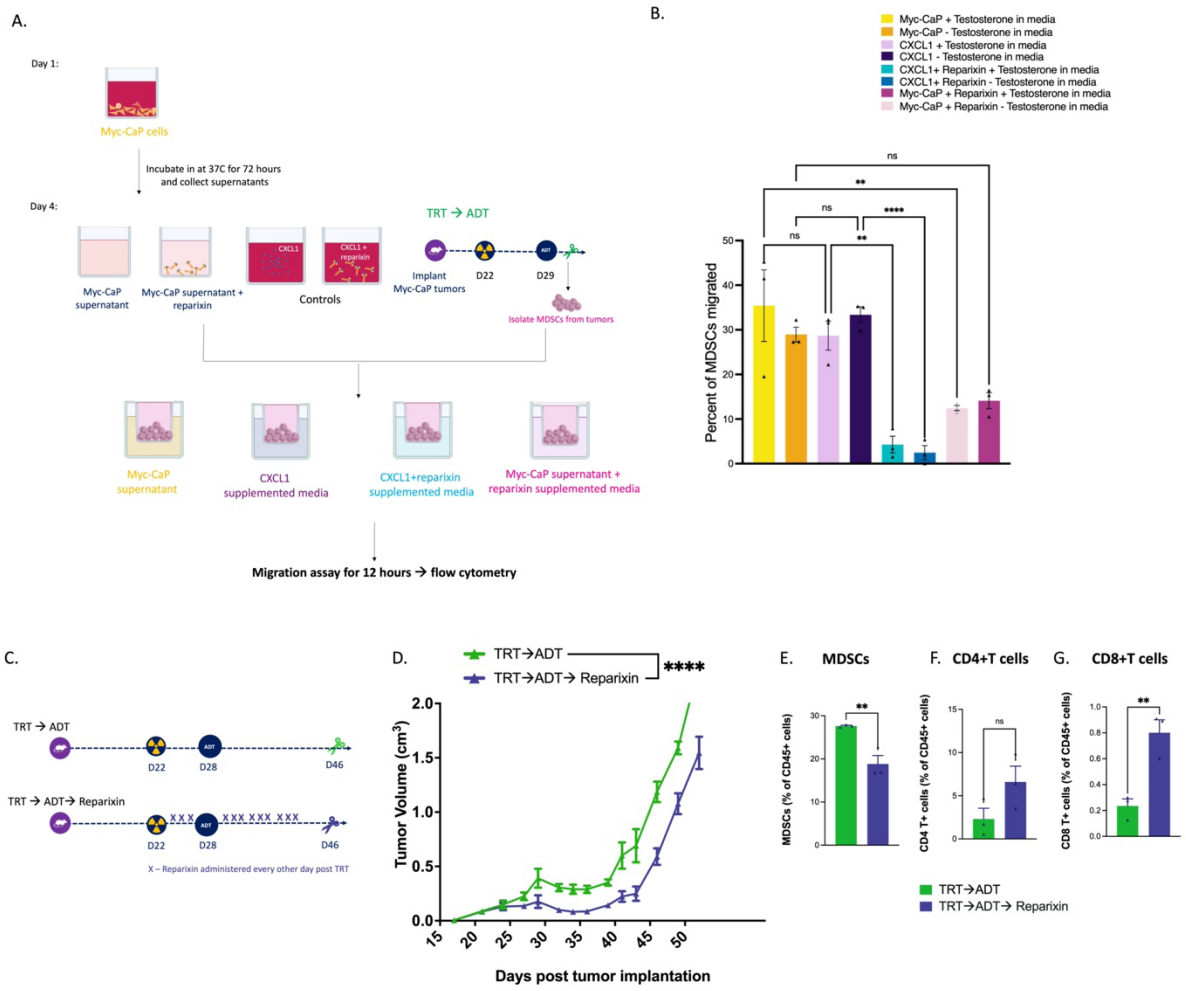

Figure 13:CXCR2 blockade improves anti-tumor efficacy in the TRT→ADT combination.

Figure 14: CXCR2 blockade improved anti-tumor responses in the TRT→ADT combination. Individual tumor growth curves from experiment shown in Figure 7D (panel A), and survival curve (panel B). Asterisks indicate **$p<0.01$ by log-rank test. Results shown are from one experiment, with n=7 animals per group.

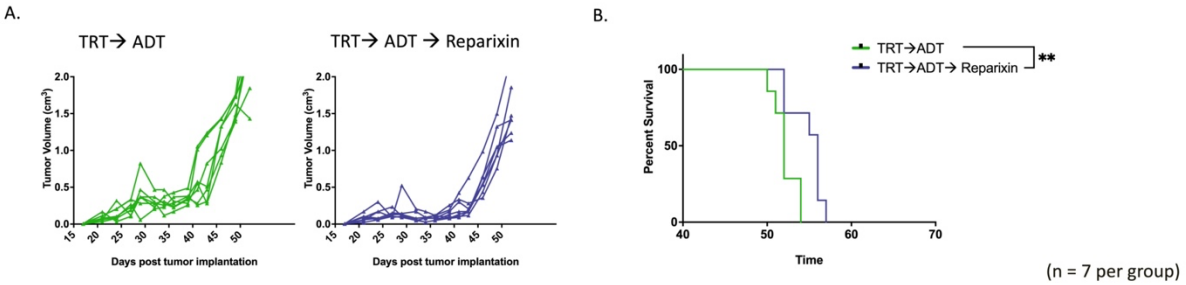

Figure 14: CXCR2 blockade improved anti-tumor responses in the TRT→ADT combination.

Figure 15: CXCR1/2 blockade improved anti-tumor responses in the ADT→TRT combination. Myc-CaP tumor cells were implanted in male FVB mice, treated with ADT→TRT as before, and then treated with reparixin, vehicle, clodronate liposomes, or anti-GR1 as indicated (schema in panel A). Shown are the tumor growth curves (panel B) and Kaplan-Meier survival curves (panel C). For tumor growth curves, comparisons were made by linear mixed effects model with Geisser-Greenhouse correction and Tukey's multiple comparisons test with individual variance; Kaplan-Meier curves were compared using the log-rank test. Asterisks demonstrate significant differences (*$p<0.05$, **$p<0.01$, and ***$p<0.001$). Results shown are from one experiment, with n=5 animals per treatment group.

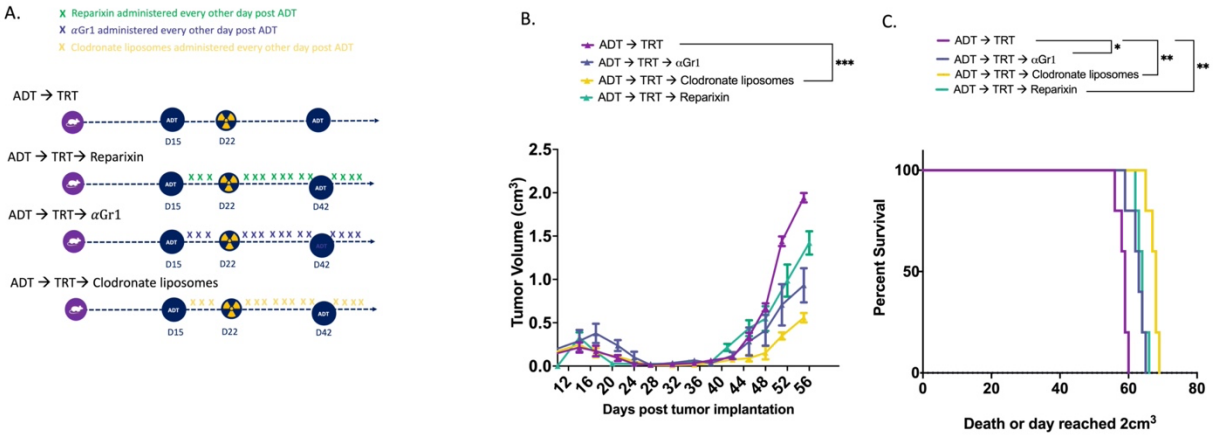

Figure 15: CXCR1/2 blockade improved anti-tumor responses in the ADT→TRT combination.

2.6 References

1. Rusthoven CG, Jones BL, Flaig TW, et al. Improved Survival With Prostate Radiation in Addition to Androgen Deprivation Therapy for Men With Newly Diagnosed Metastatic Prostate Cancer. J Clin Oncol. 2016; 34: 2835–42.

2. Sartor O, Reid RH, Hoskin PJ, et al. Samarium-153-Lexidronam complex for treatment of painful bone metastases in hormone-refractory prostate cancer. Urology. 2004; 63: 940–5.

3. Strontium-89 for palliation of pain from bone metastases in patients with prostate and breast cancer - PubMed [Internet]. [cited 28 August 2023]. Available at: https://pubmed.ncbi.nlm.nih.gov/9323260/

4. Hoskin P, Sartor O, O'Sullivan JM, et al. Efficacy and safety of radium-223 dichloride in patients with castration-resistant prostate cancer and symptomatic bone metastases, with or without previous docetaxel use: a prespecified subgroup analysis from the randomised, double-blind, phase 3 ALSYMPCA trial. Lancet Oncol. 2014; 15: 1397–406.

5. Bander NH, Milowsky MI, Nanus DM, Kostakoglu L, Vallabhajosula S, Goldsmith SJ. Phase I trial of 177lutetium-labeled J591, a monoclonal antibody to prostate-specific membrane antigen, in patients with androgen-independent prostate cancer. J Clin Oncol Off J Am Soc Clin Oncol. 2005; 23: 4591–601.

6. Tagawa ST, Milowsky MI, Morris M, et al. Phase II study of Lutetium-177-labeled anti-prostate-specific membrane antigen monoclonal antibody J591 for metastatic castration-resistant prostate cancer. Clin Cancer Res Off J Am Assoc Cancer Res. 2013; 19: 5182–91.

7. Morris MJ, Rowe SP, Gorin MA, et al. Diagnostic Performance of 18F-DCFPyL-PET/CT in Men with Biochemically Recurrent Prostate Cancer: Results from the CONDOR Phase III, Multicenter Study. Clin Cancer Res Off J Am Assoc Cancer Res. 2021; 27: 3674–82.

8. Pienta KJ, Gorin MA, Rowe SP, et al. A Phase 2/3 Prospective Multicenter Study of the Diagnostic Accuracy of Prostate Specific Membrane Antigen PET/CT with 18F-DCFPyL in Prostate Cancer Patients (OSPREY). J Urol. 2021; 206: 52–61.

9. Eder M, Schäfer M, Bauder-Wüst U, et al. 68Ga-complex lipophilicity and the targeting property of a urea-based PSMA inhibitor for PET imaging. Bioconjug Chem. 2012; 23: 688–97.

10. Sartor O, de Bono J, Chi KN, et al. Lutetium-177-PSMA-617 for Metastatic Castration-Resistant Prostate Cancer. N Engl J Med. 2021; 385: 1091–103.

11. Coulter JB, Song DY, DeWeese TL, Yegnasubramanian S. Mechanisms, Challenges, and Opportunities in Combined Radiation and Hormonal Therapies. Semin Radiat Oncol. 2022; 32: 76–81.

12. Polkinghorn WR, Parker JS, Lee MX, et al. Androgen receptor signaling regulates DNA repair in prostate cancers. Cancer Discov. 2013; 3: 1245–53.

13. Sekhar KR, Wang J, Freeman ML, Kirschner AN. Radiosensitization by enzalutamide for human prostate cancer is mediated through the DNA damage repair pathway. PLOS ONE. 2019; 14: e0214670.

14. Dal Pra A, Cury FL, Souhami L. Combining radiation therapy and androgen deprivation for localized prostate cancer—a critical review. Curr Oncol. 2010; 17: 28–38.

15. Wang C, Zhang Y, Gao W-Q. The evolving role of immune cells in prostate cancer. Cancer Lett. 2022; 525: 9–21.

16. Long X, Hou H, Wang X, et al. Immune signature driven by ADT-induced immune microenvironment remodeling in prostate cancer is correlated with recurrence-free survival and immune infiltration. Cell Death Dis. 2020; 11: 779.

17. Qin C, Wang J, Du Y, Xu T. Immunosuppressive environment in response to androgen deprivation treatment in prostate cancer. Front Endocrinol. 2022; 13: 1055826.

18. Tang S, Moore ML, Grayson JM, Dubey P. Increased CD8+ T-cell function following castration and immunization is countered by parallel expansion of regulatory T cells. Cancer Res. 2012; 72: 1975–85.

19. Roden AC, Moser MT, Tri SD, et al. Augmentation of T cell levels and responses induced by androgen deprivation. J Immunol Baltim Md 1950. 2004; 173: 6098–108.

20. Gamat M, McNeel DG. Androgen deprivation and immunotherapy for the treatment of prostate cancer. Endocr Relat Cancer. 2017; 24: T297–310.

21. Lopez-Bujanda ZA, Haffner MC, Chaimowitz MG, et al. Castration-mediated IL-8 Promotes Myeloid Infiltration and Prostate Cancer Progression [Internet]. Immunology; 2019 May [cited 12 February 2021]. Available at: http://biorxiv.org/lookup/doi/10.1101/651083

22. Lee Y, Auh SL, Wang Y, et al. Therapeutic effects of ablative radiation on local tumor require CD8+ T cells: changing strategies for cancer treatment. Blood. 2009; 114: 589–95.

23. Demaria S, Bhardwaj N, McBride WH, Formenti SC. Combining radiotherapy and immunotherapy: a revived partnership. Int J Radiat Oncol Biol Phys. 2005; 63: 655–66.

24. Kalina J, Neilson D, Comber A, et al. Immune Modulation by Androgen Deprivation and Radiation Therapy: Implications for Prostate Cancer Immunotherapy. Cancers. 2017; 9: 13.

25. Weichert JP, Clark PA, Kandela IK, et al. Alkylphosphocholine analogs for broad-spectrum cancer imaging and therapy. Sci Transl Med. 2014; 6: 240ra75.

26. Grudzinski JJ, Titz B, Kozak K, et al. A phase 1 study of 131I-CLR1404 in patients with relapsed or refractory advanced solid tumors: dosimetry, biodistribution, pharmacokinetics, and safety. PloS One. 2014; 9: e111652.

27. Ailawadhi S, Stiff PJ, Ibrahim E, et al. Fractionated Dosing of CLR 131 in Patients with Relapsed or Refractory Multiple Myeloma (RRMM). Blood. 2019; 134: 144.

28. Lubner SJ, Mullvain J, Perlman S, et al. A Phase 1, Multi-Center, Open-Label, Dose-Escalation Study of 131I-CLR1404 in Subjects with Relapsed or Refractory Advanced Solid Malignancies. Cancer Invest. 2015; 33: 483–9.

29. Grudzinski JJ, Hernandez R, Marsh I, et al. Preclinical Characterization of 86/90Y-NM600 in a Variety of Murine and Human Cancer Tumor Models. J Nucl Med. 2019; 60: 1622–8.

30. Hernandez R, Walker KL, Grudzinski JJ, et al. 90Y-NM600 targeted radionuclide therapy induces immunologic memory in syngeneic models of T-cell Non-Hodgkin's Lymphoma. Commun Biol. 2019; 2: 1–12.

31. Patel RB, Hernandez R, Carlson P, et al. Low-dose targeted radionuclide therapy renders immunologically cold tumors responsive to immune checkpoint blockade. Sci Transl Med. 2021; 13: eabb3631.

32. Potluri HK, Ferreira CA, Grudzinski J, et al. Antitumor efficacy of ^{90} Y-NM600 targeted radionuclide therapy and PD-1 blockade is limited by regulatory T cells in murine prostate tumors. J Immunother Cancer. 2022; 10: e005060.

33. Aluicio-Sarduy E, Hernandez R, Valdovinos HF, et al. Simplified and automatable radiochemical separation strategy for the production of radiopharmaceutical quality 86Y using single column extraction chromatography. Appl Radiat Isot Data Instrum Methods Use Agric Ind Med. 2018; 142: 28–31.

34. Besemer AE, Yang YM, Grudzinski JJ, Hall LT, Bednarz BP. Development and Validation of RAPID: A Patient-Specific Monte Carlo Three-Dimensional Internal Dosimetry Platform. Cancer Biother Radiopharm. 2018; 33: 155–65.

35. Bednarz B, Grudzinski J, Marsh I, et al. Murine-specific internal dosimetry for preclinical investigations of imaging and therapeutic agents. Health Phys. 2018; 114: 450–9.

36. Johnson LE, Frye TP, Chinnasamy N, Chinnasamy D, McNeel DG. Plasmid DNA vaccine encoding prostatic acid phosphatase is effective in eliciting autologous antigen-specific CD8+ T cells. Cancer Immunol Immunother CII. 2007; 56: 885–95.

37. Bolla M, Tienhoven GV, Warde P, et al. External irradiation with or without long-term androgen suppression for prostate cancer with high metastatic risk: 10-year results of an EORTC randomised study. Lancet Oncol. 2010; 11: 1066–73.

38. Roach M, Moughan J, Lawton CAF, et al. Sequence of hormonal therapy and radiotherapy field size in unfavourable, localised prostate cancer (NRG/RTOG 9413): long-term results of a randomised, phase 3 trial. Lancet Oncol. 2018; 19: 1504–15.

39. Malone S, Roy S, Eapen L, et al. Sequencing of Androgen-Deprivation Therapy With External-Beam Radiotherapy in Localized Prostate Cancer: A Phase III Randomized Controlled Trial. J Clin Oncol. 2020; 38: 593–601.

40. Ma TM, Sun Y, Malone S, et al. Sequencing of Androgen-Deprivation Therapy of Short Duration With Radiotherapy for Nonmetastatic Prostate Cancer (SANDSTORM): A Pooled Analysis of 12 Randomized Trials. J Clin Oncol. 2023; 41: 881–92.

41. Wu C-T, Chen W-C, Chen M-F. The Response of Prostate Cancer to Androgen Deprivation and Irradiation Due to Immune Modulation. Cancers. 2019; 11: 20.

42. Galon J, Costes A, Sanchez-Cabo F, et al. Type, density, and location of immune cells within human colorectal tumors predict clinical outcome. Science. 2006; 313: 1960–4.

43. Yang Y, Attwood K, Bshara W, et al. High intratumoral CD8+ T-cell infiltration is associated with improved survival in prostate cancer patients undergoing radical prostatectomy. The Prostate. 2021; 81: 20–8.

44. Gamat-Huber M, McNeel DG. Androgen deprivation as a tumour-immunomodulating treatment. Nat Rev Urol. 2020; 17: 371–2.

45. Bronte G, Conteduca V, Landriscina M, Procopio AD. Circulating myeloid-derived suppressor cells and survival in prostate cancer patients: systematic review and meta-analysis. Prostate Cancer Prostatic Dis. 2023; 26: 41–6.

46. Koinis F, Xagara A, Chantzara E, Leontopoulou V, Aidarinis C, Kotsakis A. Myeloid-Derived Suppressor Cells in Prostate Cancer: Present Knowledge and Future Perspectives. Cells. 2021; 11: 20.

47. Autio KA, Klebanoff CA, Schaer D, et al. Immunomodulatory Activity of a Colony-stimulating Factor-1 Receptor Inhibitor in Patients with Advanced Refractory Breast or Prostate Cancer: A Phase I Study. Clin Cancer Res Off J Am Assoc Cancer Res. 2020; 26: 5609–20.

48. Moeller A, Kurzrock R, Botta GP, et al. Challenges and prospects of CSF1R targeting for advanced malignancies. Am J Cancer Res. 2023; 13: 3257–65.

49. Lee J, Cacalano G, Camerato T, Toy K, Moore MW, Wood WI. Chemokine binding and activities mediated by the mouse IL-8 receptor. J Immunol Baltim Md 1950. 1995; 155: 2158–64.

50. Shi H, Han X, Sun Y, et al. Chemokine (C-X-C motif) ligand 1 and CXCL2 produced by tumor promote the generation of monocytic myeloid-derived suppressor cells. Cancer Sci. 2018; 109: 3826–39.

51. Bullock K, Richmond A. Suppressing MDSC Recruitment to the Tumor Microenvironment by Antagonizing CXCR2 to Enhance the Efficacy of Immunotherapy. Cancers. 2021; 13: 6293.

52. Goldstein LJ, Mansutti M, Levy C, et al. A randomized, placebo-controlled phase 2 study of paclitaxel in combination with reparixin compared to paclitaxel alone as front-line therapy for metastatic triple-negative breast cancer (fRida). Breast Cancer Res Treat. 2021; 190: 265–75.

53. Alfaro C, Teijeira A, Oñate C, et al. Tumor-Produced Interleukin-8 Attracts Human Myeloid-Derived Suppressor Cells and Elicits Extrusion of Neutrophil Extracellular Traps (NETs). Clin Cancer Res. 2016; 22: 3924–36.

54. Opfermann P, Derhaschnig U, Felli A, et al. A pilot study on reparixin, a CXCR1/2 antagonist, to assess safety and efficacy in attenuating ischaemia–reperfusion injury and inflammation after on-pump coronary artery bypass graft surgery. Clin Exp Immunol. 2015; 180: 131–42.

55. Nair P, Gaga M, Zervas E, et al. Safety and efficacy of a CXCR2 antagonist in patients with severe asthma and sputum neutrophils: a randomized, placebo-controlled clinical trial. Clin Exp Allergy J Br Soc Allergy Clin Immunol. 2012; 42: 1097–103.

Chapter 3

Sequence of Androgen Receptor-Targeted Vaccination with Androgen Deprivation Therapy Affects Anti-Prostate Tumor Efficacy

This work has been published in the Journal for Immunotherapy of Cancer.

Muralidhar A, Gamat-Huber M, Vakkalanka S*, et al*
Sequence of androgen receptor-targeted vaccination with androgen deprivation therapy affects anti-prostate tumor efficacy
Journal for ImmunoTherapy of Cancer 2024;**12:**e008848. doi: 10.1136/jitc-2024-008848

3.1 Abstract

Rationale: Androgen deprivation therapy (ADT) is the primary treatment for recurrent and metastatic prostate cancer. In addition to direct anti-tumor effects, ADT has immunomodulatory effects such as promoting T cell infiltration and enhancing antigen processing/presentation. Previous studies in our lab have demonstrated that ADT also leads to increased expression of the androgen receptor (AR) and increased recognition of prostate tumor cells by AR-specific CD8+ T cells. We have also demonstrated that ADT combined with a DNA vaccine encoding the androgen receptor significantly slowed tumor growth and improved survival of prostate tumor-bearing mice. The current study aimed to investigate the impact of the timing and sequencing of ADT with vaccination on the tumor immune microenvironment in murine prostate cancer models to further increase the anti-tumor efficacy of vaccines.

Methods: Male FVB mice implanted with Myc-CaP tumor cells, or male C57BL/6 mice implanted with TRAMP-C1 prostate tumor cells, were treated with a DNA vaccine encoding AR (pTVG-AR) and ADT. The sequence of administration was evaluated for its effect on tumor growth, and tumor-infiltrating immune populations were characterized.

Results: Vaccination prior to ADT (pTVG-AR → ADT) significantly enhanced anti-tumor responses and survival. This was associated with increased tumor infiltration by CD4+ and CD8+ T cells, including AR-specific CD8+ T cells. Depletion of CD8+T cells prior to ADT significantly worsened overall survival. Following ADT treatment, however, Gr1+ myeloid derived suppressor cells (MDSCs) increased, and this was associated with fewer infiltrating T cells and reduced tumor growth. Inhibiting Gr1+ MDSCs recruitment, either by using a CXCR2 antagonist or by cycling

androgen deprivation with testosterone replacement, improved anti-tumor responses and overall survival.

Conclusion: Vaccination prior to ADT significantly improved anti-tumor responses, mediated in part by increased infiltration of CD8+ T cells following ADT. Targeting MDSC recruitment following ADT further enhanced anti-tumor responses. These findings suggest logical directions for future clinical trials to improve the efficacy of prostate cancer vaccines.

3.2 Introduction

Prostate cancer is the second leading cause of cancer-related death among men in the United States [1]. Androgen deprivation therapy (ADT) plays a central role in the treatment of prostate cancer, particularly in cases of advanced or metastatic disease. The growth and progression of prostate cancer hinge on the androgen receptor (AR) pathway. ADT functions by suppressing androgens, such as testosterone, or inhibiting their binding to the AR, aiming to impede the growth of prostate cancer cells [2]. However, despite its initial efficacy, a significant challenge emerges in the form of castration resistance, with a median life expectancy of less than three years for patients with metastatic castration-resistant prostate cancer [3].

Early investigations demonstrated that ADT, achieved through surgical or chemical means, led to a reduction in prostate size and triggered tumor apoptosis [4]. In addition to its direct anti-tumor effects, there is growing evidence demonstrating that ADT exhibits immunostimulatory properties, including thymic regrowth, increased production of naïve T cells, enhanced immune cell infiltration into the prostate (both lymphoid and myeloid cells), enhanced antigen presentation and elevated antibody responses to prostate antigens [5–8]. Preclinical studies have illustrated that ADT can enhance the efficacy of various immunotherapeutic approaches such as anti-cancer vaccines, presenting a promising avenue for the strategic harnessing of both anti-tumor and immunostimulatory effects to improve immunotherapy outcomes in prostate cancer [9–13]. For example, Ardiani et al. showed that male mice, upon vaccination with a yeast-based Twist-encoded vaccine, displayed initial Twist-specific CD4+T cell proliferation. Notably, the combination of Twist vaccination and enzalutamide further enhanced CD4+ T cell proliferation compared to

control or enzalutamide-treated mice. This effect was also observed in the TRAMP model, where mice receiving the combination of the Twist vaccine and enzalutamide exhibited increased overall survival compared to control mice or those treated with monotherapy [12]. Kwilas et al. also demonstrated that a Twist poxvirus vaccine, when administered with enzalutamide, led to a significant improvement in overall survival [9]. Combining a poxviral vaccine targeting PSA, PROSTVAC, with ADT in a prostate-specific PSA transgenic mouse model demonstrated a significant increase in PSA-specific T cells and an increase in T-cell IFNγ production[14]. In a phase 2 clinical study involving patients with PSA progression, the combination of PROSTVAC and nilutamide, with nilutamide preceding the vaccine, resulted in a median time to treatment failure of 5.2 months from the initiation of combination therapy. In contrast, for patients receiving the vaccine followed by nilutamide, the median time to treatment failure was 13.9 months from the start of combination therapy, suggesting a possible benefit related to the sequence of administration of these agents [15,16].

Paradoxically, the use of ADT leads to increased expression of the AR as a compensatory mechanism [17]. In fact, castration resistance is often accompanied by mutations or gene amplifications leading to increased AR expression [18–21]. For this reason, we have previously evaluated the AR as a vaccine target, one that might be strategically targeted in combination with ADT. We previously demonstrated that ADT treatment of prostate cancer cells increased their recognition by AR-specific CD8+ T cells [22]. We also showed that a DNA vaccine encoding the ligand-binding domain (LBD) of the AR (pTVG-AR), given with or without ADT, could elicit antigen-specific CD8+ T cells, slow prostate tumor development, delay tumor growth, and prolong overall survival in murine models of prostate cancer [22,23]. In a multi-center phase I study

conducted in patients who had recently initiated ADT, we demonstrated that vaccination with pTVG-AR led to increased AR-specific Th1-biased immunity and a delayed time to castration resistance in immunized patients [24].

Given that others have demonstrated that ADT can be immunomodulatory[25,26], and there may be a sequence preference to its use with vaccination, in the current report we investigated the sequence of ADT given with the pTVG-AR DNA vaccine in preclinical murine models of prostate cancer. Our goal was to determine whether, any by what mechanism, there was a sequence preference to administration, and whether changes to the tumor immune microenvironment might inform optimal approaches that could be applied to future human clinical trials using this or other prostate cancer vaccines.

3.3 Results:

3.3.1 Sequence of vaccination and ADT, with vaccination given prior to ADT, (pTVG-AR → ADT) significantly improved anti-tumor responses in murine prostate tumor models.

We have previously reported that combining ADT with AR-targeted vaccination led to greater anti-tumor effects in murine models of prostate cancer [22]. This led to a phase I trial, demonstrating the vaccine's safety, its ability to elicit or augment T cells specific for the AR LBD, and its potential to delay castration resistance [24]. Consequently, we wished to determine whether there was an optimal use or sequence of these treatments to efficiently delay or prevent the emergence of castration-resistant disease in murine prostate tumor models. Hence, as a first study, we examined AR-targeted vaccination delivered either before or after ADT. As depicted in Figure 1A, Myc-CaP tumor cells were implanted subcutaneously in male FVB mice, and when tumors reached a volume of 0.2-0.3cm^3 they were treated with degarelix (25 mg/kg subcutaneously every 28 days). Mice were also immunized weekly with a DNA vaccine encoding the ligand binding domain of the androgen receptor (pTVG-AR), or control vector (pTVG4), beginning either one day after tumor implantation (before androgen deprivation), or one day after degarelix treatment. As shown in Figure 1B (and Figure 2), immunization prior to ADT elicited a greater anti-tumor response and significantly improved survival (Figure 1C). Similar results were found in a separate murine model of prostate cancer in which C57BL/6 mice implanted with TRAMP-C1 tumor cells (Figure 1D); AR-targeted vaccination prior to ADT resulted in a significantly greater anti-tumor response and improved overall survival (Figures 1E, 1F, and Figure 3). In this model, mice received an additional weekly vaccination prior to ADT, given the slower growth rate of these

tumors requiring 4 weeks to become palpable. Similarly, transgenic HLA-A2-expressing TRAMP mice, mice that develop autochthonous prostate tumors with age driven by the SV40 large T antigen under a prostate-specific promoter, were immunized in sequences before or after ADT, as depicted in Figure 4A. Mice that received vaccination prior to ADT showed a non-significant trend toward improvement in overall survival (Figure 4B). Overall, these findings demonstrated that vaccination in combination with ADT had a stronger anti-tumor effect in combination and was dependent on the order of administration, with pTVG-AR → ADT leading to superior anti-tumor responses.

3.3.2 ADT led to an increase in prostate tumor-infiltrating T cells and myeloid cells, and this was affected by vaccination.

It has been previously demonstrated by us and others that ADT can lead to increases in tumor infiltrating CD4+ and CD8+T cells [5,6]. We next asked whether the sequence of immunization, with immunization given prior to ADT, affected the infiltration of tumors by T cells. A similar study was performed as in Figure 5A, but tumors were collected at several time points following treatment for evaluation of immune cell compositions via flow cytometry, as shown in Figure 5A. Representative flow plots for T cells on days 21 and 36 and MDSCs on days 36 and 60 are shown in Figure 5B (and gating strategy shown in Appendix). We found that CD4+T and CD8+T cells increased in the tumor microenvironment in all mice at day 36, 14 days after ADT administration, but with the pTVG-AR → ADT combination group, CD4+T and CD8+T cells were further increased (Figures 5C and 5D) and significantly reduced by day 60. Gr-1+ MDSCs were significantly reduced at day 36 while significantly increased in all groups following ADT

regardless of vaccination (Figure 5E); there were little to no changes in regulatory CD4+ T cells (Tregs, Figure 5F). Taken together, these data suggested that ADT initially resulted in increased numbers of infiltrating T cells, which were further augmented by immunization prior to ADT. However, the effects of vaccination were transient, and at a later time point after ADT the tumor microenvironment had many Gr1+ MDSCs and few T cells.

3.3.3 Immunization prior to ADT leads to antigen-specific immune responses.

We next investigated whether immunization prior to ADT led to infiltration of antigen-specific T cells. A similar study was performed in which mice were immunized, treated with ADT, and tumors were harvested on day 37, 2 weeks following ADT (Figure 6A). Tumor-infiltrating CD8+ T cells were isolated and evaluated by IFNγ ELISPOT for AR-specific T cells (Figure 6B). We found that CD8+ T cells specific for AR, and notably for AR25, the dominant epitope for AR in FVB mice (Figure 7), were infiltrating tumors in greater numbers in mice immunized prior to receiving ADT (Figure 6C). CD8 T cells recovered from tumors following immunization also expressed more granzyme B and perforin (Figure 8). ADT was required for this infiltration, because AR-specific T cells were not detected in greater abundance following vaccination without ADT (Figure 9). We next wished to determine whether CD8+T cells elicited with vaccination prior to ADT were specifically responsible for the improved anti-tumor efficacy. Mice were treated with IgG or αCD8 for three days in the week prior to receiving ADT (Figure 6D). As shown in Figure 6E (and Figure 10), CD8+ T cell depletion after immunization and prior to ADT abrogated the delay in time to castration resistant tumor growth and significantly worsened animal survival (Figure 6F). Overall, these results indicate that CD8+ T cells elicited and/or activated by vaccination prior to ADT are crucial in mediating enhanced anti-tumor responses.

3.3.4 MDSCs increased following ADT led to impaired anti-tumor response to vaccination.

The accumulation of MDSC following ADT has been previously demonstrated in Myc-CaP tumors [30], similar to what we demonstrated in Figure 5E. MDSC are also known to accumulate in tumors and the peripheral blood of patients with advanced, castration-resistant prostate cancer, and have been implicated in the observation that advanced prostate tumors are relatively devoid of infiltrating T cells [31]. We hypothesized that ADT-induced MDSC accumulation might impair the function or presence of tumor-infiltrating T cells, even following vaccination, ultimately contributing to the development of castration-resistant tumors. To evaluate the timing and effect of ADT on MDSC infiltration, Myc-CaP tumor-bearing mice were treated with or without ADT (Figure 11A) and followed for tumor growth (Figure 11B) and overall survival (Figure 11C). Tumors were sampled from cohorts of mice with similar tumor volumes, as indicated in Figure 4B, to evaluate for the presence of tumor-infiltrating immune populations. In animals not treated with ADT, there was an increase in tumor-infiltrating CD4+ (Figure 11D) and CD8+ (Figure 11E) T cells over time, but no significant increase in MDSCs (Figure 11F). In contrast, in ADT-treated tumors, there was a marked increase in CD4+ and CD8+ T cells 12 days after ADT, but a marked decline thereafter (Figures 11D and 11E). This was associated with a concurrent significant increase in CD11b+Gr-1+ MDSCs (Figure 11F). We next sought to determine whether depletion of tumor-infiltrating MDSCs could enhance anti-tumor immune responses. As shown in Figure 11G, tumor bearing mice were treated vaccine, ADT, and control- or clodronate-encapsulated liposomes, a treatment effective at depleting precursors of MDSCs, twice a week following ADT. As shown in Figure 11H (and Figure 12), treatment with clodronate liposomes significantly improved anti-tumor responses in mice receiving AR-targeted vaccination and ADT, in either treatment sequence, as well as overall survival (Figure 11I). Tumors collected from mice treated

with clodronate liposomes at day 62 demonstrated an increase in CD4+ (Figure 11J) and CD8+ (Figure 11K) T cells. These findings suggested that treatments aimed at interrupting the infiltration of MDSC following ADT might significantly improve the treatment effects from vaccination and ADT.

3.3.5 CXCR2 blockade improves anti-tumor efficacy in the pTVG-AR→ ADT combination by infiltrating antigen-specific CD8+T cells and inhibiting recruitment of Gr1+MDSCs.

As clodronate liposomes can also deplete macrophages and do not selectively deplete MDSCs, we next wished to evaluate agents that more specifically impair MDSC recruitment or function. Blocking CXCR2 has been demonstrated to inhibit the recruitment of MDSC [32], and hence we specifically sought to determine whether inclusion of a CXCR2 inhibitor could improve the anti-tumor responses of the combination treatment (Figure 13A). As demonstrated in Figure 13B (and Figure 14), mice treated with reparixin showed improved anti-tumor responses and overall survival (Figure 13C). Tumors from mice treated in the pTVG-AR → ADT sequence exhibited a significant reduction in MDSCs (Figure 13D) and a significant increase in CD8+T cells (Figure 13F). Among tumor-infiltrating CD8+ T cells present several weeks after ADT, AR-specific CD8+ T cells were slightly but significantly increased in frequency (Figures 13G, 13H and 13I).

3.3.6 ADT followed by testosterone supplementation led to reduced accumulation of MDSCs although significantly worsened anti-tumor responses in the Myc-CaP tumor model.

Our findings indicated that prolonged treatment with ADT caused early infiltration of T cells, but this was of limited duration and eventually tumors accumulated MDSCs. This suggested that it might be preferable to use a shorter course of ADT, or use it intermittently, in combination with vaccination. Because degarelix has a long half-life, we used supplemental testosterone to quickly reverse the effects of androgen deprivation. Hence, we sought to determine whether cycling ADT and testosterone might reduce the intra-tumoral accumulation of MDSCs. Male FVB mice were implanted with Myc-CaP tumor cells and administered ADT. Testosterone (or control) was administered twice a week, two weeks post ADT (Figure 15A). As seen in the tumor growth curves, testosterone caused the tumors to grow significantly faster compared to mice treated with ADT alone (Figure 15B and Figure 16) and shortened their overall survival (Figure 15C). In a parallel experiment, tumors were harvested at post-treatment points to detect tumor infiltrating immune populations. Interestingly, we found that MDSCs were significantly reduced at day 66 following testosterone treatment (Figure 15D), but there was not an associated increase in CD4+ or CD8+T cells (Figures 15E and 15F).

3.3.7 ADT followed by testosterone supplementation reduced accumulation of MDSCs and significantly improved anti-tumor responses when combined with vaccination in TRAMP-C1 tumor-bearing mice, but not Myc-CaP tumor-bearing mice.

Given that an intermittent schedule of ADT could reduce MDSC accumulation, we next sought to determine if addition of vaccination prior to ADT could improve the anti-tumor efficacy. Myc-CaP tumors were immunized intradermally weekly with pTVG-AR or vector control one day post tumor implantation and weekly thereafter. Groups received ADT at day 22, and then received

testosterone or control 14 days later, as shown in Figure 17A. From the tumor growth curves, shown in Figure 17B (and Figure 18), treatment with vaccination improved the anti-tumor response compared to vector control, however treatment with testosterone led to faster tumor growth and shorter survival (Figure 17C). As before, treatment with testosterone led to a significant reduction of MDSCs within tumors (Figure 17D), but vaccination with ADT and testosterone did not lead to a greater infiltration of CD4+ and CD8+ T cells (Figures 17E and 17F).

Because the myc oncogene is driven by the AR promoter in Myc-CaP tumor cells, and this may have led to more rapid tumor growth following testosterone treatment, we also evaluated this approach in C57Bl/6 mice bearing TRAMP-C1 prostate tumor cells, tumors not driven by an AR-driven oncogene (Figure 17G). In this model, treatment with vaccine prior to ADT, compared to control vaccination prior to ADT, led to a greater anti-tumor response (Figure 17H, and Figure 19) and longer overall survival (Figure17I), and, unlike in the Myc-CaP model, these were further significantly improved with the addition of testosterone after ADT. This treatment was similarly associated with a significant decrease in tumor-infiltrating MDSCs in the group receiving vaccine (Figure 17J). There were no significant increases in CD4+ and CD8+ T cells detected following this treatment (Figures 17K and 17L).

3.4 Discussion and Conclusion

Following the FDA approval of Sipuleucel-T, there has been a growing interest in utilizing immunotherapy for prostate cancer treatment, either as monotherapy or in combination with other therapies. However, a current dearth of preclinical data hinders insights into how the sequencing of these therapies impacts immune cell populations within tumors and their optimal integration with ADT, the cornerstone of treatment for recurrent prostate cancer. This report aimed to investigate the timing and scheduling of ADT in combination with AR-targeted vaccination in immune-competent murine prostate tumor models. Key findings include: 1) Administering pTVG-AR → ADT enhanced anti-tumor responses more than the reverse sequence, delaying time to tumor growth and improving overall survival in several murine models; 2) pTVG-AR → ADT led to increased infiltration of CD4+ and CD8+T cells, particularly antigen-specific CD8+T cells, into the tumor microenvironment which were crucial for the observed anti-tumor effects; 3) depletion of MDSCs, or inhibiting MDSC migration using a CXCR2 antagonist, enhanced anti-tumor responses; and 4) ADT followed by testosterone supplementation modulated the tumor microenvironment by reducing MDSCs, and this could further improve the anti-tumor effect of AR-targeted vaccination in one murine prostate cancer model. These outcomes underscore the pivotal role of vaccination and ADT administration sequence in shaping the tumor immune microenvironment and influencing therapeutic responses.

ADT has been recognized for its ability to augment T-cells within human prostate tumors. Notably, the infiltration of CD8+ T cells into tumors is considered beneficial for anti-tumor immune responses [33,34]. Consequently, there has been an effort to explore strategies leveraging this

effect to enhance CD8+T cell numbers with vaccine-based approaches. However, controversy persists regarding the optimal timing and sequence of ADT administration in conjunction with immunotherapy. In a study led by Drake et al., prostate-specific CD4+ T cells that were adoptively transferred initially exhibited proliferation in mice with tumors. However, their proliferation diminished over time. Castration mitigated this tolerance, allowing for expanded effector function post-vaccination. This suggested that prostate cancer immunotherapies might be more effective after ADT [11]. In contrast, Koh et al. observed that when mice were vaccinated with DNA encoding prostate stem cell antigen (PSCA) followed by castration, this led to more PSCA-specific interferon-gamma-secreting T cells compared to castration followed by vaccination [35]. Similarly, a study by Madan et al., suggested that patients with nonmetastatic castration-resistant prostate cancer who received a PSA-targeted vaccine before second-line hormone therapy experienced improved survival compared to those who underwent hormone therapy before vaccination [16]. Sipuleucel-T, the only vaccine that has been FDA approved as a treatment for human prostate cancer, was approved for patients with castration resistance who were already being treated with ADT [36]. It has also been evaluated in sequence with ADT. For example, one study compared the administration sequence of leuprolide before sip-T (ADT → sip-T) or after sip-T (sip →ADT) in patients with non-castrate, PSA-recurrent prostate cancer. These investigators found significantly elevated PA2024-specific humoral responses when ADT was administered after sip-T treatment. T-cell responses similarly exhibited higher IFNγ production in the group receiving sip-T → ADT compared to ADT → sip-T, suggesting a similar impact of timing on immunotherapy effectiveness [37]. Our study is the first to demonstrate that vaccination prior to ADT can activate antigen-specific T cells that are then specifically recruited in greater numbers to the tumor following ADT. This could provide a mechanism for the sequence preference

that has been observed clinically. Our studies suggest a critical role for CD8 T cells, as depletion of these cells after immunization and prior to ADT abrogated the anti-tumor efficacy, however our data do not exclude a role for CD4 T cells that were also augmented after vaccination and ADT. In any case, our findings suggest that a preferred prostate cancer population for treatment with vaccines may be those who have not yet initiated androgen deprivation. This approach is already being evaluated in a neoadjuvant trial (NCT04989946) in which patients are being treated with AR-specific vaccination prior to receiving a short course of degarelix [38].

It is clear that ADT has profound effects on the prostate tumor immune microenvironment. Initially, ADT triggers a surge in T-cell infiltration, but this is later replaced by a significant increase in MDSCs [34,39]. In the Myc-CaP murine model, this change occurred within the span of days to weeks. Based on results from clinical trials evaluating ADT prior to prostatectomy, T cells appear to persist in humans several weeks to at least one month post ADT [5,40]. However, myeloid cells are known to be predominant in castration-resistant tumors and have been associated with decreased survival [5,41]. Hence, the recruitment of MDSCs following ADT needs to be considered in general for the treatment of prostate cancer, and in particular when combined with T-cell activation strategies such as vaccines. Our data, in fact, demonstrated that vaccination initiated after ADT had little treatment effect (Figure 1), however this was also slightly improved if MDSC were depleted (Supplemental Figure 9). Strategies aimed at inhibiting their immunosuppressive functions, or depleting or hindering MDSC recruitment, have been explored, including the use of CSF-1R-targeting antibodies [42]. However, these approaches have demonstrated limited success in prostate cancer clinical trials [43,44]. An approach that holds promise based on our data is CXCR2 inhibition, potentially hindering MDSC recruitment post

ADT [45,46]. Use of a CXCR2 inhibitor in combination with vaccine and ADT would be a logical direction for future clinical trials.

Our findings highlight the critical role of timing of T cell and MDSC recruitment within prostate tumors following ADT. While testosterone "reversal" of ADT modestly reduced MDSC levels, it did not lead to increased T cell infiltration as observed following clodronate liposomes or reparixin treatment. Hence, directly targeting MDSCs may be more effective than cycling androgen deprivation. However, cycling ADT is a more practical option, not requiring additional therapies, and translational approaches could involve optimizing ADT schedules using agents with shorter half-lives. Intermittent ADT, using cycles of treatment and breaks rather than continuous suppression of testosterone, has been used clinically to balance cancer control while minimizing side effects. Studies have not demonstrated this to be superior to continuous androgen deprivation, at least for metastatic prostate cancer, however, and hence this has fallen out of favor [47,48]. On the other hand, BAT therapy employs cyclical, high-dose testosterone administration aimed at restoring sensitivity to androgen signaling inhibition in patients with previously treated castration-resistant prostate cancer (CRPC) [49,50]. This has been evaluated in phase 2 trials in combination with enzalutamide (TRANSFORMER trial), as well as in combination with nivolumab (COMBAT trial), both of which have suggested clinical activity and superior quality-of-life measures [51,52]. Moreover, the use of supraphysiological levels of testosterone has been demonstrated to activate the STING pathway and downstream NFkB signaling, as well as lead to increases in tumor cell secretion of CXCL10, a chemokine associated with T cell recruitment [53], suggesting this treatment could be ideally combined with anti-tumor vaccination. Moreover, since BAT has been previously evaluated in combination with nivolumab, and we have previously demonstrated that

the anti-tumor efficacy of vaccination can be improved with concurrent PD-1 blockade in patients with prostate cancer [54,55], the combination of vaccine, BAT, and PD-1 blockade is a logical direction for clinical evaluation.

In summary, our study contributes to the understanding of how ADT might be optimally used with prostate cancer-directed immunotherapies, and AR-targeted vaccination in particular, based on its effects on the prostate cancer immune microenvironment. The administration of pTVG-AR prior to ADT exhibited superior anti-tumor responses, leading to increased infiltration of CD4+ and CD8+ T cells, and notably antigen-specific CD8+ T cells which were critical for the observed anti-tumor effects. Additionally, ADT followed by testosterone supplementation modulated the tumor microenvironment by reducing MDSCs and, when combined with vaccination, led to improved anti-tumor efficacy in at least one murine prostate cancer model. These findings suggest logical directions for future clinical trials to optimally use anti-tumor vaccines either before ADT in patients with early-stage disease or in combination with intermittent or BAT schedules of ADT for patients with later stage disease.

3.5 Figures

Figure 1: Sequence of vaccination and ADT, with vaccination given prior to ADT, (pTVG-AR → ADT) significantly improved anti-tumor responses in murine prostate tumor models.

FVB mice were implanted with Myc-CaP tumor cells and treated with degarelix (ADT), with pTVG4 (vector control) or pTVG-AR delivered before or after ADT and followed for tumor growth. Shown is a schema (panel A), tumor growth curves (panel B), and Kaplan-Meier curves depicting survival (time to a tumor size of $2cm^3$ or death, panel C). Similarly, male C57BL/6 were implanted with TRAMP-C1 tumor cells, treated with ADT, and with DNA immunization with pTVG4 or pTVG-AR initiated either before or after ADT. For tumor growth curves, asterisks demonstrate significant (*$p < 0.05$, **$p<0.01$ **$p<0.001$) differences as assessed by linear mixed effects model with Geisser-Greenhouse correction and Tukey's multiple comparisons test with individual variances. Kaplan-Meier curves were compared using the log-rank test with asterisks indicating *$p<0.05$, **$p<0.01$, and ***$p<0.001$. Results are each from one experiment, with n=7-8 animals per group, and are representative of two independent experiments.

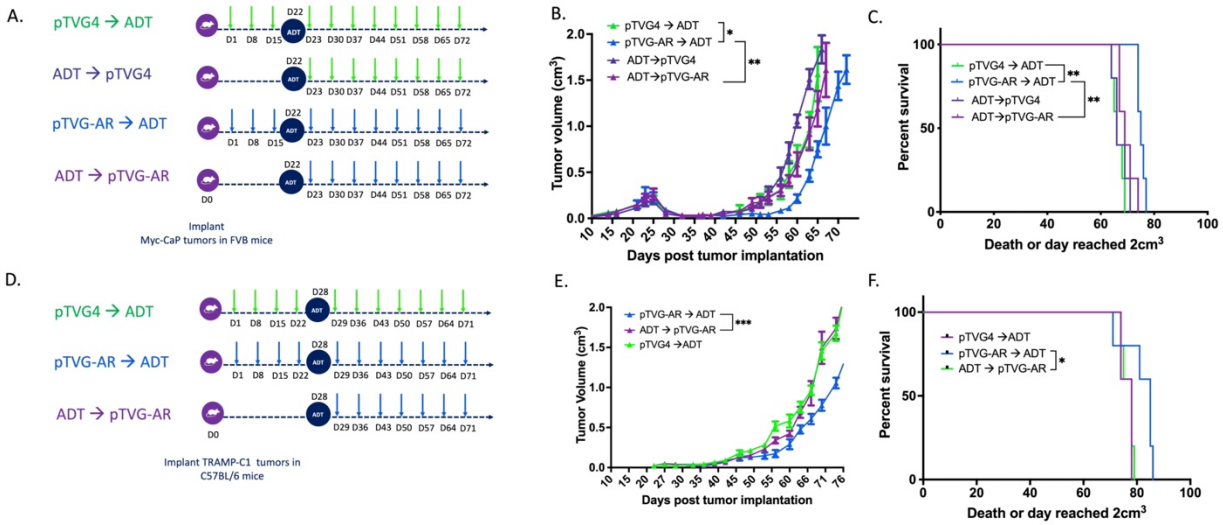

Figure 1: Sequence of vaccination and ADT, with vaccination given prior to ADT, (pTVG-AR → ADT) significantly improved anti-tumor responses in murine prostate tumor models.

Figure 2: Sequence of vaccination and ADT, with vaccination given prior to ADT, (pTVG-AR → ADT) significantly improved anti-tumor responses in Myc-CaP/FVB tumor model. (A)Tumor growth study in the Myc-CaP/FVB model and (B) survival in a repeat experiment from that shown in Figure 1B and 1C. (C) Individual tumor growth curves from experiment shown in Figure 1B.

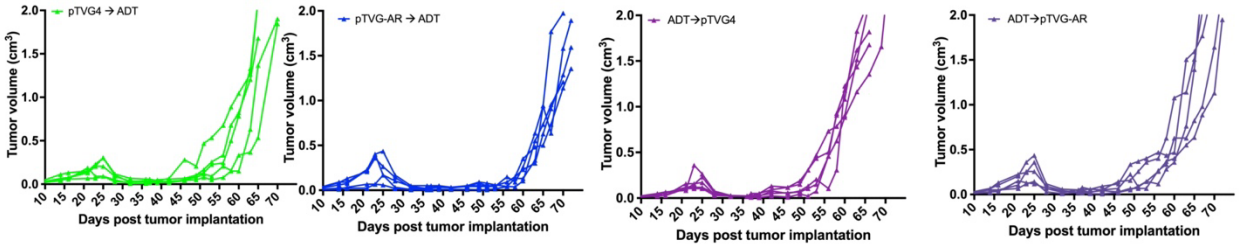

Figure 2: Sequence of vaccination and ADT, with vaccination given prior to ADT, (pTVG-AR → ADT) significantly improved anti-tumor responses in Myc-CaP/FVB tumor model.

Figure 3: Sequence of vaccination and ADT, with vaccination given prior to ADT, (pTVG-AR → ADT) significantly improved anti-tumor responses in TRAMP-C1/C57BL/6 tumor model. Individual tumor growth curves from experiment shown in Figure 1E. Results are from one experiment and are representative of two independent experiments.

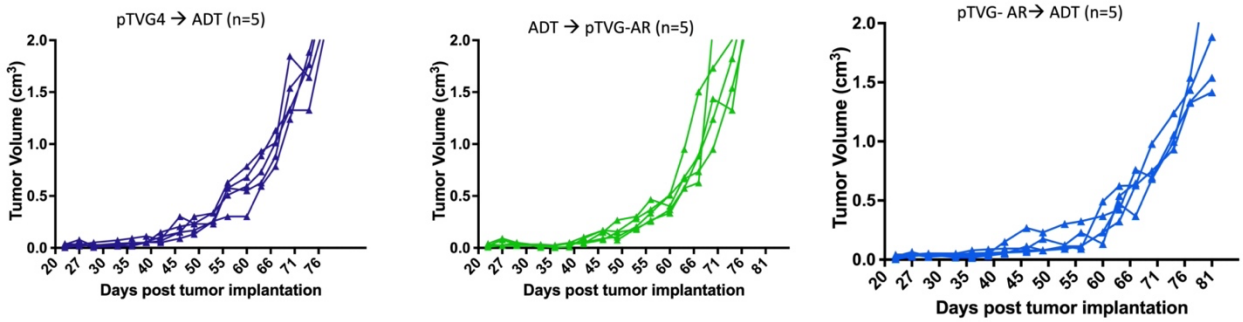

Figure 3: Sequence of vaccination and ADT, with vaccination given prior to ADT, (pTVG-AR → ADT) significantly improved anti-tumor responses in TRAMP-C1/C57BL/6 tumor model.

Figure 4: Sequence of vaccination and ADT, with vaccination given prior to ADT, (pTVG-AR → ADT) seemed to improve anti-tumor responses in A2-TRAMP tumor model. Groups of 10 male A2-TRAMP mice were treated beginning at 16 or 20 weeks of age with DNA immunization and ADT and followed for survival (schema in panel A). Shown are the Kaplan-Meier survival curves (panel B).

Figure 4: Sequence of vaccination and ADT, with vaccination given prior to ADT, (pTVG-AR → ADT) seemed to improve anti-tumor responses in A2-TRAMP tumor model.

Figure 5: ADT led to an increase in prostate tumor-infiltrating T cells and myeloid cells, and T cell infiltration was increased with vaccination prior to ADT. Myc-CaP tumor cells were implanted in male FVB mice and treated with ADT, and DNA immunization was delivered before or after ADT. Additional groups received either vector (pTVG4) or vaccine (pTVG-AR) alone, without ADT. Tumors were sampled at different days for flow cytometry analysis. Shown are a schema (panel A) and representative dot plots (panel B) of CD4+CD3+ and CD8+CD3+ T cells (collected on days 21 and 36), or CD11b+Gr1+ MDSCs (panel H, collected on days 36 and 60). CD4+ T cells (panel C), CD8+ T cells (panel D), and CD11b+Gr-1+ MDSC (panel E) are shown as a percentage of CD45+ cells. CD4+FoxP3+ Tregs (panel F) are shown as a percentage of CD4+ cells. Panels C-F were compared using one-way ANOVA with Tukey's multiple comparisons test; asterisks indicate *$p<0.05$, **$p<0.01$, and ***$p<0.001$. Results are from one experiment and are representative of two independent experiments.

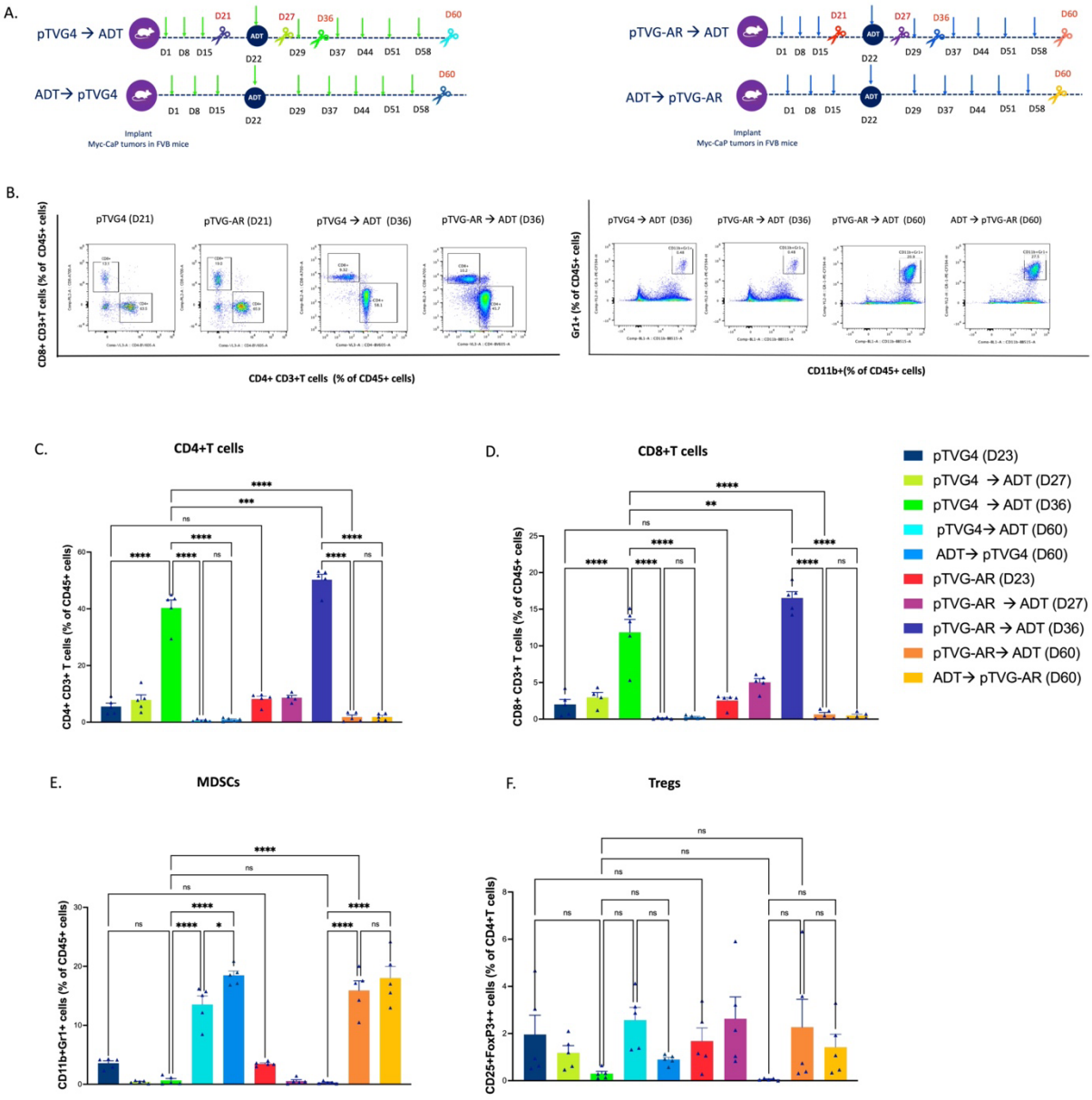

Figure 5: ADT led to an increase in prostate tumor-infiltrating T cells and myeloid cells, and T cell infiltration was increased with vaccination prior to ADT.

Figure 6: Immunization prior to ADT led to infiltration of tumors by antigen-specific CD8+ T cells.

Myc-CaP tumor cells were implanted in male FVB mice, treated with ADT and DNA immunization as described before, and tumors were harvested two weeks after ADT (schema in panel A). CD8+CD3+T cells were isolated and IFNγ ELISPOT was performed with media alone, AR pool peptides, AR-25, or anti-CD3/anti-CD28 beads. Raw data are shown in panel B and quantified in panel C. Myc-CaP tumor cells were implanted in male FVB mice, treated with ADT and DNA immunization before or after ADT, and mice received IgG (control) or anti-CD8 depleting antibody on days 16, 18 and 20, before ADT treatment (schema in panel D). Shown are the tumor growth curves (panel E) and Kaplan-Meier survival curves (panel F). Panel C was compared using unpaired-t tests. Tumor growth curve comparisons were made using one-way ANOVA with Tukey's multiple comparisons test. Kaplan-Meier curves were compared using the log-rank test. Asterisks indicate *$p<0.05$, **$p<0.01$, and ***$p<0.001$. Results are from one experiment and are representative of two independent experiments.

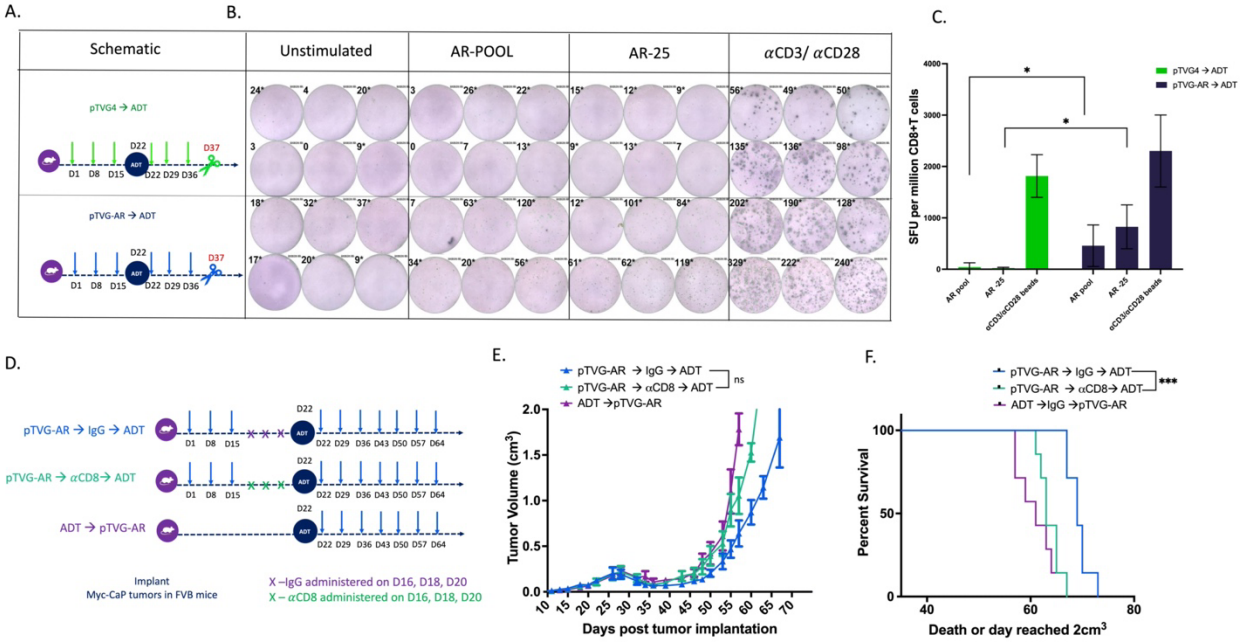

Figure 6: Immunization prior to ADT led to infiltration of tumors by antigen-specific CD8+ T cells.

Figure 7: Identification of AR-25 as the dominant epitope in the FVB background by IFNγ ELISA. Naïve FVB male mice were immunized with pTVG4 or pTVG-AR weekly for 4 weeks. Splenocytes were isolated and stimulated with 15-mer peptides (1-62 epitopes of AR) for 72 hours and IFNγ ELISA was performed. Shown is the quantification of IFNγ ELISA.

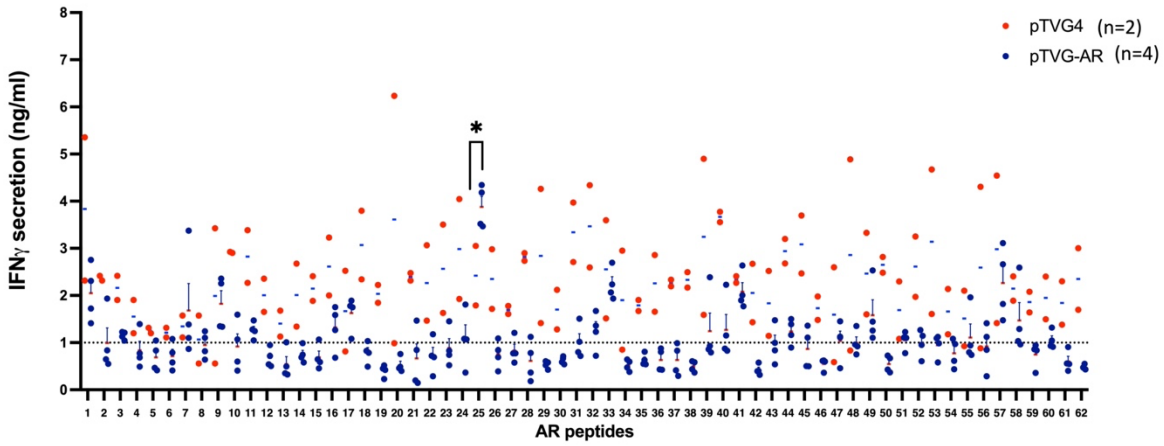

Figure 7: Identification of AR-25 as the dominant epitope in the FVB background by IFNγ ELISA.

Figure 8: Immunization prior to ADT had higher infiltration of CD8+T cells with increased Granzyme B, Perforin and TNFα expression. Myc-CaP tumor cells were implanted in male FVB mice and treated with ADT, and DNA immunization before or after ADT, with tumors sampled at day 36 for flow cytometry analysis. Shown are the MFI of Granzyme B, Perforin and TNFα (panels A-C) on CD8+CD3T cells Panels A-C were compared using student's t test with asterisks indicating *$p<0.05$, **$p<0.01$, and ***$p<0.001$.

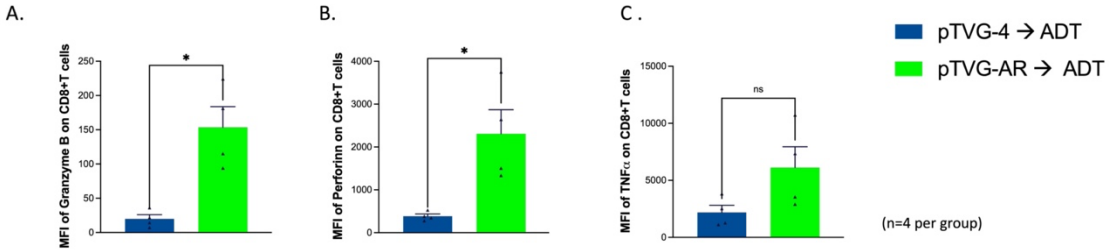

Figure 8:Immunization prior to ADT had higher infiltration of CD8+T cells with increased Granzyme B, Perforin and TNFα expression.

Figure 9: Immunization prior to ADT led to antigen-specific immune responses. Myc-CaP tumor cells were implanted in male FVB mice, treated with DNA immunization or ADT and DNA immunization, and tumors were harvested on day 36 as shown in panel A. CD8+CD3+T cells were isolated and IFNγ ELISPOT was performed with media alone or AR-25. Raw data are shown in panel B and quantified in panel C.

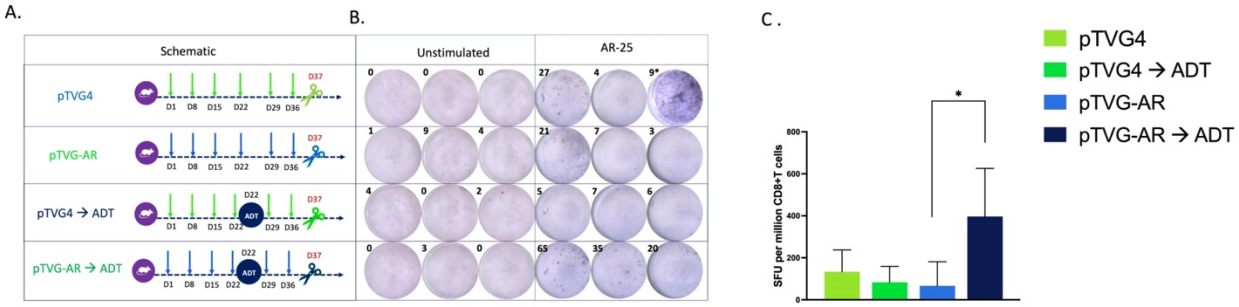

Figure 9: Immunization prior to ADT led to antigen-specific immune responses.

Figure 10: Depletion of CD8+T cells in the pTVG-AR → ADT sequence worsened anti-tumor responses. Individual tumor growth curves from experiment shown in Figure 3E. Results are from one experiment and are representative of two independent experiments.

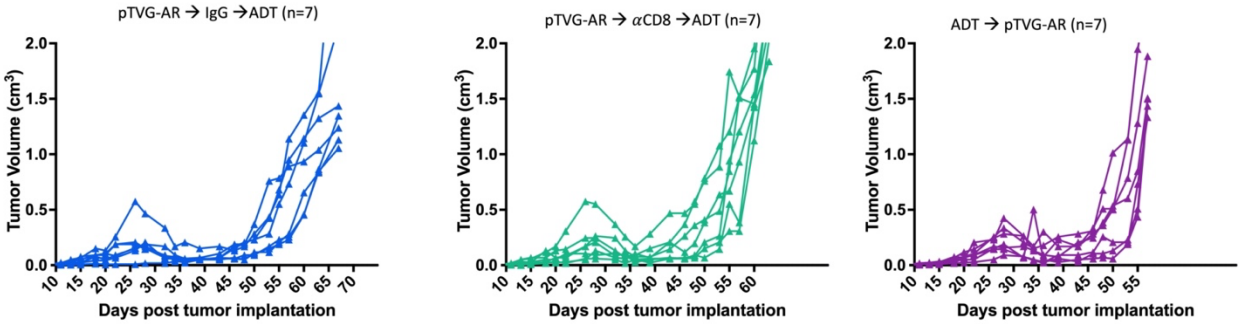

Figure 10: Depletion of CD8+T cells in the pTVG-AR → ADT sequence worsened anti-tumor responses.

Figure 11: ADT leads to infiltration of MDSCs, and depletion of these populations improved anti-tumor responses in combination with DNA vaccines. Myc-CaP tumor cells were implanted in male FVB mice and treated with ADT or control as indicated in panel A. Shown are the tumor growth curves and time points at which groups of animals were euthanized for tumor assessments (panel B) and Kaplan-Meier survival curves (panel C). Tumors collected were evaluated by flow cytometry for CD4+ T cells (panel D), and CD8+ T cells (panel E) and CD11b+Gr-1+ MDSC (panel F). Myc-CaP tumor cells were implanted in male FVB mice, treated as before, and then received control- or clodronate-encapsulated liposomes as indicated (schema in panel G). Shown are the tumor growth curves (panel H) and Kaplan-Meier survival curves (panel me). In a parallel study, tumors were collected at day 62 and evaluated by flow cytometry for CD4+ T cells (panel J), and CD8+ T cells (panel K) and CD11b+Gr-1+ MDSC (panel L). For tumor growth curves, asterisks demonstrate significant ($p < 0.05$) differences as assessed by linear mixed effects model with Geisser-Greenhouse correction and Kaplan-Meier curves were compared using the log-rank test with asterisks indicating *$p<0.05$, **$p<0.01$, and ***$p<0.001$. For panels D-F and J-L, comparisons were made using one-way ANOVA with Tukey's multiple comparisons test; asterisks indicate *$p<0.05$, **$p<0.01$, and ***$p<0.001$. Results are from single experiments with n=5 (panels D-F) or 3 (panels J-L) mice per group.

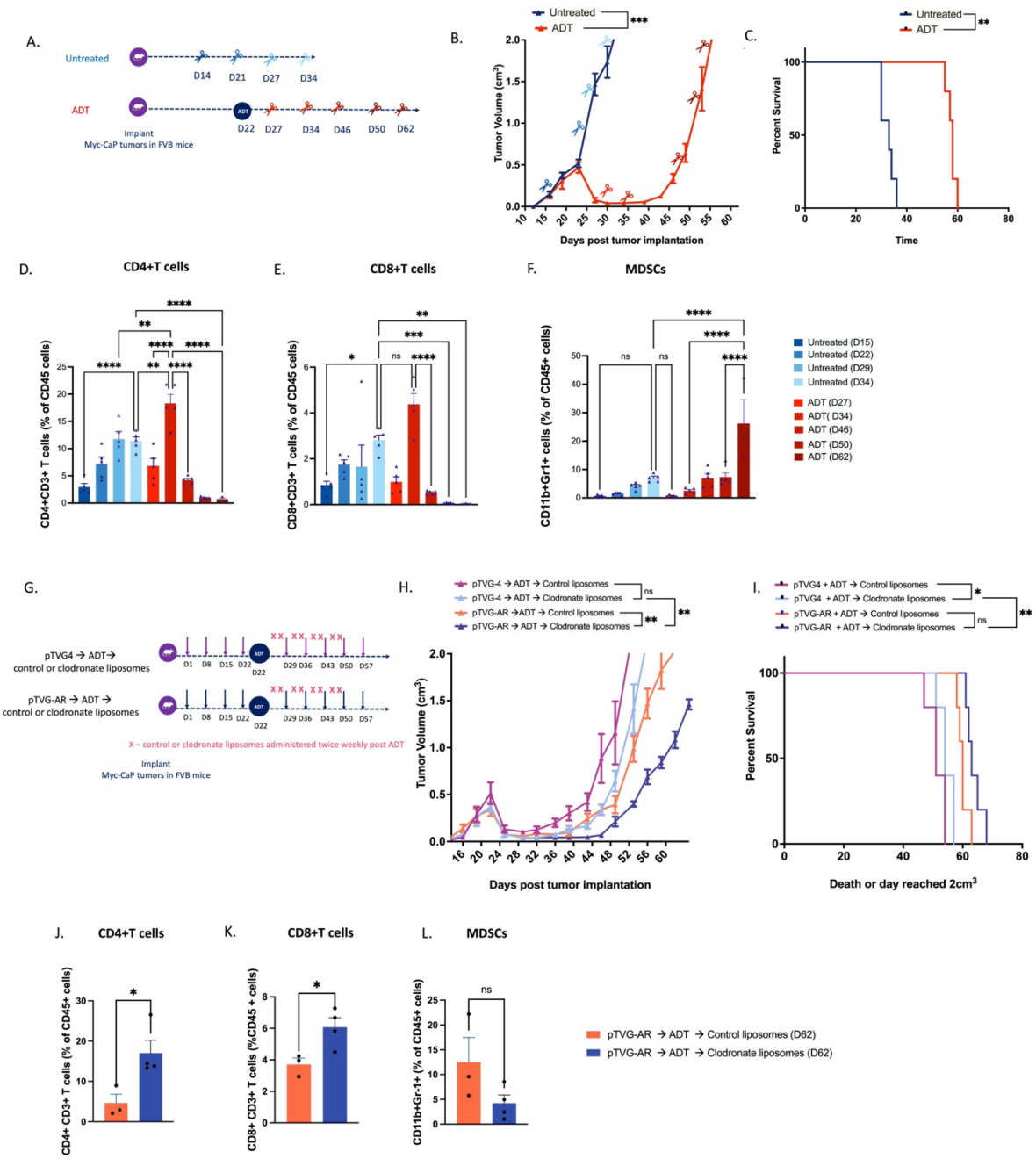

Figure 11: ADT leads to infiltration of MDSCs, and depletion of these populations improved anti-tumor responses in combination with DNA vaccines

Figure 12: Clodronate liposome treatment significantly improved anti-tumor responses in the combination groups. Myc-CaP tumor cells were implanted in male FVB mice, treated with ADT followed by DNA immunization then treated with clodronate liposomes or mice were treated with control or clodronate liposomes as control(schema in panel A). Shown are the tumor growth curves (panel B) and Kaplan-Meier survival curves (panel C). Individual tumor growth curves from experiment shown in 5B (panel D). Individual tumor growth curves from experiment shown in Figure 4H. Results are from one experiment and are representative of two independent experiments panel E). Results are from one experiment and are representative of two independent experiments. For tumor growth curves, comparisons were made by linear mixed effects model with Geisser-Greenhouse correction and Tukey's multiple comparisons test with individual variance; Kaplan-Meier curves were compared using the log-rank test. Asterisks demonstrate significant differences (*$p<0.05$, **$p<0.01$, and ***$p<0.001$). Results shown are from one experiment, with n=5 animals per treatment group

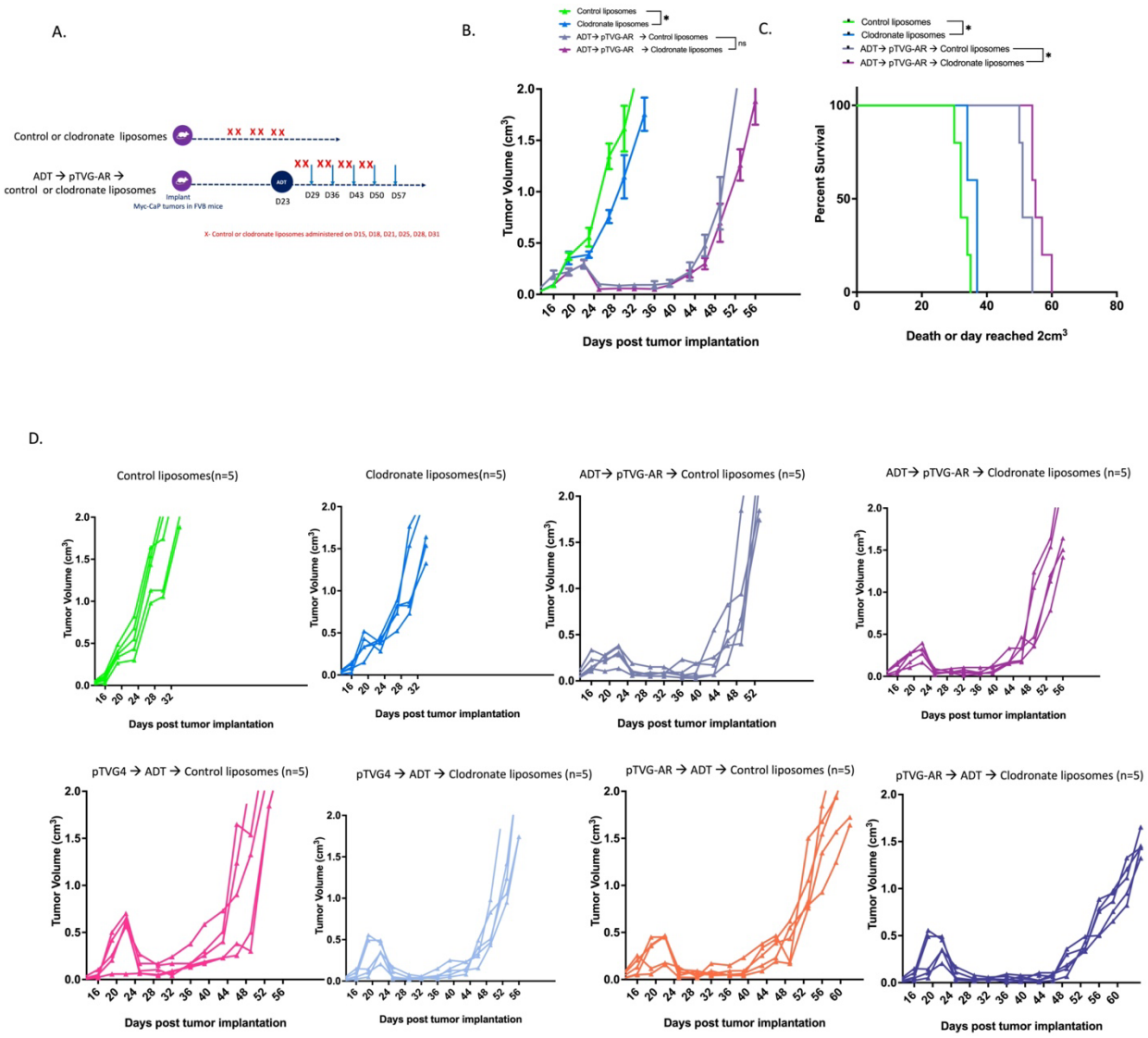

Figure 12: Clodronate liposome treatment significantly improved anti-tumor responses in the combination groups.

Figure 13: CXCR2 blockade improved anti-tumor efficacy in the pTVG-AR→ADT combination. Myc-CaP tumor cells were implanted in male FVB mice, treated with vaccine, ADT and reparixin as indicated in panel A. Shown are the tumor growth curves (panel B) and Kaplan-Meier survival curves (panel C). A similar study was performed, and tumors were collected on day 56 and evaluated by flow cytometry for CD4+ T cells (panel D), and CD8+ T cells (panel E) and CD11b+Gr-1+ MDSC (panel F). In a parallel experiment, tumors were harvested on day 37 and CD8+CD3+T cells were isolated (schema in panel G). IFNγ ELISPOT was performed with media alone, AR pool peptides, AR-25, or anti-CD3/anti-CD28 beads, with results as shown in panel H and quantified in panel I. For tumor growth curves, asterisks demonstrate significant ($p < 0.05$) differences as assessed by linear mixed effects model with Geisser-Greenhouse correction and Kaplan-Meier curves were compared using the log-rank test with asterisks indicating *$p<0.05$, **$p<0.01$, and ***$p<0.001$. For panels D-F, comparisons were made using one-way ANOVA with Tukey's multiple comparisons test; asterisks indicate *$p<0.05$, **$p<0.01$, and ***$p<0.001$. Panel I was compared using unpaired-t tests. Results are from single experiments with n=5 mice per group.

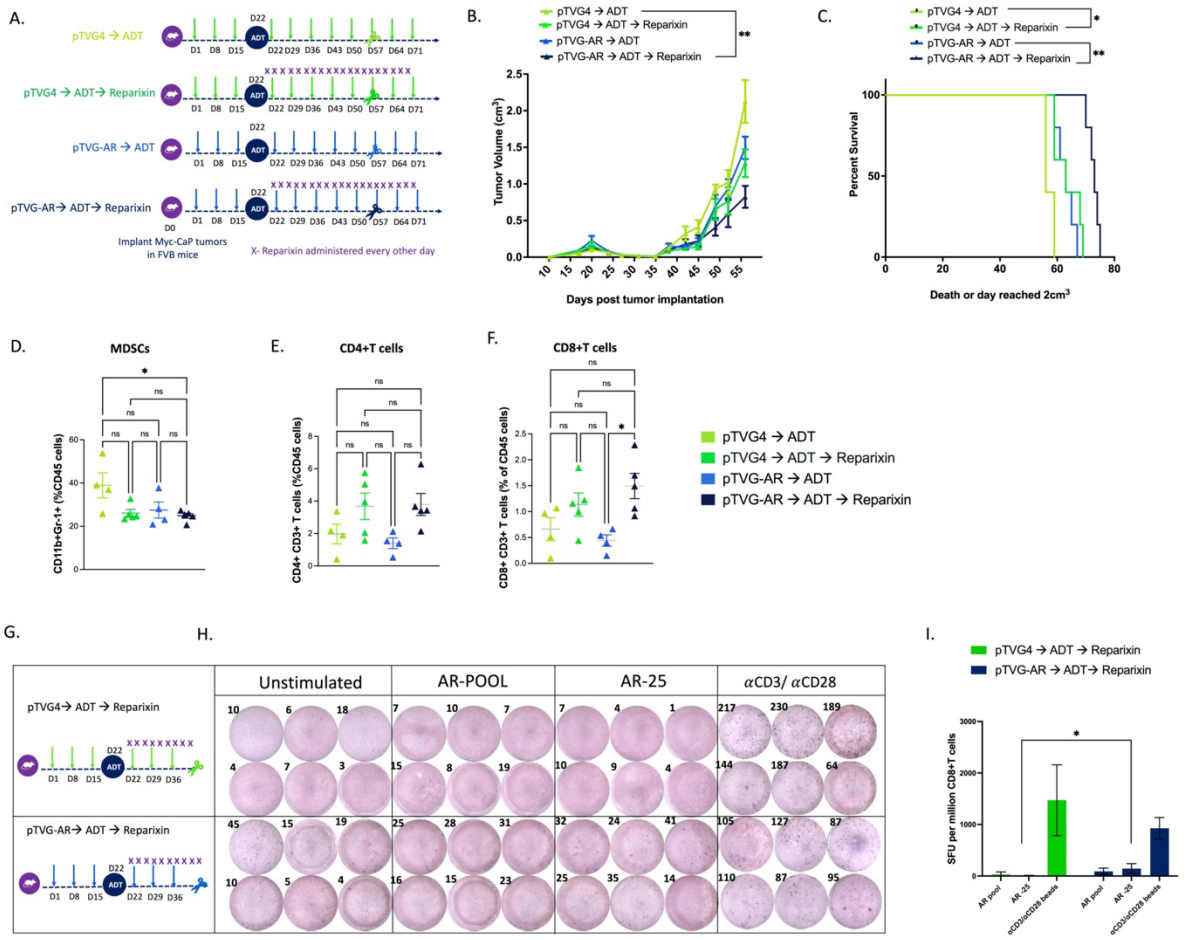

Figure 13: CXCR2 blockade improved anti-tumor efficacy in the pTVG-AR -> ADT combination.

Figure 14: CXCR2 blockade improved antitumor efficacy in the pTVG-AR→ADT combination. Individual tumor growth curves from experiment shown in Figure 7B. Results are from one experiment.

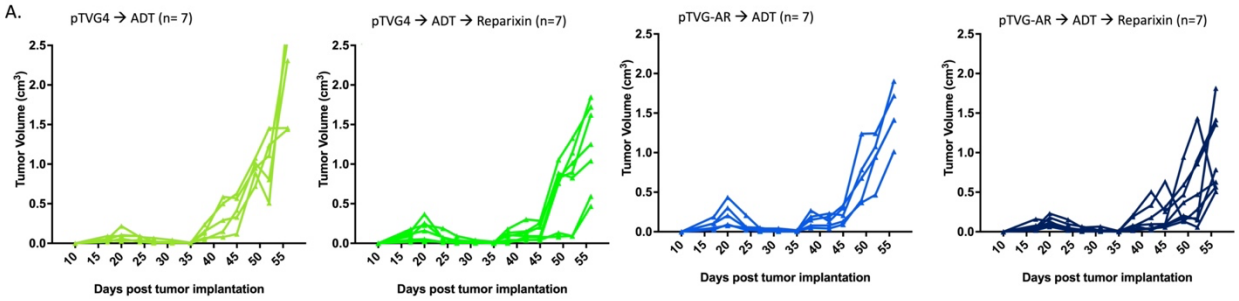

Figure 14: CXCR2 blockade improved antitumor efficacy in the pTVG-AR→ADT combination.

Figure 15: ADT and testosterone reversal led to reduced accumulation of MDSCs although significantly worsened anti-tumor responses in the Myc-CaP tumor model.

Myc-CaP tumor cells were implanted in male FVB mice, treated with ADT and testosterone as indicated in panel A. Shown are the tumor growth curves (panel B) and Kaplan-Meier survival curves (panel C). In a parallel study, tumors were collected on days 34, 46 and 66 and evaluated by flow cytometry for CD11b+Gr-1+ MDSC (panel D), CD4+ T cells (panel E), and CD8+ T cells (panel F). For tumor growth curves, asterisks demonstrate significant ($p < 0.05$) differences as assessed by linear mixed effects model with Geisser-Greenhouse correction and Kaplan-Meier curves were compared using the log-rank test with asterisks indicating *$p<0.05$, **$p<0.01$, and ***$p<0.001$. For panels D-F, comparisons were made using one-way ANOVA with Tukey's multiple comparisons test; asterisks indicate *$p<0.05$, **$p<0.01$, and ***$p<0.001$. Results are from one experiment with n=5 mice per group.

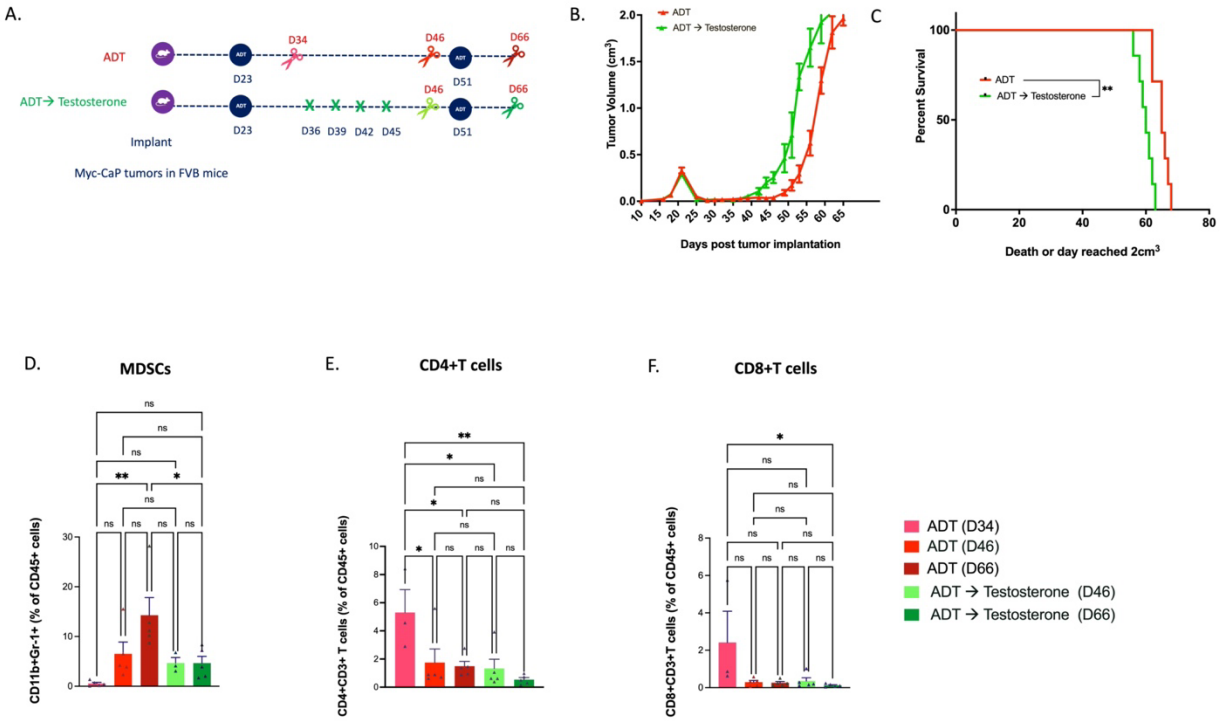

Figure 15: ADT and testosterone reversal led to reduced accumulation of MDSCs although significantly worsened anti-tumor responses in the Myc-CaP tumor model.

Figure 16: ADT and testosterone reversal worsened anti-tumor responses in the Myc-CaP tumor model. Individual tumor growth curves from experiment shown in Figure 5B. Results are from one experiment and are representative of two independent experiments.

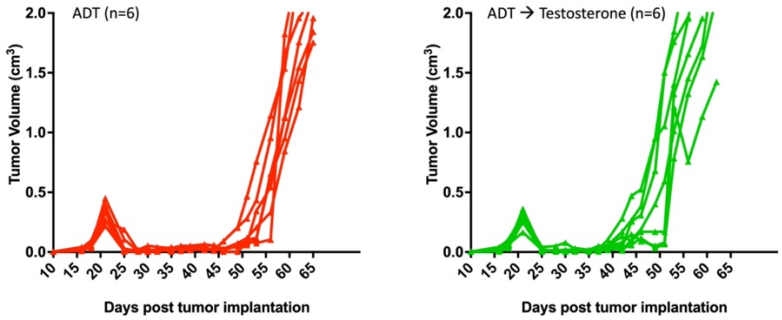

Figure 16: ADT and testosterone reversal worsened anti-tumor responses in the Myc-CaP tumor model.

Figure 17: ADT and testosterone reversal led to reduced accumulation of MDSC and significantly improved anti-tumor responses when combined with vaccination in the TRAMP-C1 tumor model but not in the Myc-CaP model. Myc-CaP tumor cells were implanted in male FVB mice and treated with ADT and DNA immunization with or without testosterone, as indicated in panel A. Shown are the tumor growth curves (panel B) and Kaplan-Meier survival curves (panel C). A similar study was performed, and tumors were collected on days 56 and evaluated by flow cytometry for CD11b+Gr-1+ MDSC (panel D), CD4+ T cells (panel E), and CD8+ T cells (panel F). TRAMP-C1 tumor cells were implanted in male C56BL/6 mice, treated with ADT and DNA vaccination with or without testosterone as indicated in panel G. Shown are the tumor growth curves (panel H) and Kaplan-Meier survival curves (panel I). A similar study was performed, and tumors were collected on days 56 and evaluated by flow cytometry for CD11b+Gr-1+ MDSCs (panel J), CD4+ T cells (panel K), and CD8+ T cells (panel L). For tumor growth curves, asterisks demonstrate significant ($p < 0.05$) differences as assessed by linear mixed effects model with Geisser-Greenhouse correction and Kaplan-Meier curves were compared using the log-rank test with asterisks indicating *$p<0.05$, **$p<0.01$, and ***$p<0.001$. For panels D-F and J-L comparisons were made using one-way ANOVA with Tukey's multiple comparisons test; asterisks indicate *$p<0.05$, **$p<0.01$, and ***$p<0.001$. Results are from one experiment with n=5 mice per group.

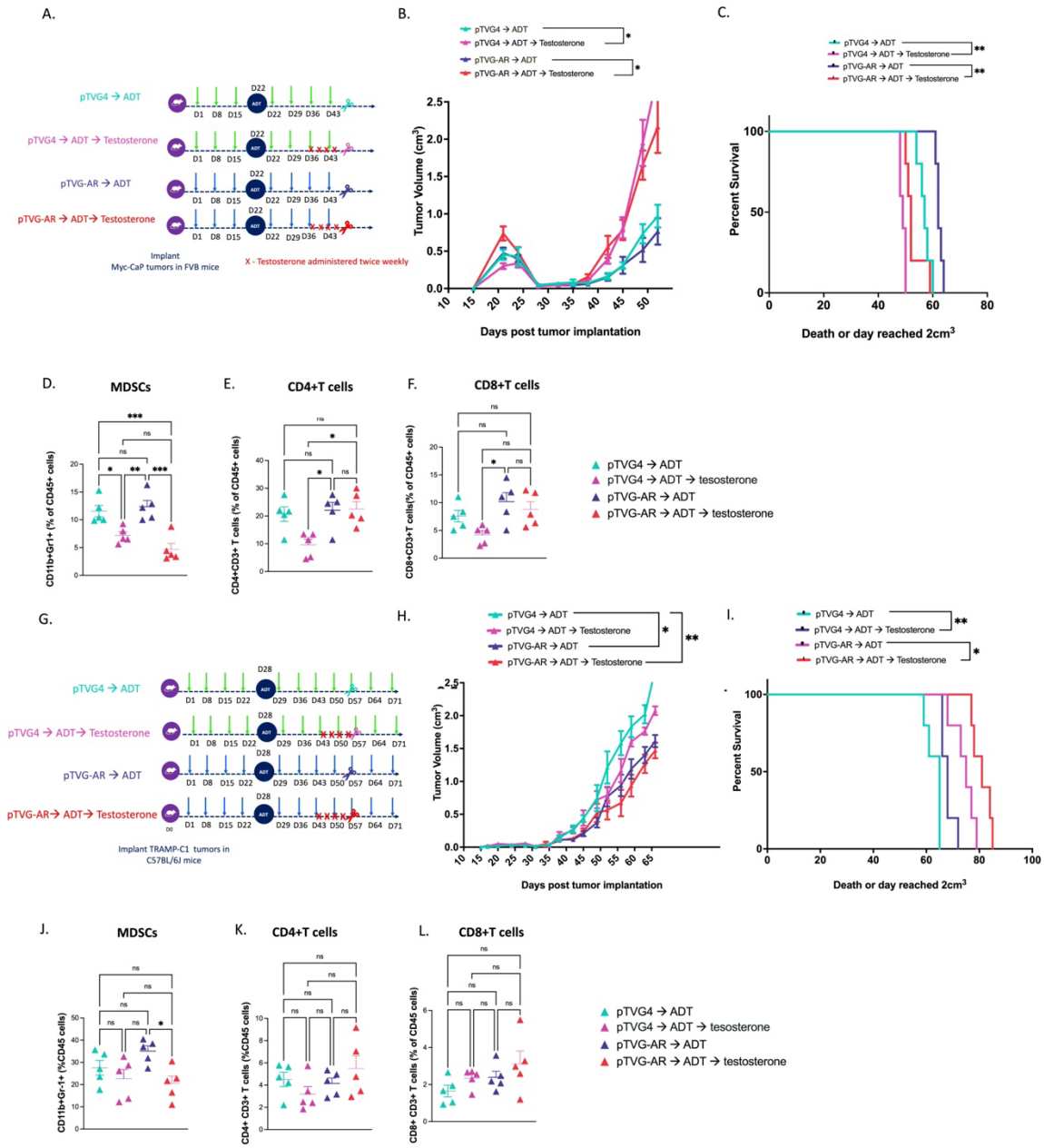

Figure 17: ADT and testosterone reversal led to reduced accumulation of MDSC and significantly improved anti-tumor responses when combined with vaccination in the TRAMP-C1 tumor model but not in the Myc-CaP model.

Figure 18: ADT and testosterone reversal in combination with vaccination worsened anti-tumor responses in the Myc-CaP tumor model. Individual tumor growth curves from experiment shown in Figure 6B. Results are from one experiment and are representative of two independent experiments.

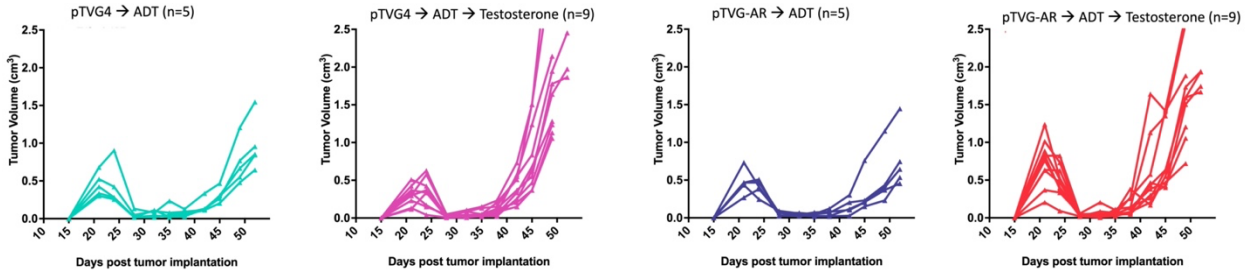

Figure 18: ADT and testosterone reversal in combination with vaccination worsened anti-tumor responses in the Myc-CaP tumor model.

Figure 19: ADT and testosterone reversal in combination with vaccination improved anti-tumor responses in the TRAMP-C1 tumor model. Individual tumor growth curves from experiment shown in Figure 6H. Results are from one experiment and are representative of two independent experiments.

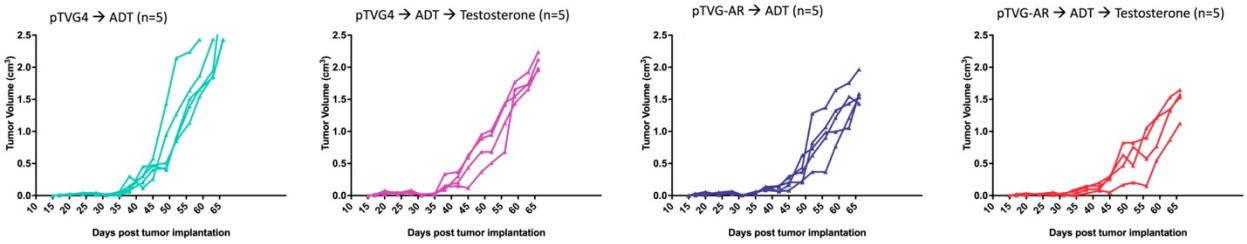

Figure 19: ADT and testosterone reversal in combination with vaccination improved anti-tumor responses in the TRAMP-C1 tumor model.

3.5 References

1. Siegel RL, Miller KD, Wagle NS, Jemal A. Cancer statistics, 2023. CA Cancer J Clin. 2023; 73: 17–48.

2. Perlmutter MA, Lepor H. Androgen Deprivation Therapy in the Treatment of Advanced Prostate Cancer. Rev Urol. 2007; 9: S3–8.

3. Garcia JA, Rini BI. Castration-resistant prostate cancer: Many treatments, many options, many challenges ahead. Cancer. 2012; 118: 2583–93.

4. HUGGINS C, STEVENS RE Jr, HODGES CV. STUDIES ON PROSTATIC CANCER: II. THE EFFECTS OF CASTRATION ON ADVANCED CARCINOMA OF THE PROSTATE GLAND. Arch Surg. 1941; 43: 209–23.

5. Mercader M, Bodner BK, Moser MT, et al. T cell infiltration of the prostate induced by androgen withdrawal in patients with prostate cancer. Proc Natl Acad Sci U S A. 2001; 98: 14565–70.

6. Morse MD, McNeel DG. T cells localized to the androgen-deprived prostate are TH1 and TH17 biased. The Prostate. 2012; 72: 1239–47.

7. Gannon PO, Poisson AO, Delvoye N, Lapointe R, Mes-Masson A-M, Saad F. Characterization of the intra-prostatic immune cell infiltration in androgen-deprived prostate cancer patients. J Immunol Methods. 2009; 348: 9–17.

8. Potluri HK, Ng TL, Newton MA, et al. Antibody profiling of patients with prostate cancer reveals differences in antibody signatures among disease stages. J Immunother Cancer. 2020; 8: e001510.

9. Kwilas AR, Ardiani A, Dirmeier U, Wottawah C, Schlom J, Hodge JW. A poxviral-based cancer vaccine the transcription factor twist inhibits primary tumor growth and metastases in a model of metastatic breast cancer and improves survival in a spontaneous prostate cancer model. Oncotarget. 2015; 6: 28194–210.

10. Tang S, Moore ML, Grayson JM, Dubey P. Increased CD8+ T-cell function following castration and immunization is countered by parallel expansion of regulatory T cells. Cancer Res. 2012; 72: 1975–85.

11. Drake CG, Doody ADH, Mihalyo MA, et al. Androgen ablation mitigates tolerance to a prostate/prostate cancer-restricted antigen. Cancer Cell. 2005; 7: 239–49.

12. Ardiani A, Farsaci B, Rogers CJ, et al. Combination therapy with a second-generation androgen receptor antagonist and a metastasis vaccine improves survival in a spontaneous prostate cancer model. Clin Cancer Res Off J Am Assoc Cancer Res. 2013; 19: 6205–18.

13. Luchner M, Reinke S, Milicic A. TLR Agonists as Vaccine Adjuvants Targeting Cancer and Infectious Diseases. Pharmaceutics. 2021; 13: 142.

14. Arredouani MS, Tseng-Rogenski SS, Hollenbeck BK, et al. Androgen ablation augments human HLA2.1-restricted T cell responses to PSA self-antigen in transgenic mice. The Prostate. 2010; 70: 1002–11.

15. Arlen PM, Gulley JL, Todd N, et al. Antiandrogen, vaccine and combination therapy in patients with nonmetastatic hormone refractory prostate cancer. J Urol. 2005; 174: 539–46.

16. Madan RA, Gulley JL, Schlom J, et al. Analysis of overall survival in patients with nonmetastatic castration-resistant prostate cancer treated with vaccine, nilutamide, and combination therapy. Clin Cancer Res Off J Am Assoc Cancer Res. 2008; 14: 4526–31.

17. Kokontis J, Takakura K, Hay N, Liao S. Increased androgen receptor activity and altered c-myc expression in prostate cancer cells after long-term androgen deprivation. Cancer Res. 1994; 54: 1566–73.

18. Karantanos T, Corn PG, Thompson TC. Prostate cancer progression after androgen deprivation therapy: mechanisms of castrate resistance and novel therapeutic approaches. Oncogene. 2013; 32: 5501–11.

19. Labaf M, Li M, Ting L, et al. Increased AR expression in castration-resistant prostate cancer rapidly induces AR signaling reprogramming with the collaboration of EZH2. Front Oncol. 2022; 12: 1021845.

20. Visakorpi T, Hyytinen E, Koivisto P, et al. In vivo amplification of the androgen receptor gene and progression of human prostate cancer. Nat Genet. 1995; 9: 401–6.

21. Shafi AA, Yen AE, Weigel NL. Androgen receptors in hormone-dependent and castration-resistant prostate cancer. Pharmacol Ther. 2013; 140: 223–38.

22. Olson BM, Gamat M, Seliski J, et al. Prostate Cancer Cells Express More Androgen Receptor (AR) Following Androgen Deprivation, Improving Recognition by AR-Specific T Cells. Cancer Immunol Res. 2017; 5: 1074–85.

23. Olson BM, Johnson LE, McNeel DG. The androgen receptor: a biologically relevant vaccine target for the treatment of prostate cancer. Cancer Immunol Immunother CII. 2013; 62: 585–96.

24. Kyriakopoulos CE, Eickhoff JC, Ferrari AC, et al. Multicenter Phase 1 Trial of a DNA Vaccine Encoding the Androgen Receptor Ligand Binding Domain (pTVG-AR, MVI-118) in Patients with Metastatic Prostate Cancer. Clin Cancer Res Off J Am Assoc Cancer Res. 2020; 26: 5162–71.

25. Long X, Hou H, Wang X, et al. Immune signature driven by ADT-induced immune microenvironment remodeling in prostate cancer is correlated with recurrence-free survival and immune infiltration. Cell Death Dis. 2020; 11: 779.

26. Gamat-Huber M, McNeel DG. Androgen deprivation as a tumour-immunomodulating treatment. Nat Rev Urol. 2020; 17: 371–2.

27. Benten WP, Wunderlich F, Mossmann H. Testosterone-induced suppression of self-healing Plasmodium chabaudi malaria: an effect not mediated by androgen receptors? J Endocrinol. 1992; 135: 407–13.

28. Oshida K, Waxman DJ, Corton JC. Chemical and Hormonal Effects on STAT5b-Dependent Sexual Dimorphism of the Liver Transcriptome. PLoS ONE. 2016; 11: e0150284.

29. Monajemi M, Pang YCF, Bjornson S, Menzies SC, van Rooijen N, Sly LM. Malt1 blocks IL-1β production by macrophages in vitro and limits dextran sodium sulfate-induced intestinal inflammation in vivo. J Leukoc Biol. 2018; 104: 557–72.

30. Xu P, Yang JC, Chen B, et al. Androgen receptor blockade resistance with enzalutamide in prostate cancer results in immunosuppressive alterations in the tumor immune microenvironment. J Immunother Cancer. 2023; 11: e006581.

31. Bronte G, Conteduca V, Landriscina M, Procopio AD. Circulating myeloid-derived suppressor cells and survival in prostate cancer patients: systematic review and meta-analysis. Prostate Cancer Prostatic Dis. 2023; 26: 41–6.

32. Bullock K, Richmond A. Suppressing MDSC Recruitment to the Tumor Microenvironment by Antagonizing CXCR2 to Enhance the Efficacy of Immunotherapy. Cancers. 2021; 13: 6293.

33. Galon J, Costes A, Sanchez-Cabo F, et al. Type, density, and location of immune cells within human colorectal tumors predict clinical outcome. Science. 2006; 313: 1960–4.

34. Yang Y, Attwood K, Bshara W, et al. High intratumoral CD8+ T-cell infiltration is associated with improved survival in prostate cancer patients undergoing radical prostatectomy. The Prostate. 2021; 81: 20–8.

35. Koh YT, Gray A, Higgins SA, Hubby B, Kast WM. Androgen ablation augments prostate cancer vaccine immunogenicity only when applied after immunization. The Prostate. 2009; 69: 571–84.

36. Gardner TA, Elzey BD, Hahn NM. Sipuleucel-T (Provenge) autologous vaccine approved for treatment of men with asymptomatic or minimally symptomatic castrate-resistant metastatic prostate cancer. Hum Vaccines Immunother. 2012; 8: 534–9.

37. Antonarakis ES, Kibel AS, Yu EY, et al. Sequencing of Sipuleucel-T and Androgen Deprivation Therapy in Men with Hormone-Sensitive Biochemically Recurrent Prostate

Cancer: A Phase II Randomized Trial. Clin Cancer Res Off J Am Assoc Cancer Res. 2017; 23: 2451–9.

38. University of Wisconsin, Madison. Phase I/II Trial of Androgen Deprivation, With or Without pTVG-AR, and With or Without T-Cell Checkpoint Blockade, in Patients With Newly Diagnosed, High-Risk Prostate Cancer [Internet]. clinicaltrials.gov; 2023 Dec [cited 31 December 2023]. Report No.: NCT04989946. Available at: https://clinicaltrials.gov/study/NCT04989946

39. Sanaei M, Salimzadeh L, Bagheri N. Crosstalk between myeloid-derived suppressor cells and the immune system in prostate cancer: MDSCs and immune system in Prostate cancer. J Leukoc Biol. 2020; 107: 43–56.

40. Obradovic A, Dallos MC, Zahurak ML, et al. T-Cell Infiltration and Adaptive Treg Resistance in Response to Androgen Deprivation With or Without Vaccination in Localized Prostate Cancer. Clin Cancer Res Off J Am Assoc Cancer Res. 2020; 26: 3182–92.

41. Idorn M, Køllgaard T, Kongsted P, Sengeløv L, Thor Straten P. Correlation between frequencies of blood monocytic myeloid-derived suppressor cells, regulatory T cells and negative prognostic markers in patients with castration-resistant metastatic prostate cancer. Cancer Immunol Immunother CII. 2014; 63: 1177–87.

42. Wang Y, Jia A, Bi Y, et al. Targeting Myeloid-Derived Suppressor Cells in Cancer Immunotherapy. Cancers. 2020; 12: 2626.

43. Autio KA, Klebanoff CA, Schaer D, et al. Immunomodulatory Activity of a Colony-stimulating Factor-1 Receptor Inhibitor in Patients with Advanced Refractory Breast or Prostate Cancer: A Phase I Study. Clin Cancer Res Off J Am Assoc Cancer Res. 2020; 26: 5609–20.

44. Moeller A, Kurzrock R, Botta GP, et al. Challenges and prospects of CSF1R targeting for advanced malignancies. Am J Cancer Res. 2023; 13: 3257–65.

45. Lopez-Bujanda ZA, Haffner MC, Chaimowitz MG, et al. Castration-mediated IL-8 Promotes Myeloid Infiltration and Prostate Cancer Progression [Internet]. Immunology; 2019 May [cited 12 February 2021]. Available at: http://biorxiv.org/lookup/doi/10.1101/651083

46. Lee J, Cacalano G, Camerato T, Toy K, Moore MW, Wood WI. Chemokine binding and activities mediated by the mouse IL-8 receptor. J Immunol Baltim Md 1950. 1995; 155: 2158–64.

47. Magnan S, Zarychanski R, Pilote L, et al. Intermittent vs Continuous Androgen Deprivation Therapy for Prostate Cancer: A Systematic Review and Meta-analysis. JAMA Oncol. 2015; 1: 1261–9.

48. Hussain M, Tangen CM, Berry DL, et al. Intermittent versus continuous androgen deprivation in prostate cancer. N Engl J Med. 2013; 368: 1314–25.

49. Denmeade S, Antonarakis ES, Markowski MC. Bipolar androgen therapy (BAT): A patient's guide. The Prostate. 2022; 82: 753–62.

50. Markowski MC, Wang H, Sullivan R, et al. A Multicohort Open-label Phase II Trial of Bipolar Androgen Therapy in Men with Metastatic Castration-resistant Prostate Cancer (RESTORE): A Comparison of Post-abiraterone Versus Post-enzalutamide Cohorts. Eur Urol. 2021; 79: 692–9.

51. Denmeade SR, Wang H, Agarwal N, et al. TRANSFORMER: A Randomized Phase II Study Comparing Bipolar Androgen Therapy Versus Enzalutamide in Asymptomatic Men With Castration-Resistant Metastatic Prostate Cancer. J Clin Oncol Off J Am Soc Clin Oncol. 2021; 39: 1371–82.

52. Markowski MC, Taplin M-E, Aggarwal RR, et al. Overall survival (OS) and biomarker results from combat: A phase 2 study of bipolar androgen therapy (BAT) plus nivolumab for patients with metastatic castrate-resistant prostate cancer (mCRPC). J Clin Oncol. 2022; 40: 5064–5064.

53. Kumar R, Mendonca J, Owoyemi O, et al. Supraphysiological testosterone induces ferroptosis and activates immune pathways through nucleophagy in prostate cancer. Cancer Res. 2021; 81: 5948–62.

54. McNeel DG, Eickhoff JC, Wargowski E, et al. Phase 2 trial of T-cell activation using MVI-816 and pembrolizumab in patients with metastatic, castration-resistant prostate cancer (mCRPC). J Immunother Cancer. 2022; 10: e004198.

55. McNeel DG, Emamekhoo H, Eickhoff JC, et al. Phase 2 trial of a DNA vaccine (pTVG-HP) and nivolumab in patients with castration-sensitive non-metastatic (M0) prostate cancer. J Immunother Cancer. 2023; 11: e008067.

Chapter 4

Anti-tumor efficacy of ADT in combination with AR targeted therapies and anti-PD-1 is limited by regulatory T cells in murine prostate models.

4.1 Abstract

Background: While Androgen deprivation therapy (ADT) is pivotal in prostate cancer treatment, its effectiveness with different ADT agents on T-cell responses is complex and not yet fully understood. Our study expands upon previous research indicating that combining AR vaccination with ADT enhances AR specific CD8+T cell infiltration. We directly compare various ADT approaches, including AR degraders and AR antagonists, to determine their synergy with AR-specific immunization. Subsequently, we identify the optimal combination for enhancing anti-tumor responses using checkpoint blockade.

Methods: Prostate cancer cell lines were cultured under testosterone-replete and -deficient conditions to assess changes in AR expression post-androgen deprivation. Subsequent AR-specific T-cell recognition assays were performed after treating tumor cells with various AR-targeted agents. In vivo experiments involved combining ADT with AR-targeted vaccination and either Enzalutamide or ARV110 with anti-PD-1 in murine prostate tumor models. Tumor growth, survival rates, and immune cell infiltration were monitored and evaluated.

Results: Androgen deprivation led to a significant increase in AR expression in androgen-dependent prostate tumor cells. Additionally, enhanced AR expression post-androgen deprivation augmented AR-specific T-cell recognition, particularly with AR antagonists such as Bicalutamide and Enzalutamide. In vivo studies demonstrated that combining ADT with AR vaccination and Enzalutamide resulted in superior anti-tumor responses and prolonged survival compared to ARV110. Furthermore, Enzalutamide treatment in combination with ADT and AR vaccination increased CD4+ and CD8+ T-cell infiltration within the tumor microenvironment, with a notable

presence of effector memory CD8+ T cells. However, when combined with anti-PD-1, there was an increase in the infiltration of regulatory T cells (Tregs).

Conclusion: Our findings highlight the potential of combining ADT with AR-targeted vaccination and Enzalutamide to enhance anti-tumor responses in prostate cancer. Enzalutamide, as opposed to ARV110, demonstrated superior efficacy in improving T-cell infiltration and generating memory CD8+ T-cell populations within the tumor microenvironment. While the addition of PD-1 blockade to this combination showed only modest benefits, it led to an increase in intratumoral regulatory CD4+T cells, suggesting a complex interplay between immune activation and regulation with combination therapies. Overall, our study provides valuable insights into optimizing therapeutic strategies for prostate cancer treatment.

4.2 Introduction

Androgen deprivation therapy (ADT) is widely recognized as the primary treatment approach for prostate cancer. Its mechanism involves the suppression of androgens, notably testosterone, with the aim of inhibiting the proliferation of prostate cancer cells. While initially effective, a substantial portion of patients progress to advanced stages or develop castration resistance. In such cases, where median life expectancy is often less than three years, additional therapeutic strategies are necessitated to target the androgen receptor (AR) axis [1,2] . Consequently, therapies focusing on the AR signaling axis remain actively pursued. Some of these interventions operate by inhibiting androgen production as a first-line treatment (e.g., GnRH agonists or antagonists such as leuprolide, goserelin, or degarelix; abiraterone; TAK-700) [3]. Others involve blocking the binding of androgen to the AR (e.g., bicalutamide, flutamide, enzalutamide, apalutamide, darolutamide), and/or by degrading the androgen receptor (e.g., galeterone, TRC253, ASC-J9, or proteolysis targeting chimeras (PROTACs) targeting the AR, such as ARV-110 and ARCC-4) [4,5]. Although these agents have exhibited promising results in both pre-clinical and clinical trials, there exists a significant need to understand how these treatments can be optimally combined.

Beyond the primary effect of killing tumor cells, emerging evidence suggests that ADT exhibits immunostimulatory properties. These include thymic regrowth, increased production of naïve T cells, enhanced infiltration of immune cells into the prostate, elevated antigen presentation, and heightened antibody responses to prostate antigens. These findings have sparked considerable interest in leveraging the immunomodulatory effects of ADT to enhance the efficacy of immune therapy in prostate cancer [6,7].

Despite advancements in immune therapy for other cancers, effectively treating advanced stage prostate cancer remains challenging. Ardiani et al. treated murine prostate tumors with a

combination of enzalutamide and a vaccine targeting the Twist antigen and demonstrated increase of functional Twist-specific CD8+ T cells and resulted in significantly increased overall survival of the mice compared to treatments with Twist vaccine alone (27.5 weeks vs 10.3 weeks) [8]. We have previously shown that ADT treatment of prostate cancer cells can enhance their recognition by AR-specific CD8+ T cells [9]. Additionally, in pre-clinical models, the sequence of treatments with DNA vaccination preceding ADT has been demonstrated to be superior [10]. Moreover, in a multi-center phase I study involving patients recently initiated on ADT, vaccination with pTVG-AR was shown to elicit increased AR-specific Th1-biased immunity and a delayed time to castration resistance in immunized patients [11].

Furthermore, a phase 2 trial assessing the combination of a DNA vaccine encoding PAP (MVI-816) and pembrolizumab demonstrated a promising 6-month disease control rate. However, further randomized clinical trials are required to confirm these results [12].

In the phase III IMbassador250 study, combining atezolizumab, an anti-PD-L1 antibody, with enzalutamide failed to extend survival in metastatic prostate cancer, despite preclinical research strongly suggesting elevated PD-L1 expression in enzalutamide-resistant castration-resistant prostate cancer cells [13]. This highlights the urgent need for further investigation into the mechanisms of resistance within the prostate tumor microenvironment, which hinder the effectiveness of immunotherapies. Additionally, enzalutamide treatment has been associated with CD8+ T cell exhaustion and decreased levels of interferon-gamma (IFN-γ), indicating additional mechanisms underlying treatment failure that may require enhancing CD8+ T cell responses [14,15].

In our previous research, we discovered that DNA or peptide vaccines, designed to activate tumor-specific CD8+ T cells, inadvertently triggered the expression of multiple checkpoint receptors. These receptors act to dampen the anti-tumor response, thereby reducing the efficacy of the vaccination. Specifically, we observed that antigens with high affinity for MHC-I resulted in prolonged contact between CD8+ T cells and antigen-presenting cells (APCs). This prolonged interaction led to an increase in various immune checkpoints, including PD-1, CTLA-4, LAG-3, and TIM-3 on activated cells, compared to those activated with lower affinity epitopes. Remarkably, we found that combining vaccines encoding high-affinity epitopes with PD-1 or PD-L1 blocking antibodies restored their anti-tumor efficacy [16].

In a separate investigation, we noted that immunization strategies leading to increased antigen expression also increased LAG-3 expression on tumor antigen-specific CD8+ T cells. This upregulation of LAG-3 similarly impeded the anti-tumor response and vaccination with LAG-3 blocking antibodies improved anti-tumor efficacy [17].

These findings underscore the significance of blocking the regulatory pathways induced by vaccination to enhance anti-tumor responses. Moreover, they highlight checkpoint receptor upregulation as a prominent mechanism of tumor resistance to vaccination. Additionally, our data indicate that T-cell activating therapies can induce the expression of various checkpoint receptors.

Given that previous studies have illustrated the immunomodulatory effects of ADT, and our prior research has demonstrated the augmentation of anti-tumor responses by AR-DNA vaccination preceding ADT, and that checkpoint blockade further augments anti-tumor efficacy of AR-targeted vaccination, in the current report we investigated effective combination of ADT alongside

the AR targeted therapies, specifically AR degrader (ARV110) or AR antagonist (enzalutamide) and checkpoint blockade in murine models of prostate cancer. Our primary aim was to examine changes in the tumor immune microenvironment to identify the optimal combination for integrating checkpoint blockade and to elucidate the underlying mechanisms. Additionally, we aim to analyze alterations in the tumor immune microenvironment to provide insights that can guide optimal strategies for future clinical trials involving this or similar prostate cancer vaccines.

4.3 Results:

4.3.1 Enzalutamide increases expression of the androgen receptor in prostate cancer cell lines.

Previously, we demonstrated that reducing testosterone levels (androgen deprivation therapy, ADT) resulted in increased expression of the androgen receptor (AR) in tumor cells, leading to enhanced recognition by AR-specific CD8+ T cells. In clinical practice, ADT is often combined with AR antagonists, while AR degraders are also under investigation. While one approach increases AR expression and the other decreases it, our hypothesis was that AR degradation might enhance MHC class I presentation of AR by tumor cells. Expanding on our previous findings, we cultured a panel of three prostate cell lines—human prostate cancer line 22Rv1 and androgen-dependent murine lines Myc-CaP and TRAMP-C1—in both testosterone-replete and -deficient conditions for 72 hours. (Figure 1A). Analysis revealed a significant rise in AR expression in androgen-dependent prostate tumor cells following androgen deprivation, as demonstrated by intracellular staining using an AR antibody. (Figure. 1B). Quantitative assessments of AR expression amplitude further supported these findings.

4.3.2 AR-specific T cells have increased recognition of androgen-deprived tumor cells

To evaluate the impact of increased AR expression post-androgen deprivation on AR-specific T-cell effector function against prostate tumor cells, we treated 22Rv1 cells with various AR-targeted agents (ARV110, Bicalutamide, Dip-G, Enzalutamide, Flutamide, and Galeterone) for 72 hours. Subsequently, these cells were co-cultured with splenocytes from HLA-A2 transgenic mice previously immunized with the HLA-A2 restricted epitope AR811 (Fig. 2A) and were then

assessed for AR-specific function using IFN-gamma ELISPOT (Fig. 2B). Notably, CD8+ T cell recognition of tumor cells was significantly elevated with AR antagonists such as Bicalutamide and Enzalutamide rather than AR degraders such as ARV110, DipG, and Galeterone. Consequently, we concluded that the enhanced recognition of prostate tumor cells treated with AR antagonists rather than AR degraders by AR-specific CD8+ T cells was primarily attributable to increased AR expression.

4.3.3 Androgen deprivation Therapy in combination AR targeted vaccination and Enzalutamide rather than ARV110 improved anti-tumor responses in-vivo.

We and others have previously shown that that ADT can increase the infiltration of tumor-infiltrating CD4+ and CD8+ T cells in murine prostate cancer models. Additionally, AR vaccination prior to ADT further augmented T cell infiltration into tumors. We aimed to determine whether combining ARV110 or enzalutamide with ADT (degarelix) and AR-vaccination could enhance anti-tumor responses. Using Myc-CaP tumor cells implanted in male FVB mice (Figure 3A), we initiated treatments when tumors reached a volume of 0.2-0.3cm^3 and administering degarelix (25 mg/kg subcutaneously every 28 days) alongside daily enzalutamide or ARV110 five times a week until the end of the study. Mice were also immunized weekly with a DNA vaccine encoding the androgen receptor's ligand-binding domain (pTVG-AR) or a control vector (pTVG4), starting one day after tumor implantation. Notably, immunization prior to ADT combined with enzalutamide compared to ARV110 led to a greater anti-tumor response and significantly improved survival rates (Figure 3B and 3C). Similar outcomes were observed in a separate model using TRAMP-C1 tumor cells in C57BL/6 mice (Figure 3D), where pre-ADT vaccination followed by enzalutamide significantly enhanced anti-tumor responses and overall survival

(Figures 3E and 3F). In the TRAMP-C1 model, due to the slower tumor growth necessitating 4 weeks for palpability, mice received an additional weekly vaccination before ADT. Overall, our results suggest superior anti-tumor efficacy of enzalutamide in combination with vaccination and ADT compared to ARV110.

4.3.4 Vaccination prior to ADT followed by enzalutamide led to decreased prostate tumor-infiltrating T cells and increased regulatory T cell populations in the Myc-CaP FVB model.

We then explored whether immunization prior to ADT, followed by either enzalutamide or ARV110, influenced T cell infiltration. A similar experiment as depicted in Figure 1A was performed, with tumors harvested two weeks post-ADT and subsequent administration of enzalutamide or ARV110 for immune cell composition assessment via flow cytometry, as illustrated in Figure 4A. Our analysis revealed an overall decrease in CD4+ and CD8+ T cells within the tumor microenvironment in mice treated with vaccination followed by ADT and enzalutamide by day 36 (panels B and C). Furthermore, Gr-1+ MDSCs remained low in all groups (panel D) while regulatory CD4+T cells (Tregs) were notably lower in the ARV110-treated group compared to enzalutamide (panel E). These findings collectively indicate that ADT initially induces an influx of infiltrating T cells, a response further enhanced by AR-vaccination, however with enzalutamide treatment, the infiltration of T cells is abrogated.

4.3.5 Vaccination prior to ADT followed by enzalutamide did not affect activation, proliferation or memory T cell populations however increased PD-1 and LAG-3 expression on CD8+T cells.

A similar study was conducted to further analyze the immunophenotype of CD8+ T cells within the tumor microenvironment (Figure 4A). Tumor-infiltrating CD8+ T cells in the group treated with enzalutamide, with or without vaccination, in combination with ADT, exhibited no alterations in proliferation (Ki67+ CD8+ T cells), activation (CD69 MFI), memory populations (CD44+ CD8+ T cells), or CD44+ CD27- CD62L- effector memory CD8+ T cells compared to ARV110. However, treatment with enzalutamide followed by vaccination and ADT led to a significant increase in PD-1 MFI (panel F) and LAG-3 MFI (panel G) on CD8+ T cells, while no changes were observed in TIGIT MFI (panel H). Additionally, there was a notable increase in CTLA-4 MFI (panel I) on CD8+ T cells. Taken together, these data suggest that enzalutamide treatment caused lower infiltration CD8+T cells and express high levels of immune checkpoint molecules.

4.3.6 Addition of PD-1 blockade to ADT, AR targeted vaccination and Enzalutamide slightly improved anti-tumor responses in-vivo.

Due to the increased PD-1 expression on CD8 +T cells following ADT and AR vaccination and enzalutamide treatment, we hypothesized that blockade of the PD-1/PD-L1 axis in combination with enzalutamide would further improve antitumor efficacy. To test this hypothesis, we implanted prostate tumors and initiated immunization the day after, followed by PD-1 blockade the subsequent day and weekly thereafter (Figure 3A, B). Tumor growth was monitored over time. In the Myc-CaP model, combining anti-PD-1 with enzalutamide showed a slight additional benefit to the combination (Figure 3D) but did not significantly improve overall survival.

4.4 Discussion

Since the FDA approval of pembrolizumab for prostate cancer with microsatellite instability (MSI), there has been a surge of interest in utilizing immunotherapy for prostate cancer, especially when combined with other treatment modalities. However, considering the limited clinical impact observed in several trials, there is an urgent need to understand how the combination of these therapies affects immune cell populations within tumors. Additionally, further investigation is needed to determine the optimal form of ADT to combine with immunotherapy. This report aimed to investigate ADT in combination with optimal AR targeted agents (AR antagonists or degraders with AR DNA vaccination) and immune checkpoint blockade in immune-competent murine prostate tumor models. Key findings include: 1) Administering pTVG-AR → ADT→ Enzalutamide enhanced anti-tumor responses compared to ARV110 delaying time to tumor growth and significantly improving overall survival; 2) pTVG-AR → ADT→ Enzalutamide led to decreased infiltration of CD4+ and CD8+T cells into the tumor microenvironment while increasing regulatory T cells; 3) pTVG-AR → ADT→ Enzalutamide increased PD-1 and LAG-3 expression on CD8+T cells; 4) pTVG-AR → ADT→ αPD-1→ Enzalutamide modestly improved anti-tumor responses although not significantly. These outcomes underscore the pivotal role of infiltrating immune populations in shaping the tumor immune microenvironment and influencing therapeutic responses. Additionally, this is the first study combining AR-targeted vaccination with ARV110 in in-vivo immune competent models.

The pivotal role of androgen receptor (AR) signaling in prostate development, normal prostate function, and the progression of prostate cancer, particularly in castration-resistant states, is well-established [18]. Additionally, the transient and gradual response observed with enzalutamide treatment, coupled with the persistence of AR expression in prostate cancer cells that develop

resistance to AR-targeted therapy, underscores the potential benefits of developing novel therapies that target residual AR activity for patients with castration-resistant prostate cancer (CRPC) who have become resistant to current treatments [19,20]. Salami et al. demonstrated the ability of AR PROTACs to degrade AR at low nanomolar concentrations, addressing some of the limitations associated with current AR antagonists used in CRPC therapy. [21]. However, our study sheds light on the importance of understanding the immune-mediated mechanisms of action of AR degraders compared to AR antagonists.

Recent studies have revealed that androgen receptor (AR) activity suppresses interferon-gamma (IFN-γ) transcription in T cells, and blocking AR can restore CD8+ T cells' ability to produce IFN-γ. These findings emphasize the importance of thorough inhibition of androgen signaling within the tumor microenvironment (TME) to maximize therapeutic efficacy[22]. However, despite the potency of enzalutamide as an AR antagonist, research by Xu et al. indicates that resistance to AR blockade induced by enzalutamide in prostate cancer can lead to immunosuppressive alterations within the tumor immune microenvironment [12]. This includes the infiltration of tumor-associated macrophages and regulatory T cell populations, which aligns with our own findings suggesting potential detrimental effects of prolonged enzalutamide use on tumor suppression. Furthermore Pu et al., demonstrated that that AR antagonists may have off target effects on T cells affecting their function.

Combining enzalutamide with ADT not only enhanced T-cell responsiveness to PD-1 antibodies but also extended survival in a mouse model of prostate cancer [22]. Additionally, in other mouse experiments, Shen et al. found that combining ADT with anti-PD-1 and/or anti-CTLA-4 significantly delays the development of castration resistance, reduces tumor volume, and prolongs survival in some cases [22,23]. However, in a randomized phase III trial of enzalutamide with or

without atezolizumab (anti-PD-L1) in 759 men with metastatic CRPC who progressed on abiraterone (androgen synthesis inhibitor) failed to meet the primary endpoint of overall survival (OS), suggesting other resistant mechanisms at play. However, our experiments did not demonstrate additional improvement with the addition of PD-1 antibody, suggesting that combining multiple checkpoint inhibitors may yield enhanced outcomes. Several clinical trials have investigated the efficacy of checkpoint inhibitors in combination with ADT for treating metastatic castration-resistant prostate cancer (mCRPC), but with limited success [22].

In summary, our findings suggest that the combination of AR-targeted vaccination and ADT with enzalutamide yields better outcomes compared to ARV110. However, this combination leads to the infiltration of Tregs and upregulates the expression of immune checkpoints. The addition of anti-PD-1 did not substantially enhance anti-tumor responses; nevertheless, there were limitations to our approach. Firstly, we employed only one specific combination of anti-PD-1, based on the hypothesis that reducing PD-1 expression on CD8+ T cells would enhance antitumor efficacy. However, since this resulted in further increased Tregs, it would have been logical to combine it with a Treg-depleting antibody to augment the antitumor efficacy of the combination. Additionally, our in-vivo studies of the tumor microenvironment utilized only one murine tumor model, MyC-CaP, recognized as an immunologically "cold" prostate tumor model, making it difficult to further characterize CD8+T cells for effector and memory phenotypes. Furthermore, ARV110 is predominantly utilized in enzalutamide-resistant models. Nevertheless, our results do not rule out the possibility that optimizing the combination of enzalutamide and ARV110 with AR-targeted vaccination could lead to significant improvements. Therefore, future investigations will seek to explore these therapies in diverse tumor models and integrate multiple checkpoint inhibitors in combination.

4.5 Figures

Figure 1: Enzalutamide increases expression of the androgen receptor in prostate cancer cell lines.

Prostate cell lines (androgen-dependent prostate cancer cell lines: 22Rv1, Myc-CaP and TRAMP-C1) cultured in either androgen-replete (FCS) or androgen-deprived (CSS) medium for 72 hours (panel A) and analyzed for androgen receptor protein expression intracellular staining by flow cytometry and quantified for (B) geometric mean and representative flow cytometry plots of AR expression.

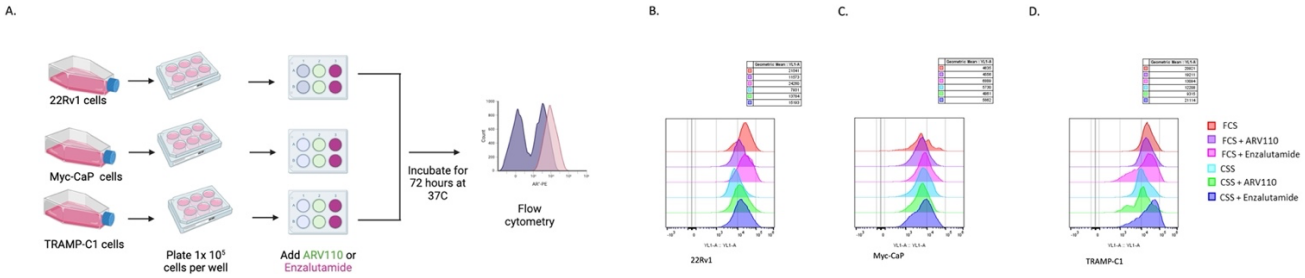

Figure 1: Enzalutamide increases expression of the androgen receptor in prostate cancer cell lines.

Figure 2: AR-specific T cells have increased recognition of androgen-deprived tumor cells treated with AR antagonists compared to AR degraders. Prostate cell line 22Rv1cultured in either media alone, ARV110 or Enzalutamide medium for 72 hours (panel A) and co-cultured with splenocytes from HHD mice that were AR811or control immunized. IFNγ ELISPOT was performed. Raw data are shown in panel B and quantified in panel C.

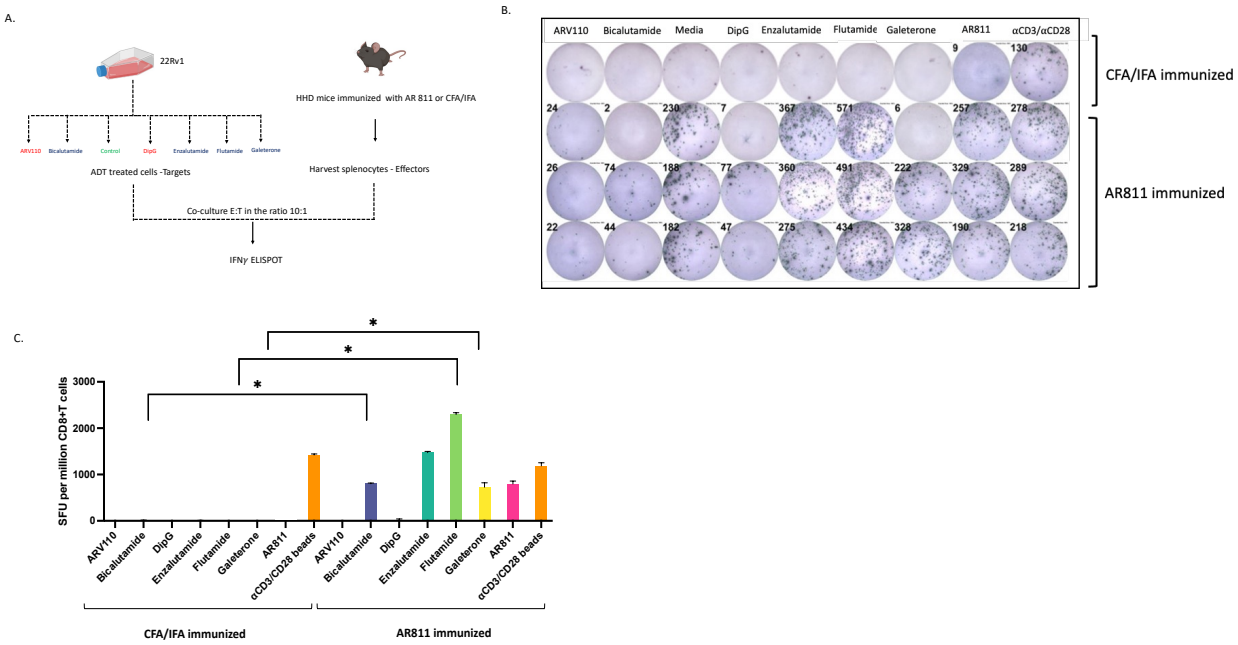

Figure 2: AR-specific T cells have increased recognition of androgen-deprived tumor cells treated with AR antagonists compared to AR degraders.

Figure 3: Vaccination prior to ADT followed by enzalutamide rather than ARV110 significantly improved anti-tumor responses in murine prostate tumor models.

FVB mice were implanted with Myc-CaP tumor cells and treated with degarelix (ADT), with pTVG4 (vector control) or pTVG-AR delivered before ADT followed by Enzalutamide or ARV110 given 5X a week and followed for tumor growth. Shown is a schema (panel A), tumor growth curves (panel B), and Kaplan-Meier curves depicting survival (time to a tumor size of $2cm^3$ or death, panel C). Similarly, male C57BL/6 were implanted with TRAMP-C1 tumor cells, treated with ADT, and with DNA immunization with pTVG4 or pTVG-AR initiated before ADT and followed by Enzalutamide or ARV110 given 5X a week. Shown is a schema (panel D), tumor growth curves (panel E), and Kaplan-Meier curves depicting survival (time to a tumor size of $2cm^3$ or death, panel F). For tumor growth curves, asterisks demonstrate significant (*$p < 0.05$, **$p<0.01$ ***$p<0.001$) differences as assessed by linear mixed effects model with Geisser-Greenhouse correction and Tukey's multiple comparisons test with individual variances. Kaplan-Meier curves were compared using the log-rank test with asterisks indicating *$p<0.05$, **$p<0.01$, and ***$p<0.001$. Results are each from one experiment, with n=7 animals per group, and are representative of two independent experiments.

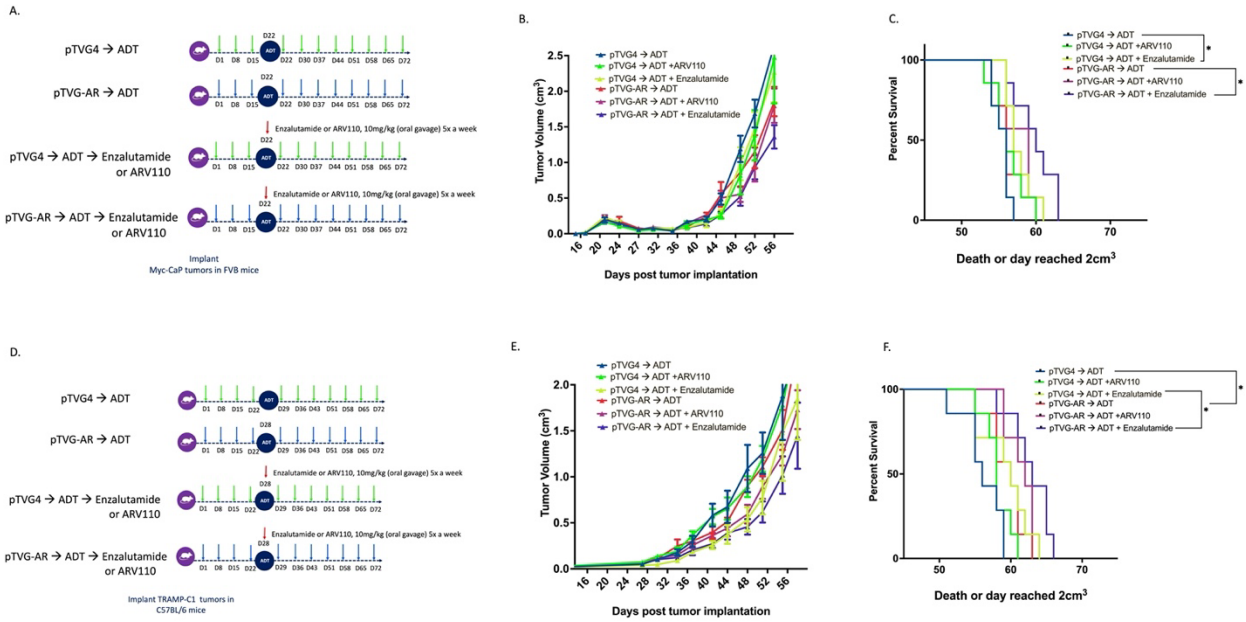

Figure 3: Vaccination prior to ADT followed by enzalutamide rather than ARV110 significantly improved anti-tumor responses in murine prostate tumor models.

Figure 4: Vaccination prior to ADT followed by enzalutamide led to decreased prostate tumor-infiltrating T cells and increased regulatory T cell populations in the Myc-CaP FVB model.

Myc-CaP tumor cells were implanted in male FVB mice and treated with ADT, and DNA immunization was delivered before ADT followed by enzalutamide or ARV110. Tumors were sampled at day 36 for flow cytometry analysis. Shown are a schema (panel A), CD4+ T cells (panel B), CD8+ T cells (panel C), and CD11b+Gr-1+ MDSC (panel D) are shown as a percentage of CD45+ cells. CD4+FoxP3+ Tregs (panel E) are shown as a percentage of CD4+ cells.

Panels B-E were compared using one-way ANOVA with Tukey's multiple comparisons test; asterisks indicate *$p<0.05$, **$p<0.01$, and ***$p<0.001$. Results are from one experiment and are representative of two independent experiments.

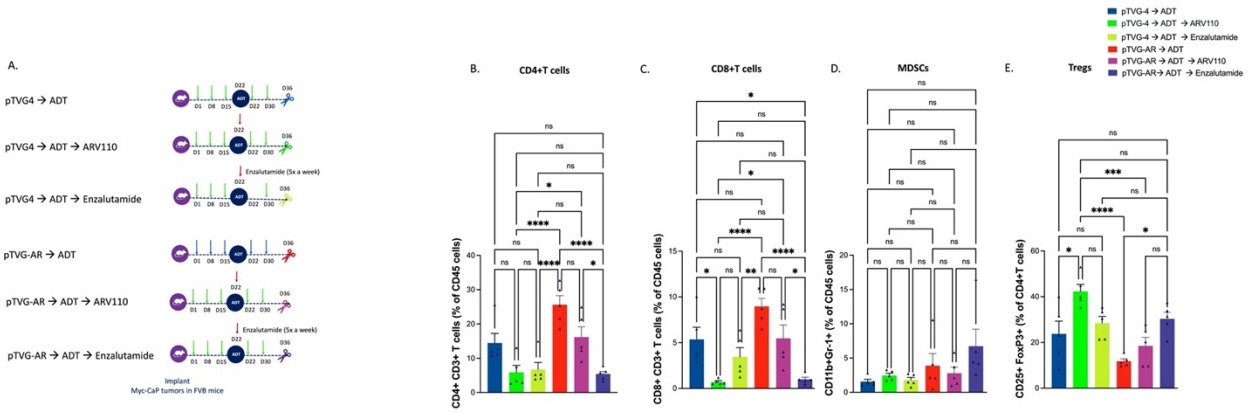

Figure 4: Vaccination prior to ADT followed by enzalutamide led to decreased prostate tumor-infiltrating T cells and increased regulatory T cell populations in the Myc-CaP FVB model.

Figure 5: Vaccination prior to ADT followed by enzalutamide did not affect activation, proliferation or memory T cell populations however increased PD-1 and LAG-3 expression on CD8+T cells.

Myc-CaP tumor cells were implanted in male FVB mice and treated with ADT, and DNA immunization was delivered before ADT followed by enzalutamide or ARV110. Tumors were sampled at day 36 for characterizing CD8+T cells. Shown are a schema (panel A), Ki67+CD8+CD3+ T cells (panel B), CD69 MFI on CD8+T cells (panel C), CD44+ memory CD8+ T cells (panel D), CD44+CD27-CD62L- effector memory CD8+ T cells (panel E). Shown are PD-1 MFI (panel F), LAG-3 MFI (panel G), TIGIT MFI (panel H) and CTLA-4 MFI (panel I) on CD8+T cells. Comparisons were made using one-way ANOVA with Tukey's multiple comparisons test asterisks indicating *$p<0.05$, **$p<0.01$, and ***$p<0.001$. Results are from one experiment.

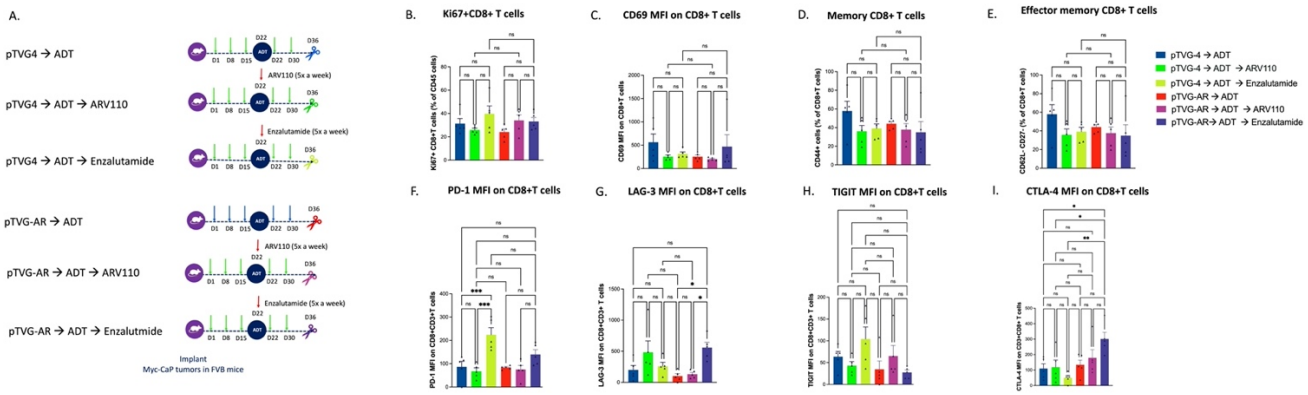

Figure 5: Vaccination prior to ADT followed by enzalutamide did not affect activation, proliferation or memory T cell populations however increased PD-1 and LAG-3 expression on CD8+T cells.

Figure 6: Vaccination prior to ADT followed by enzalutamide and anti-PD-1 did not improve anti-tumor responses in murine prostate tumor models.

FVB mice were implanted with Myc-CaP tumor cells and treated with pTVG4 (vector control) or pTVG-AR, followed by anti-PD-1 weekly until the end of the study. ADT was initiated on day 24, followed by enzalutamide administration, and the mice were monitored for tumor progression thereafter. Shown is a schema (panel A), tumor growth curves (panel B), and Kaplan-Meier curves depicting survival (time to a tumor size of $2cm^3$ or death, panel C). For tumor growth curves, asterisks demonstrate significant (*$p < 0.05$, **$p<0.01$ ***$p<0.001$) differences as assessed by linear mixed effects model with Geisser-Greenhouse correction and Tukey's multiple comparisons test with individual variances. Kaplan-Meier curves were compared using the log-rank test with asterisks indicating *$p<0.05$, **$p<0.01$, and ***$p<0.001$. Results are each from one experiment, with n=7 animals per group, and are representative of two independent experiments.

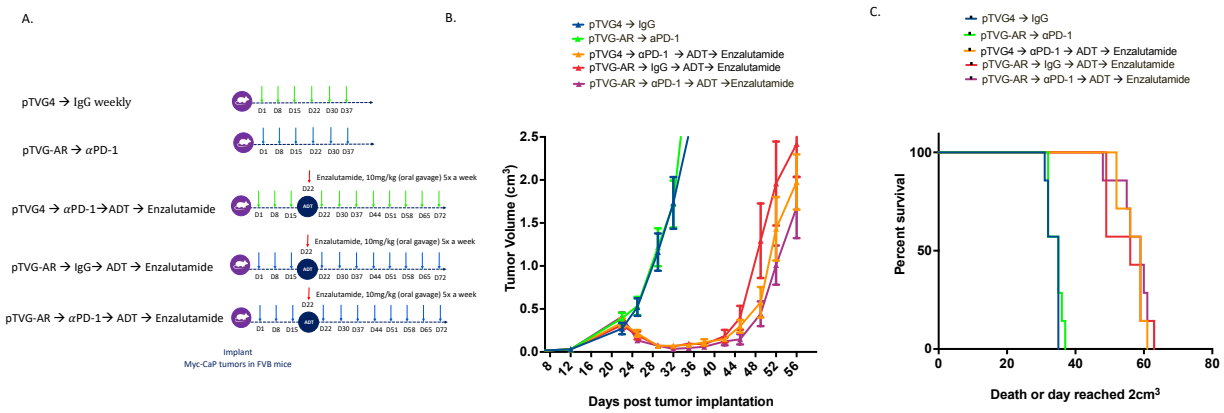

Figure 6: Vaccination prior to ADT followed by enzalutamide and anti-PD-1 did not improve anti-tumor responses in murine prostate tumor models.

4.6 References

1. Lallous N, Dalal K, Cherkasov A, Rennie P. Targeting Alternative Sites on the Androgen Receptor to Treat Castration-Resistant Prostate Cancer. IJMS. 2013; 14: 12496–519.

2. Heemers HV. Targeting Androgen Receptor Action for Prostate Cancer Treatment: Does the Post-Receptor Level Provide Novel Opportunities? Int J Biol Sci. 2014; 10: 576–87.

3. Fontana F, Marzagalli M, Montagnani Marelli M, Raimondi M, Moretti RM, Limonta P. Gonadotropin-Releasing Hormone Receptors in Prostate Cancer: Molecular Aspects and Biological Functions. International Journal of Molecular Sciences. 2020; 21: 9511.

4. Jia X, Han X. Targeting androgen receptor degradation with PROTACs from bench to bedside. Biomedicine & Pharmacotherapy. 2023; 158: 114112.

5. Neklesa T, Snyder LB, Willard RR, et al. ARV-110: An oral androgen receptor PROTAC degrader for prostate cancer. JCO. 2019; 37: 259–259.

6. Long X, Hou H, Wang X, et al. Immune signature driven by ADT-induced immune microenvironment remodeling in prostate cancer is correlated with recurrence-free survival and immune infiltration. Cell Death Dis. 2020; 11: 779.

7. Conteduca V, Caffo O, Scarpi E, et al. Immune Modulation in Prostate Cancer Patients Treated with Androgen Receptor (AR)-Targeted Therapy. JCM. 2020; 9: 1950.

8. Ardiani A, Farsaci B, Rogers CJ, et al. Combination therapy with a second-generation androgen receptor antagonist and a metastasis vaccine improves survival in a spontaneous prostate cancer model. Clin Cancer Res. 2013; 19: 6205–18.

9. Olson BM, McNeel DG. CD8+ T cells specific for the androgen receptor are common in patients with prostate cancer and can lyse prostate tumor cells. Cancer Immunol Immunother. 2011; 60: 781–92.

10. Muralidhar A, Gamat-Huber M, Vakkalanka S, McNeel DG. Sequence of androgen receptor-targeted vaccination with androgen deprivation therapy affects anti-prostate tumor efficacy. J Immunother Cancer. 2024; 12: e008848.

11. Kyriakopoulos CE, Eickhoff JC, Ferrari AC, et al. Multicenter Phase 1 Trial of a DNA Vaccine Encoding the Androgen Receptor Ligand Binding Domain (pTVG-AR, MVI-118) in Patients with Metastatic Prostate Cancer. Clin Cancer Res. 2020; 26: 5162–71.

12. McNeel DG, Eickhoff JC, Wargowski E, et al. Phase 2 trial of T-cell activation using MVI-816 and pembrolizumab in patients with metastatic, castration-resistant prostate cancer (mCRPC). J Immunother Cancer. 2022; 10: e004198.

13. Powles T, Yuen KC, Gillessen S, et al. Atezolizumab with enzalutamide versus enzalutamide alone in metastatic castration-resistant prostate cancer: a randomized phase 3 trial. Nat Med. 2022; 28: 144–53.

14. Xu P, Yang JC, Chen B, et al. Androgen receptor blockade resistance with enzalutamide in prostate cancer results in immunosuppressive alterations in the tumor immune microenvironment. J Immunother Cancer. 2023; 11: e006581.

15. Kwon H, Schafer JM, Song N-J, et al. Androgen Conspires with the CD8+ T Cell Exhaustion Program and Contributes to Sex Bias in Cancer. Sci Immunol. 2022; 7: eabq2630.

16. D J, Dg M. Toll-like receptor agonist combinations augment mouse T-cell anti-tumor immunity via IL-12- and interferon ß-mediated suppression of immune checkpoint receptor expression. Oncoimmunology [Internet]. 2022 [cited 22 May 2024]; 11. Available at: https://pubmed.ncbi.nlm.nih.gov/35340661/

17. Zahm CD, Moseman JE, Delmastro LE, G. Mcneel D. PD-1 and LAG-3 blockade improve anti-tumor vaccine efficacy. Oncoimmunology. 10: 1912892.

18. Kregel S, Chen JL, Tom W, et al. Acquired resistance to the second-generation androgen receptor antagonist enzalutamide in castration-resistant prostate cancer. Oncotarget. 2016; 7: 26259–74.

19. Watson PA, Arora VK, Sawyers CL. Emerging mechanisms of resistance to androgen receptor inhibitors in prostate cancer. Nat Rev Cancer. 2015; 15: 701–11.

20. Salami J, Alabi S, Willard RR, et al. Androgen receptor degradation by the proteolysis-targeting chimera ARCC-4 outperforms enzalutamide in cellular models of prostate cancer drug resistance. Commun Biol. 2018; 1: 1–9.

21. Guan X, Polesso F, Wang C, et al. Androgen receptor activity in T cells limits checkpoint blockade efficacy. Nature [Internet]. 2022 [cited 30 April 2022]; Available at: https://www.nature.com/articles/s41586-022-04522-6

22. Shen Y-C, Ghasemzadeh A, Kochel CM, et al. Combining intratumoral Treg depletion with androgen deprivation therapy (ADT): preclinical activity in the Myc-CaP model. Prostate Cancer Prostatic Dis. 2018; 21: 113–25.

Chapter 5

Summary and Future Directions

5.1 Summary

The overall goal of this thesis was to investigate the effects of ADT on the prostate tumor microenvironment and to use this information to inform rational treatment combination of TRT and immunotherapy. I hypothesized that ADT, when combined with the optimal choice of immune-stimulating therapies and/or radioisotope, would result in improved anti-tumor efficacy. I explored the impact of ADT treatment with TRT, AR-targeted vaccination alone or in combination with checkpoint blockade on the composition of the tumor immune microenvironment and on tumor growth.

Chapter 2 delved into the utilization of combined approaches involving ADT and TRT in murine prostate cancer models. Specifically, 90Y-NM600 TRT with ADT, with a focus on exploring immune modulation effects and the critical considerations of timing and order in this combined therapy strategy. Our findings revealed that administering ADT followed by TRT (ADT→TRT) conferred notable benefits compared to the reverse sequence. This was evidenced by a prolonged delay in tumor growth and enhanced overall survival. Moreover, ADT→TRT correlated with a sustained presence of activated and memory CD8+ T cells within the tumor microenvironment, while the TRT→ADT regimen led to increased infiltration of functionally active Myeloid-Derived Suppressor Cells (MDSCs), which suppressed CD8+ T cell function. Additionally, blocking CXCR2, the receptor for CXCL1 and CXCL2, effectively impeded MDSC migration and bolstered the anti-tumor response in the TRT→ADT group. These observed outcomes underscore the pivotal role of the sequence in which ADT and TRT are administered in shaping the tumor immune microenvironment, thereby influencing therapeutic efficacy. Furthermore, the identification of

molecular targets, such as CXCR2 blockade, provides mechanistic insights to the development of novel approaches aimed at augmenting treatment outcomes as shown in the schematic below.

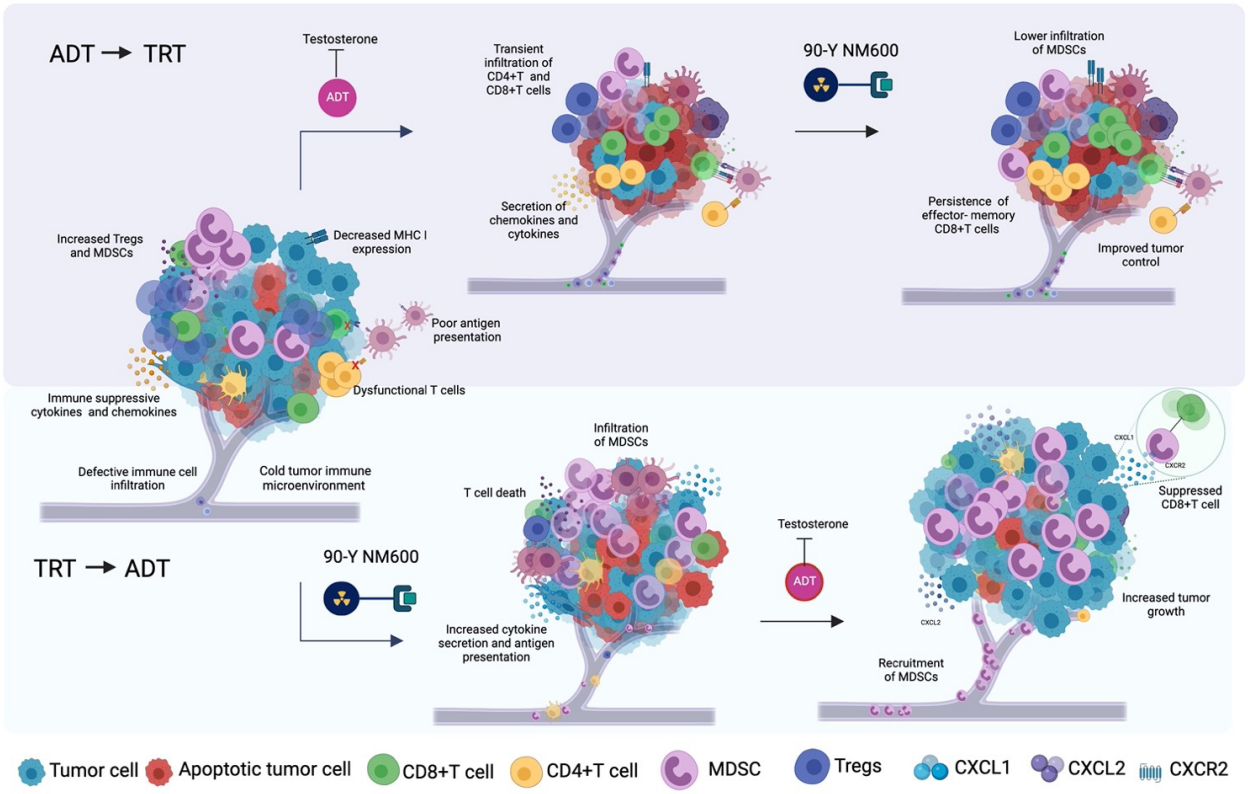

Chapter 3 delved into the combination of ADT and tumor-specific vaccination. Specifically, it assessed the combination of degarelix and pTVG-AR, a DNA vaccine encoding the androgen receptor's ligand-binding domain. Our findings indicated that administering pTVG-AR before ADT (pTVG-AR → ADT) elicited stronger anti-tumor responses compared to the reverse sequence. This regimen led to a delay in tumor growth and improved overall survival across several murine models. Notably, pTVG-AR → ADT resulted in increased infiltration of CD4+ and CD8+ T cells, particularly antigen-specific CD8+ T cells, into the tumor microenvironment, which proved pivotal for the observed anti-tumor effects. Furthermore, depleting MDSCs or inhibiting

their migration using a CXCR2 antagonist augmented anti-tumor responses. Additionally, intermittent ADT strategies, wherein ADT preceded testosterone supplementation, modulated the tumor microenvironment by reducing MDSCs. This modulation further enhanced the anti-tumor effect of AR-targeted vaccination in a murine prostate cancer model. These outcomes underscore the critical role of vaccination and the sequence of ADT administration in shaping the tumor immune microenvironment and influencing therapeutic responses as shown in the schematic below.

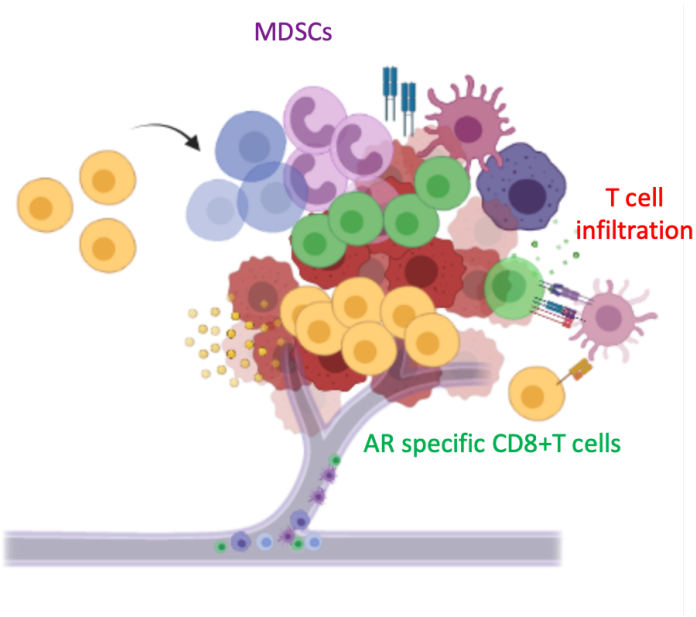

Chapter 4 was focused on determining the most effective form of ADT to combine with AR targeted vaccination. This study aimed to explore ADT in combination with optimal AR targeted agents, such as AR antagonists or degraders, along with AR targeted vaccination and immune checkpoint blockade in immune-competent murine prostate tumor models. Our findings revealed that administering pTVG-AR before ADT followed by Enzalutamide (pTVG-AR → ADT → Enzalutamide) yielded enhanced anti-tumor responses compared to ARV110, resulting in a delay in tumor growth and a significant improvement in overall survival across several murine models,

however led to reduced infiltration of CD4+ and CD8+ T cells into the tumor microenvironment while elevating regulatory T cells. Additionally, this regimen increased PD-1 and LAG-3 expression on CD8+ T cells. Although not statistically significant, pTVG-AR → ADT → αPD-1 → Enzalutamide modestly improved anti-tumor responses. These findings underscore the crucial role of infiltrating immune populations in shaping the tumor immune microenvironment and influencing therapeutic outcomes as shown in the schematic below.

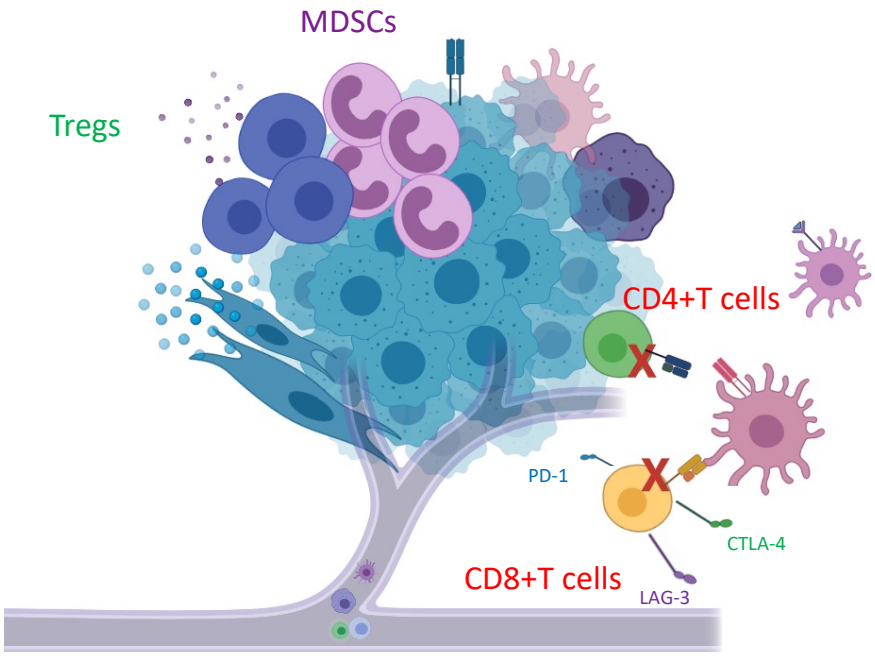

5.2 Discussion and Future Directions

Although we've demonstrated that ADT induces various immunomodulatory effects within the prostate tumor microenvironment, our findings overall indicate that combinations of ADT and immunotherapy are effective in prostate cancer treatment in immune competent murine prostate models. However, their effectiveness heavily relies on the sequence and timing of therapies, as well as the selection of therapies in combination. We've observed that ADT combined with TRT or AR targeted vaccination yields enhanced anti-tumor efficacy when ADT preceded TRT or when AR targeted vaccination preceded ADT while AR antagonists rather than AR degraders in combination with AR targeted vaccination yielded better anti-tumor responses.

Our data reveal that the primary mechanisms of resistance to regimens combining immunotherapy with ADT appear to vary depending on the specific type of targeted immunotherapy utilized. Resistance mediated by Tregs was observed with AR antagonists and ADT initially, but not with ADT combined with TRT or vaccination which was heavily infiltrated by MDSCs. This underscores the critical need to thoroughly investigate the effectiveness of combination therapies and potential sources of resistance before advancing to clinical trials. Despite the approval of various AR targeted therapies and ^{177}Lu-PSMA-617 for metastatic castration-resistant prostate cancer (mCRPC), several clinical trials have initiated exploration of these agents in combination with ADT, without first establishing a mechanistic rationale for these combinations in preclinical models.

Chapter 2 highlights that while NM600 can effectively deliver doses safely, other TRT agents may offer higher selectivity for prostate tumors. Specifically, PSMA 617 presents a promising TRT approach with high specificity for human prostate cancers, making it highly translatable. However,

utilizing PSMA-617 in preclinical studies poses challenges due to the absence of an adequate tumor model. Mouse prostate tissue, including Myc-CaP and TRAMP-C1 tumors, expresses minimal levels of PSMA, limiting its applicability in such models. However, efforts are underway to develop mouse PSMA-transduced cell lines suitable for implantation in immune-competent mouse models, thereby facilitating further TRT-related investigations. Conversely, alpha emitters such as Ac-225 could offer enhanced efficacy in targeting radio-resistant and immune-suppressive populations like MDSCs, potentially circumventing the necessity for supplementary MDSC-depleting or recruitment-inhibition therapies.

Moreover, the combination of ADT and TRT, alongside AR vaccination, holds promise in further enhancing antigen-specific CD8+ T cell responses. Alternatively, the use of alpha emitters such as Ac-225 may be more suitable for ablating radio-resistant and immune-suppressive populations like MDSCs which may further avoid the use of additional MDSC depleting or inhibition therapies. Additionally, the combination of ADT and TRT in combination with AR vaccination can be used to further enhance CD8+T cells.

Chapter 3 focused on the challenge faced in enhancing the effectiveness of ADT when combined with AR targeted vaccination, mainly due to the infiltration of MDSCs. Multiple strategies have been explored to target MDSCs in prostate cancer patients, encompassing approaches such as depletion, inhibition of expansion, differentiation, or combinations thereof. For instance, a clinical trial (NCT03177187) is underway to assess the efficacy of the CXCR2 antagonist AZD5069, combined with enzalutamide, in patients with mCRPC. Additionally, investigations are ongoing into targeting VEGF, a factor associated with MDSC expansion, through a clinical trial (NCT03964337) utilizing cabozantinib, a tyrosine kinase inhibitor that impedes the VEGF pathway. Another approach revolves around depleting MDSCs from the circulation. For example,

a clinical trial (NCT03709550) is evaluating decitabine, a hypomethylating agent, for its potential to selectively deplete monocytic MDSCs (Mo-MDSCs) in patients with mCRPC. Moreover, efforts are being made to inhibit the differentiation of MDSCs into immunosuppressive phenotypes. Clinical trials are investigating agents like curcumin and white button mushroom extract, hypothesized to facilitate the differentiation of MDSCs into anti-tumor macrophages or antigen-presenting cells, respectively. Additionally, targeting MDSC-induced suppressive mechanisms emerges as a promising therapeutic strategy. Clinical trials are examining combinations of drugs such as abiraterone, tildrakizumab (anti-IL-23 antibody), ipatasertib (AKT inhibitor), atezolizumab (anti-PD-L1 antibody), and docetaxel to inhibit MDSC function or bolster anti-tumor immune responses. Moreover, there is an urgent need to deepen our understanding of the mechanism underlying the T cell-MDSC switch post ADT treatment. Advancing this understanding will be crucial for devising more effective strategies to overcome MDSC-mediated immunosuppression and enhance the therapeutic outcomes of ADT combined with AR targeted vaccination.

In Chapter 4, our observations revealed that the effectiveness of ADT with vaccination depended on the specific type of ADT utilized. Contrary to our hypothesis, degradation of the AR did not result in increased MHC class I presentation of the AR or enhance infiltration of AR-specific T cells. However, treatment with AR antagonists led to upregulation of AR expression. When combined with AR vaccination, this regimen improved anti-tumor responses but also increased the infiltration of regulatory T cells (Tregs) in vivo. Tregs are known to confer resistance in this combination therapy, particularly as they exhibit high resistance to radiation. Thus, depletion of Tregs may still be necessary for optimal efficacy alongside ADT and enzalutamide treatment.

Alternatively, blocking other immune checkpoint molecules such as CTLA-4, PD-1, and/or LAG-3 could potentially overcome Treg-mediated resistance and enhance infiltration of CD8+ T cells.

Given the recruitment of MDSCs at later stages with ADT, future studies will focus on intermittent approaches of ADT in combination with checkpoint blockade. This strategy will aim to address the immunosuppressive effects of MDSCs and optimize the therapeutic response by strategically timing ADT administration alongside checkpoint blockade.

Overall, while ADT has shown various immune modulatory effects, understanding its implications in different tumor volumes is crucial. The immune response triggered by ADT-mediated antigen delivery likely varies based on the tumor's size and stage. Combining ADT with conventional treatments such as or radiation therapy could be especially effective in shrinking larger tumors and priming them for immune-mediated elimination. Furthermore, investigating how tumor volume affects ADT-mediated immune modulation could help design rational combination therapies.

In conclusion, exploring the relationship between tumor volume and ADT-mediated immune modulation is essential in cancer immunotherapy. By uncovering the complex interplay among ADT, tumor size, and the immune environment, we can refine treatment strategies and advance personalized therapies for cancer patients.

Chapter 6

Materials and Methods

Most of this work is published or is currently being prepared as part of research manuscripts to be submitted for publication in The Journal of Immunotherapy in Cancer.

6.1 Material and Methods – Chapter 2

6.1.1 Radiosynthesis of ^{90}Y-NM600:

Briefly, $^{86}YCl_3$ was provided by the University of Wisconsin-Madison cyclotron group after proton bombardment of enriched [^{86}Sr] SrCO3 solid targets in a PETtrace biomedical cyclotron and elution of ^{86}Y from a diglycolamide extraction resin column [33]. Clinical grade $^{90}YCl_3$ and NM600 were obtained from PerkinElmer (Shelton, CT) and Archeus Technologies (Madison, WI) respectively. NM600 was radiolabeled with ^{90}Y or ^{86}Y and purified as previously described [29,30]. Briefly, 185–370 MBq (5 - 10 mCi) of $^{86/90}$Y was buffered with 0.1 M NaOAc (pH 5.5) and mixed with 55-110 nmol (50-100 μg). The reaction was incubated for 30 min at 95°C under constant shaking (500 rpm). $^{86/90}$Y-NM600 was purified by a solid-phase extraction cartridge (HLB; Waters) and eluted in 2 mL of 200-proof ethanol. The eluate was then evaporated and dried under a nitrogen stream, and $^{86/90}$Y-NM600 was reconstituted in excipient (saline containing 0.1% v/v Tween20). Radiochemical yield was assessed by instant thin-layer chromatography (iTLC) using silica-impregnated paper as the stationary phase and run using 50 mM ethylenediaminetetraacetic acid, which moves the free radiometals with the solvent front ($R_f = 1$) while $^{86/90}$Y-NM600 remains at the origin ($R_f = 0$). iTLC chromatograms were developed using a cyclone phosphor-plate imager and analyzed with Optiquant software (PerkinElmer). Radiochemical purity and stability were determined via radiolabeled high-performance liquid chromatography (HPLC) using a reverse-phase 250 × 3.00 mm C18 Luna 5 μm 100 Å column (Phenomenex) and a water:acetonitrile gradient (5% MeCN: 0–2 min; 5%–65% MeCN: 2–30 min; 65%–90% MeCN: 30–35 min; 90%–5% MeCN: 35–45 min). The final radiochemical purity obtained consistently surpassed 95% with an average molar specific activity of 18 GBq/μmol for

both ^{90}Y-NM600 and ^{86}Y-NM600 (n > 5). Additionally, HPLC chromatograms indicated that both ^{90}Y-NM600 and ^{86}Y-NM600 were stable in mouse serum over at least 48h [29].

6.1.2 Cell lines:

TRAMP-C1 (CRL-2730) and Myc-CaP (CRL-3255) cell lines were obtained from ATCC (Manassas, VA), maintained according to ATCC recommendations, and tested for mycoplasma contamination.

6.1.3 Mice:

FVB/NJ mice (stock #001800) and C57BL/6J mice (stock #000664) were obtained from The Jackson Laboratory (Bar Harbor, ME) and housed in micro insulator cages under aseptic conditions. NRG mice were graciously provided by Dr. Paul Sondel (University of Wisconsin-Madison). All animal studies were conducted under an IACUC-approved protocol.

6.1.4 Tumor implantation and tumor growth studies:

1 x 10^6 Myc-CaP cells, resuspended in PBS, were implanted subcutaneously into the right flank of 4–6-week-old male FVB mice or 6–10-week-old male NRG mice. Similarly, wild type male C57BL/6J mice aged 4-6 weeks were injected subcutaneously with 1 x 10^6 TRAMP-C1 cells in 1:1 ratio in PBS: Matrigel (Corning, NY. CB354248) into the right flank. Twelve to fifteen days post injection, when tumors were palpable and similarly sized (0.2-0.3cm^3), mice were randomized into treatment groups. Tumors were measured twice weekly via calipers until the tumors reached 2cm^3. Tumor volumes were calculated as (long axis x short $axis^2$)/2.

6.1.5 Androgen deprivation therapy:

Mice were treated subcutaneously with either degarelix (25mg/kg) or a vehicle sham treatment (PBS) every 28 days starting when the tumor volume reached ~ 0.2-0.3cm^3 in size.

6.1.6 Dosimetry estimation:

Dosimetry estimations were performed as previously reported using a Monte Carlo-based dosimetry assessment platform, Radionuclide Assessment Platform for Internal Dosimetry (RAPID) [34,35]. The dosimetry and biodistribution of ^{90}Y-NM600 have been previously published for murine Myc-CaP and TRAMP-C1 prostate tumors [29,32].

6.1.7 TRT administration:

^{90}Y-NM600 250μCi ~ 9.25MBq was injected into the tail vein of tumor-bearing mice one week before or after the start of ADT. Based on dosimetry studies, a single dose of 250μCi injected activity delivered 5-6Gy absorbed dose to TRAMP-C1 tumors and 16-20Gy to Myc-CaP tumors [29,32].

6.1.8 Antibody treatments:

All antibody treatments, anti-CD4 (BioXcell BP0003-1), anti-CD8 (BioXcell BP0061) and IgG2a isotype (BioXcell BP0085), were administered as 200μg intraperitoneal injections, on days 2, 4, and 6 post ADT or TRT. 200μg anti-mouse Gr-1 antibody (clone RB6-8C5) (BD Pharmingen 552985) was administered intraperitoneally three times a week post TRT administration.

6.1.9 Flow cytometry:

Tumors were collected at different time points, then digested for 1-2 hours at 37°C in mouse cell culture medium: RPMI 1640 with L-glutamine, 10% fetal calf serum (FCS), 200 U/mL Pen/Strep, 5% sodium pyruvate, 5% HEPES, and 50 μM β-MeOH supplemented with 2 mg/mL collagenase,

0.2 mg/mL DNAse I, and 1 tablet protease inhibitor (Sigma-Aldrich, St. Louis, MO, 11697498001) per 50 mL digest solution. Digests were then passed through 100 μm screens. 5 x 10^6 cells were plated and Fc blocked (BD, Franklin Lakes, NJ, 553142) for 20 min at 4°C. Cells were then stained for 30 min at 4°C with the viability dye Ghost Dye Red 780 (Tonbo 13-0865 T100) and the following antibodies: CD11b-BB515 (BD 564454), CD25-BB700 (BD 566498), GR-1-PE-CF594 (BD 562710), CD3-PE-Cy7 (eBiosciences Thermo Fisher Scientific, Waltham, MA 25-0031-82), MHCII-BV421 (Biolegend San Diego, CA 107632), CD45-BV510 (BD 563891), CD4-BV605 (Biolegend 100451), CD19-BV711 (BD 563157), CD11c-APC (BD 550261), CD8-AF700 (100730), CD44-AF488 (Biolegend 103016), CD45- PerCP-Cy5.5 (Biolegend 103132), KLRG-1-PE (Biolegend 138408), CD69-PE-CF594 (BD 562455), CD62L-BV510 (Biolegend 104441), CD103-BV605 (Biolegend 121453), CD27-BV785 (Biolegend 124241), CD4-APC-Cy7 (Biolegend 561830). Cells were then fixed and permeabilized with the eBiosciences Foxp3/Transcription Factor Staining Buffer Set overnight at 4°C (Thermo Fisher 00-5523-00). Cells were then stained with intracellular antibodies for 30 min at 4°C: FoxP3-PE (Thermo Fisher 12-5773-82), Ki67-BV421 (BD 562899). Flow cytometry was performed on a Thermo Fisher Attune NxT cytometer and data were analyzed using FlowJo V.10. Gates were set according to a fluorescence-minus-one control. Flow cytometry data was reported as either the % of populations among all CD45+ events or as a frequency per gm of tumor tissue.

6.1.10 CXCR2 antagonist:

CXCR2 antagonist, reparixin (Selleckchem, Houston, Texas), was reconstituted in Tween-80 and PBS in a 1:4 ratio and administered subcutaneously at 5mg/kg on the left flank thrice a week for three weeks post TRT administration.

6.1.11 CD8+T cell suppression assay:

Spleens were harvested from naïve FVB mice and passed through 100 µm screens. CD8+ T cells were isolated from splenocytes via immunomagnetic negative selection (StemCell #19853), then labeled with carboxyfluorescein succinimidyl ester (CFSE, Biolegend #423801) according to the manufacturer's instructions. Tumors were collected from treated tumor-bearing mice on day 36, processed into single cell suspensions as above, and CD11b+Gr-1+Ly-6G+ MDSCs were isolated (Miltenyi Biotec #130-094-538). 1×10^5 labeled CD8 +T cells were cultured together with MDSCs at a 1:1 ratio. CD8+ T cells were stimulated with anti-CD3/anti-CD28 coated beads (Thermo Fisher 11 456D) at a ratio of 2 beads per CD8+ T cell. Cells were cultured with 30 units/mL of human IL-2 for 72 hours in 96-well plates before analysis via flow cytometry.

6.1.12 ELISA:

ELISA was performed as previously described [36]. Briefly, Immulon plates (Thermo Fisher, Waltham, MA) were coated with anti-mouse IFNγ antibody (BD #551216) and incubated overnight at 4°C. Plate were then blocked with PBS/1% BSA before adding standards (BD #554587) or cell culture supernatants and incubated overnight at 4°C. The next day, biotin-conjugated anti-mouse IFNγ antibody was added (BD #554410), followed by avidin-HRP (BioRad Hercules, CA, 170-6528). TMB Substrate (Kirkegaard and Perry, Gaithersburg, MD, 50-76-01) was added and OD was measured at 450nm.

6.1.13 Luminex assay:

50µL of sera or conditioned media from *in vitro* assays were evaluated for 26 different cytokines and chemokines using the Cytokine & Chemokine 26-Plex Mouse ProcartaPlex™ Panel 1 (Thermo Fisher EPX260-26088-901) according to the manufacturer's instructions. The plate was

read on a Luminex MagPix instrument. Analytes were divided according to their type, Th1 (IFN gamma, IL-12p70, IL-18, IL-27, IL-2, TNF alpha, GMCSF, IL-1 beta), Th2 (IL-4, IL-5, IL-6, IL-9, IL-10, IL-13, GMCSF), Th17 (IL-17A, IL-22, IL-23), and chemokines (CXCL10, CXCL1, CCL2, CCL7, CCL3, CCL4, CXCL2, CCL5, CCL11).

***In-vitro* chemotaxis assay:**

3 x10^5 cells (Myc-CaP cells and/or T cells including CD4 and CD8 T cells isolated from naïve FVB mice splenocytes) were plated in regular media, charcoal-stripped media (regular media with charcoal-stripped FBS (Thermo#12676029), ^{90}Y containing media (23.3μCi ~ 0.86MBq of ^{90}Y per 1mL media) or ^{90}Y-containing charcoal-stripped media, in 6-well plates (n=3 replicates per media condition). Wells containing T cells were stimulated with anti-CD3/anti-CD28 coated beads at a ratio of 2 beads per CD8 +T cell. Supernatants were collected after incubation for 72 hours. 1 x 10^5 MDSCs isolated from tumors as described above were added to the top chamber of the transwell and cultured for 12 hours with the conditioned media in the bottom well. In related experiments, 5 ng/mL recombinant CXCL1 was used as a positive control, and MDSCs were pre-treated with 4mM reparixin. In other related experiments, conditioned media from T cells were added to the Myc-CaP conditioned media in a 1:1 ratio. After incubation, cells were collected from the bottom well, stained, and analyzed via flow cytometry. The absolute number of MDSCs was determined and the percent migration was calculated as the fraction of MDSCs present in the bottom well of the total number of MDSCs plated in the transwell

6.1.14 Statistical analysis:

Tumor growth data, comparing group means among treatment groups, were analyzed by fitting a linear mixed-effects model with Geisser-Greenhouse correction. The data were analyzed via analysis of variance (ANOVA) followed by Tukey's multiple-comparison test. Survival analysis

was conducted using a Mantel-Cox log-rank test. For all comparisons, p values ≤ 0.05 were considered statistically significant with asterisks *$p<0.05$, **$p<0.01$, and ***$p<0.001$. All statistical analyses were performed using GraphPad Prism software v10.0.3.

Materials and methods – Chapter 3

6.2.1 Cell lines:

TRAMP-C1 and Myc-CaP cell lines were obtained from ATCC (Manassas, VA) and maintained according to ATCC recommendations and tested for mycoplasma contamination.

6.2.2 Mice:

FVB/NJ mice (stock #001800) and C57BL/6 mice (stock #000664) were obtained from The Jackson Laboratory (Bar Harbor, ME) and housed in micro insulator cages under aseptic conditions. A2/TRAMP mice were generated by crossing homozygous TRAMP mice and HHDII-DR1 mice [23]. All animal studies were conducted under an IACUC-approved protocol.

6.2.3 Tumor implantation:

FVB mice were implanted with 1 x 10^6 cells in PBS into the flank of 4–6-week-old FVB mice, or 6–10-week-old NRG mice, respectively. Similarly, wild type-male C57BL/6J mice aged 4-6 weeks were injected subcutaneously into the flank with 1 x 10^6 TRAMP-C1 cells in 1:1 ratio in PBS: Matrigel (Corning, NY. CB354248).

6.2.4 Tumor growth studies:

Tumors were measured twice weekly via calipers until the tumors reached 2 cm^3. Tumor volumes were calculated as (long axis x short $axis^2$) / 2. Mice were randomized to treatment groups and treatments were started when the tumor volume reached 0.1-0.2 cm^3.

6.2.5 Androgen deprivation therapy:

Mice were treated subcutaneously with either degarelix (25mg/kg) (Ferring Pharmaceuticals, Parsippany, NJ) or a vehicle sham (PBS) treatment every 28 days starting when the tumor volume reached 0.1-0.2 cm^3.

6.2.6 DNA immunization:

100mg of pTVG4 or pTVG-AR (GeneScript, Piscataway, NJ) per mouse was administered intradermally in the ear pinna of TRAMP-C1 or Myc-CaP tumor-bearing mice. The first dose of vaccine was given the day after tumor implantation, with additional doses given weekly afterwards in the pTVG4 → ADT and pTVG-AR → ADT groups. For ADT → pTVG4 and ADT → pTVG-AR groups, the immunizations were started one day after ADT administration. In the A2-TRAMP studies, immunizations were started when mice reached 16 weeks of age, for 4 weeks, followed by ADT administered every 28 days. In the pTVG4 →ADT and pTVG-AR →ADT groups, a boost was administered prior to ADT. Conversely, in the ADT →pTVG4 and ADT → pTVG-AR groups, immunizations were initiated after ADT, with subsequent boosts administered post ADT every 28 days.

6.2.7 Testosterone administration:

Mice were administered 0.9 mg testosterone cypionate (Cipla USA, Warren, NJ). This was resuspended in 100µl of sesame oil and delivered subcutaneously twice a week for two weeks beginning 14 days post ADT treatment [27,28].

6.2.8 CXCR2 antagonist:

CXCR2 antagonist, reparixin (Selleckchem, Houston, TX), was reconstituted in Tween-80 and PBS in a 1:4 ratio and administered subcutaneously at 5mg/kg on the left flank thrice a week for three weeks post ADT administration.

6.2.9 Clodronate liposomes:

Mice were injected with clodronate liposomes intravenously, using 200µL of 5mg/ml suspension of clodronate liposomes (Liposoma clodronate liposomes, Amsterdam, The Netherlands), twice weekly for three weeks post ADT treatment. Control groups received empty liposomes at the same dose and schedule [29].

6.2.10 Flow cytometry:

Tumors were collected from mice at different time points following different treatments, then digested for 1-2 hours at 37°C in mouse cell culture medium: RPMI 1640 with L-glutamine, 10% fetal calf serum (FCS), 200 U/mL Pen/Strep, 5% sodium pyruvate, 5% HEPES, and 50 µM β-MeOH supplemented with 2 mg/mL collagenase, 0.2 mg/mL DNAse I, and 1 tablet protease inhibitor (Sigma-Aldrich, St. Louis, MO, Cat# 11697498001) per 50 mL digest solution. Digests were then passed through 100 µm screens. 5 x 10^6 cells were plated and Fc blocked (BD, Franklin Lakes, NJ, 553142) for 20 min at 4°C. Cells were then stained for 30 min. at 4°C with the viability dye Ghost Dye Red 780 (Tonbo 13-0865 T100) and the following antibodies: CD11b-BB515 (BD 564454), CD25-BB700 (BD 566498), GR-1-PE-CF594 (BD 562710), CD3-PE-Cy7 (eBiosciences Thermo Fisher Scientific, Waltham, MA 25-0031-82), MHCII-BV421 (Biolegend San Diego, CA 107632), CD45-BV510 (BD 563891), CD4-BV605 (Biolegend 100451), CD19-BV711 (BD 563157), CD11c-APC (BD 550261), CD8-AF700 (100730) and cells were then fixed and permeabilized with the eBioscience Foxp3/Transcription Factor Staining Buffer Set overnight at 4°C (Thermo Fisher 00-5523-00). Cells were then stained with intracellular antibodies for 30 min. at 4°C: FoxP3-PE (Thermo Fisher 12-5773-82), Ki67-BV421 (BD 562899), TNFα (Biolegend 506323), Granzyme B (Thermo Fisher 61-8898-82) Perforin-FITC (Biolegend 353309). Flow

cytometry was performed on a Thermo Fisher Attune NxT cytometer and data were analyzed using FlowJo V.10 software. Gates were set according to fluorescence minus one control.

6.2.11 Enzyme-linked immunospot assay (ELISPOT):

Measures of antigen-specific immune response were performed by IFNγ ELISPOT (Bio-Techne, R&D Systems, Minneapolis, MN). Briefly, CD8+T cells were harvested from tumors of treated mice using EasySep™ Mouse CD8+ T Cell Isolation Kit (Stemcell Technologies, Cat# 19853) following ADT treatment and added together with splenocytes from naïve FVB mice as feeder cells in a 1:10 ratio. AR25 (SRMLYFAPDLVFNEY), a 15-mer AR-specific dominant CD8+ peptide epitope in FVB mice, or a pool of 62 15-mer amino acids spanning the amino acid sequence of the AR ligand-binding domain, was used as a measure for antigen-specific response measured after 48 hours of antigen stimulation. Positive control included stimulating the CD8+T cells with αCD3/αCD28 coated beads (Thermo Fisher, Cat# 11 456D) at a ratio of 2 beads per CD8 +T cell. Experimental results are shown as the number of IFNγ spot-forming units (SFU) per 10^5 CD8+ T cells normalized against media-alone control wells.

6.2.12 Statistical analysis:

Tumor growth data were analyzed by fitting a linear mixed-effects model with Geisser-Greenhouse correction and used to compare group means among treatment groups. Flow cytometry data were analyzed via analysis of variance (ANOVA) followed by Tukey's multiple-comparison test when comparing all conditions to baseline, or planned contrasts when comparing only two conditions at each time point. Survival analysis was conducted using a Mantel-Cox log-rank test. For all comparisons, p values ≤ 0.05 were considered statistically significant with asterisks *p<0.05, **p<0.01, and ***p<0.001. For ELISPOT analyses, comparisons between

treatment groups and media only controls were made using a Student's t test, with $p < 0.05$ defining a significant antigen-specific T-cell response. One-way ANOVA with Tukey's multiple comparisons test was performed for time course experiments with asterisks indicating $*p < 0.05$, $**p<0.01$, and $***p<0.001$. All analysis was performed on GraphPad Prim version 10.0.0, GraphPad Software, Boston, Massachusetts USA.

Materials and Methods – Chapter 4

6.3.1 Cell lines:

TRAMP-C1 and Myc-CaP cell lines were obtained from ATCC (Manassas, VA) and maintained according to ATCC recommendations and tested for mycoplasma contamination.

6.3.2 Mice:

FVB/NJ mice (stock #001800) and C57BL/6 mice (stock #000664) were obtained from The Jackson Laboratory (Bar Harbor, ME) and housed in micro insulator cages under aseptic conditions. A2/TRAMP mice were generated by crossing homozygous TRAMP mice and HHDII-DR1 mice [23]. All animal studies were conducted under an IACUC-approved protocol.

6.3.3 Tumor implantation:

FVB mice were implanted with 1 x 10^6 cells in PBS into the flank of 4–6-week-old FVB mice. Similarly, wild type-male C57BL/6J mice aged 4-6 weeks were injected subcutaneously into the flank with 1 x 10^6 TRAMP-C1 cells in 1:1 ratio in PBS: Matrigel (Corning, NY. CB354248).

6.3.4 Tumor growth studies:

Tumors were measured twice weekly via calipers until the tumors reached 2 cm^3. Tumor volumes were calculated as (long axis x short $axis^2$) / 2. Mice were randomized to treatment groups and treatments were started when the tumor volume reached 0.1-0.2 cm^3.

6.3.5 Androgen deprivation therapy:

Mice were treated subcutaneously with either degarelix (25mg/kg) (Ferring Pharmaceuticals, Parsippany, NJ) or a vehicle sham (PBS) treatment every 28 days starting when the tumor volume reached 0.1-0.2 cm^3.

6.3.6 DNA immunization:

100mg of pTVG4 or pTVG-AR (GeneScript, Piscataway, NJ) per mouse was administered intradermally in the ear pinna of TRAMP-C1 or Myc-CaP tumor-bearing mice. The first dose of vaccine was given the day after tumor implantation, with additional doses given weekly afterwards in the pTVG4 → ADT and pTVG-AR → ADT groups.

6.3.6 ARV110 and Enzalutamide administration:

Mice were treated with ARV110 (10 mg/kg) (MedChem Express, NJ, #HY-138641) or Enzalutamide (10 mg/kg) (MedChem Express, NJ, #HY-70002) or a vehicle sham (PBS) treatment five times a week starting when the mice received degarelix.

6.3.7 Antibody treatments

All antibodies were administered at 200 μg intraperitoneally weekly post DNA immunization. Anti-PD-1 antibody was produced by Envigo (Madison, WI) and Armenian Hamster IgG (BioXCell BE0091) was used as control.

6.3.8 Flow cytometry:

Tumors were collected from mice at different time points following different treatments, then digested for 1-2 hours at 37°C in mouse cell culture medium: RPMI 1640 with L-glutamine, 10% fetal calf serum (FCS), 200 U/mL Pen/Strep, 5% sodium pyruvate, 5% HEPES, and 50 μM β-MeOH supplemented with 2 mg/mL collagenase, 0.2 mg/mL DNase I, and 1 tablet protease inhibitor (Sigma-Aldrich, St. Louis, MO, Cat# 11697498001) per 50 mL digest solution. Digests were then passed through 100 μm screens. 5 x 10^6 cells were plated and Fc blocked (BD, Franklin Lakes, NJ, 553142) for 20 min at 4°C. Cells were then stained for 30 min. at 4°C with the viability dye Ghost Dye Red 780 (Tonbo 13-0865 T100) and the following antibodies: CD11b-BB515 (BD

564454), CD25-BB700 (BD 566498), GR-1-PE-CF594 (BD 562710), CD3-PE-Cy7 (eBiosciences Thermo Fisher Scientific, Waltham, MA 25-0031-82), MHCII-BV421 (Biolegend San Diego, CA 107632), CD45-BV510 (BD 563891), CD4-BV605 (Biolegend 100451), CD19-BV711 (BD 563157), CD11c-APC (BD 550261), CD8-AF700 (100730) and cells were then fixed and permeabilized with the eBioscience Foxp3/Transcription Factor Staining Buffer Set overnight at 4°C (Thermo Fisher 00-5523-00). Cells were then stained with intracellular antibodies for 30 min. at 4°C: FoxP3-PE (Thermo Fisher 12-5773-82), Ki67-BV421 (BD 562899). Flow cytometry was performed on a Thermo Fisher Attune NxT cytometer and data were analyzed using FlowJo V.10 software. Gates were set according to fluorescence minus one control.

6.3.9 In vitro AR expression by flow cytometry

For AR intracellular staining, cells were stained with a Live/Dead GhostDye 780 Live/Dead Stain (Tonbo Biosciences) for tumor cells cultured in vitro with or without Enzalutamide for 72 hours at 37C, and intracellularly stained with PE conjugated antibody directed against the AR (LS bio, MA, LS-C184175)

6.3.10 Ex-vivo Enzyme-linked immunospot assay (ELISPOT) assay:

Measures of antigen-specific immune response were performed by IFNγ ELISPOT (Bio-Techne, R&D Systems, Minneapolis, MN). Briefly, 22RV1 cells were treated with ARV110, bicalutamide, media alone as control, Dip G, enzalutamide and flutamide and co-cultured with splenocytes from HHD mice immunized with AR811 mice as feeder cells in a 1:10 ratio. Positive control included stimulating the splenocytes with AR811, a 15-mer AR-specific dominant CD8+ peptide epitope in HHD mice, or anti-CD3/anti-CD28 coated beads (Thermo Fisher, Cat# 11 456D) at a ratio of 2

beads per CD8 +T cell. Experimental results are shown as the number of IFNγ spot-forming units (SFU) per 10^5 CD8+ T cells normalized against media-alone control wells.

6.3.11 Statistical analysis:

Tumor growth data were analyzed by fitting a linear mixed-effects model with Geisser-Greenhouse correction and used to compare group means among treatment groups. Flow cytometry data were analyzed via analysis of variance (ANOVA) followed by Tukey's multiple-comparison test when comparing all conditions to baseline, or planned contrasts when comparing only two conditions at each time point. Survival analysis was conducted using a Mantel-Cox log-rank test. For all comparisons, p values ≤ 0.05 were considered statistically significant with asterisks *p<0.05, **p<0.01, and ***p<0.001. For ELISPOT analyses, comparisons between treatment groups and media only controls were made using a student's t test, with $p < 0.05$ defining a significant antigen-specific T-cell response. One-way ANOVA with Tukey's multiple comparisons test was performed for time course experiments with asterisks indicating *p < 0.05, **p<0.01, and ***p<0.001. All analysis was performed on GraphPad Prim version 10.0.0, GraphPad Software, Boston, Massachusetts USA.

Appendix – Chapter 4

Flow cytometry gating strategies.

Flow gating strategy for T cells and MDSC populations. CD4+ and CD8+ T cells were selected within the CD3+CD45+ cell population after applying gating criteria for single cells and live-dead staining. MDSCs (CD11b+Gr1+ cells) were gated within the CD45+ cell population and Regulatory T cells (Tregs) were gated on CD4+T cells.

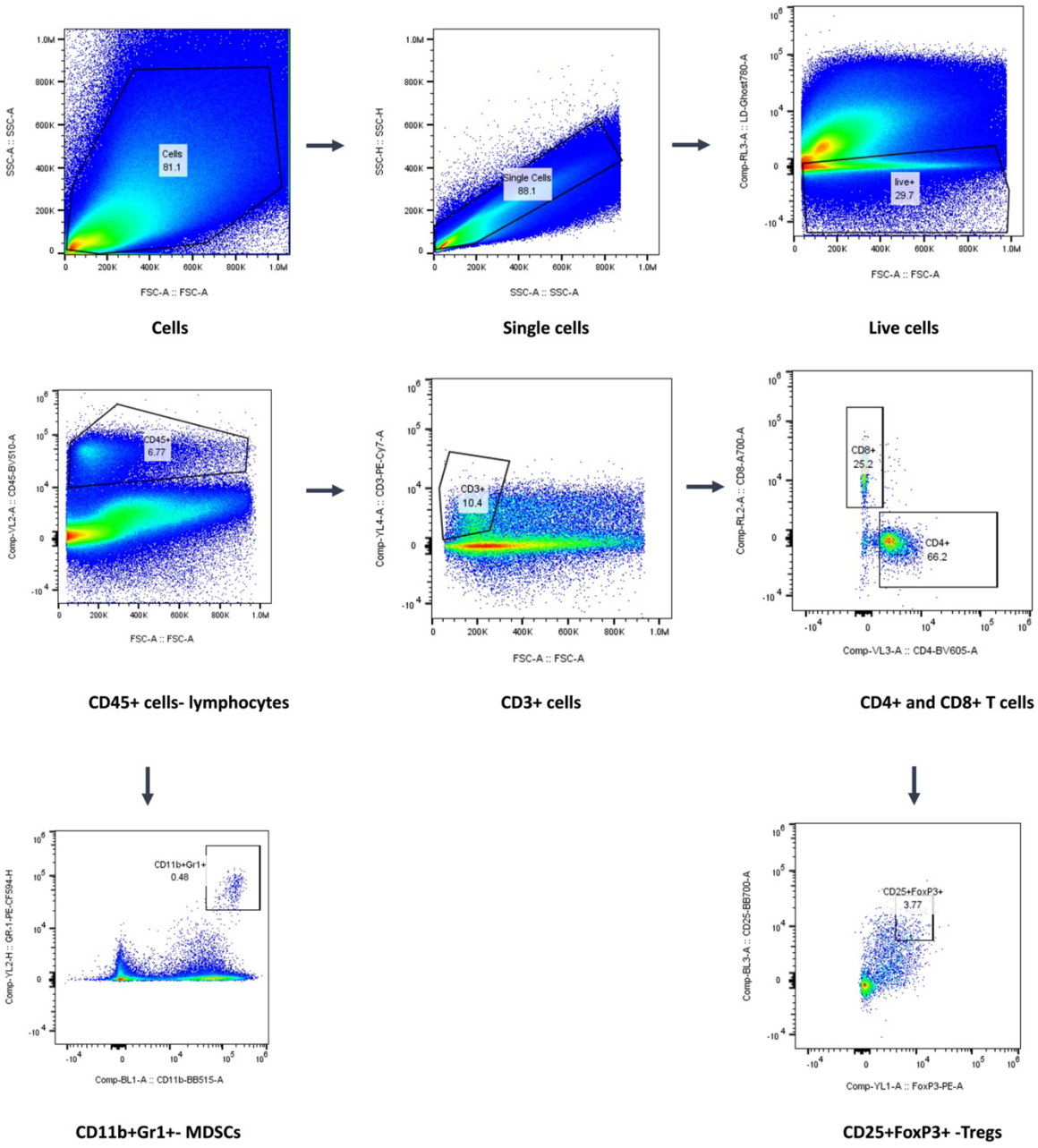

Flow gating strategy for T cell and MDSC populations.

Flow gating strategy for immunophenotyping CD8+T cell subtypes. Memory CD8+ T cells were identified within the CD44+ cell subset, which was subsequently subdivided into central and effector memory populations based on the expression of CD62L+CD27+ and CD62L-CD27-, respectively. Resident memory cells (CD69+CD103+) were gated within the CD44+CD8+ T cell population.

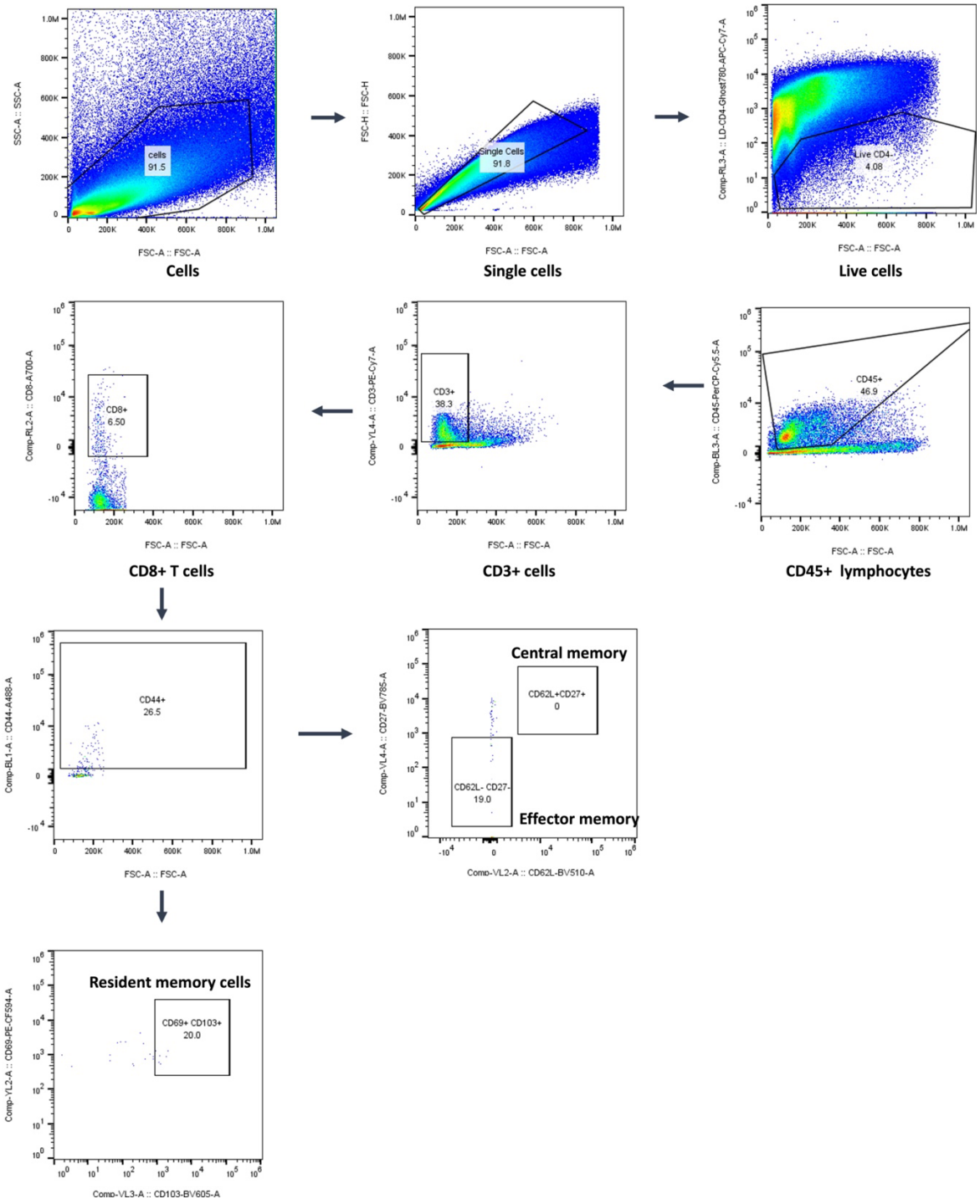

Flow gating strategy for immunophenotyping CD8+T cell subtypes.